Singh, Avtar

AUTOMATIC WAVEFORM DETECTION AND MODEL PARAMETER ESTIMATION FOR OPTOKINETIC NYSTAGMUS

City University of New York PH.D. 1982

AUTOMATIC WAVEFORM DETECTION AND MODEL PARAMETER ESTIMATION FOR OPTOKINETIC NYSTAGMUS

by

AVTAR SINGH

A dissertation submitted to the Graduate Faculty in Engineering in partial fulfillment of the requirements for the degree of Doctor of Philosophy

The City University of New York

1982

This manuscript has been read and accepted by the Graduate Faculty in Engineering in satisfaction of the dissertation requirement for the degree of Doctor of Philosophy.

8/23/82
date

F. E. Thau
Chairman of Examining Committee

9/30/82
date

Executive Officer

Professor F. E. Thau (Mentor)

Professor T. Raphan

Professor B. Cohen

Professor G. Kranc

Professor N. Shienberg

Supervisory Committee

The City University of New York

Abstract

AUTOMATIC WAVEFORM DETECTION AND PARAMETER ESTIMATION
FOR
OPTOKINETIC NYSTAGMUS

by

Avtar Singh

Adviser: Professor Frederick E. Thau

The purpose of this dissertation is to contribute to a precise understanding of the oculomotor system responsible for eye movements. The attempt to acquire this understanding is made through the signal processing of oculomotor responses and the parameter estimation of a model for the generation of slow eye movements. The slow eye movement system is important since it describes the tracking capability of the eye and thus gives clues to the pathological state of the neural system where these movements are generated.

In response to head rotation or to optokinetic stimulation, slow and rapid eye movements are made which together form nystagmus. The first step in the analysis of an eye movement record is to develop an algorithm that separates the slow and quick phase eye movements. These movements can then be related to the oculomotor system parameters and to the stimulus. The most commonly used technique for recording eye position, electrooculography (EOG), records muscle and skin artifacts along with changes in eye position. Thus one must identify and distinguish between waveforms in the presence of noise.

The detection algorithm presented in this dissertation compares a window of eye position samples to functional representations of quick and slow eye movements. Based upon minimizing the probability of error,

a decision function is formulated. Its value is then compared to a threshold to determine whether the latest sample in the window belongs to a slow or a rapid eye movement. Two kinds of errors can be made in the detection process. The first kind is: when all the samples in the window are from one kind of movement and it is detected as the other kind. This kind of error is due to the inherent noise on the samples. The second kind of error occurs when the data window consists of samples from both kinds of movements. This error is due to the frequency of transitions between movements, the temporal relations between movements and the window width used. An expression for the probability of error accounting for both kinds of errors is derived.

Once a quick phase or a saccade has been detected, it is removed by subtracting the saccadic jump and extrapolating the slow eye position during a saccade. This generates a cumulative slow phase position whose differentiation yields the slow phase eye velocity. The differentiator algorithm is based on least squares straight line fit to the data. The saccadic detection, the cumulative slow phase position, and slow phase velocity generation algorithms are implemented on a mini-computer for real-time signal processing. The implementation allows a sampling interval as small as 2msec and can be controlled from external inputs for optimal performance.

The slow phase velocity as obtained from the processing of an optokinetic nystagmus is utilized in the parameter estimation of a model for the system which generates optokinetic nystagmus (OKN) and optokinetic after-nystagmus (OKAN). The parameter estimation is based upon a least squares curve fitting technique which is implemented to generate recursively the model parameters. The parameter estimation obtained in this manner is used to evaluate the OKN and OKAN model. The estimation and evaluation programs are written in assembly language for optimization and on-line processing.

Contribution of this research lie in the application of detection theory, nonlinear digital filtering, and parameter estimation to the analysis of the oculomotor system. The implementation of various algorithms for the real-time signal processing and the on-line parameter estimation is another contribution of this dissertation. The direction chosen here has a great potential for further investigations.

ACKNOWLEDGEMENTS

I wish to thank all the members of my Doctoral Committee consisting of Professors Frederick E. Thau, Theodore Raphan, Bernard Cohen, George Kranc and Norman Shienberg. My special thanks go to late Professor Ralph Mckel who helped start this work, but could not see its completion.

Professor F. E. Thau provided constant invaluable assistance in conducting this research. The numerous hours spent with him discussing the problem led to an elegant solution. His help in the writing of this dissertation was also very educational. Professor T. Raphan of the Mount Sinai School of Medicine guided in defining the problem, helped in computer implementations, and also in the writing of this dissertation. Professor B. Cohen also of the Mount Sinai School of Medicine was instrumental in the selection of this research area and in bringing out the practical importance of this work.

I also like to thank the following individuals, who were helpful in one way or the other: Drs D. Weitzman and V. Matsuo of the Mount Sinai School of Medicine; Professor J. Vallely, F. Gonzalez, L. Kovach and R. Svaarer of the County College of Morris. Thanks are paid to Mrs D. Weisland and Mrs H. Yung for typing the manuscript.

The partial finacial and equipment support as obtained from the City University of New York, Mount Sinai School of Medicine, County College of Morris, National Aeronautics and Space Administration and the National Semiconductor is highly appreciated and acknowledged.

Avtar Singh

TABLE OF CONTENTS

LIST OF TABLES

LIST OF ILLUSTRATIONS

CHAPTER 1

INTRODUCTION

1.1 Rationales and Motivation

This dissertation is concerned with the signal processing involved in detecting rapid eye movements during nystagmus induced by optokinetic and vestibular stumuli. The detection must be done in the presence of noise since the most commonly used eye movement recording techniques such as electrooculography (EOG) are noisy due to muscle and skin artifacts as well as electrode noise. The problem then becomes one of distinguishing between two waveforms i.e. the slow phase and quick phase in the presence of noise. In order to derive a slow phase eye velocity response waveform, the quick phase movements must be suppressed and the resulting position waveform be differentiated. Therefore, the signal processing involves extrapolation and differentiation of noisy signals.

A second problem addressed in this dissertation is the parameter identification of a model for the generation of optokinetic nystagmus and optokinetic-after nystagmus (OKN and OKAN). In the design of signal processing and parameter identification algorithms, an important consideration in this thesis is their implementation on a small general-purpose computer.

Recent studies on nystagmus generation have uncovered basic mechanisms underlying the generation of the slow phases of nystagmus. In addition, relationships have been found relating characteristics

of slow phase eye velocity of nystagmus to head velocity and surround velocity. It has thus become important to analyze slow phases of nystagmus in pathological states to determine which parameters of the slow eye movements are modified. Parametric models for the generation of nystagmus are important, since these models lead to a better understanding of functional aspects of brain structures controlling the oculomotor system response. In addition, parameters of a slow phase system model have the potential of being used in the diagnosis procedure. The computer implementation of signal processing and parameter identification techniques is important from the point of view of real-time and on-line analysis of oculomotor system responses.

The approach taken in this dissertation for the problem described above is as follows. As a first step, a technique based upon 'Baye's likelihood ratio detector' for the detection of quick phases/saccades is developed and implemented on a computer. 'Baye's likelihood ratio detector' which minimizes the probability of detection error is used to derive a sufficient statistic, the value of which leads to assign a window of data to one of the two processes namely quick phase or a slow phase. The implementation of this technique is easier and the detector equations can be used to compute the probability of error for given noise contents and other processing errors.

The next step of signal processing involves generation of a waveform which exclusively represents the slow phase system response. This is done by subtracting the saccadic jump and piecing together

slow phases of nystagmus. The gap left by the saccadic interval is bridged by an extrapolated waveform. The error introduced by extrapolation is likely to be negligible as the saccadic intervals are far smaller than the slow phase intervals. The waveform generated in this manner represents cumulative slow phase position which when differentiated yields slow phase eye velocity. The differentiator algorithm must satisfy the conditions that it is fast enough to keep the program cycle time small and be relatively immune to noise in the signal. The least squares straight line fit to the data yields such an algorithm for the digital differentiator.

The model for the neural mechanism generating slow phases of optokinetic and optokinetic-after nystagmus has been proposed by Raphan and Cohen [8]. The signal processing scheme described in this thesis yields the waveforms needed to carry out such an identification. A least squares curve fitting technique is considered to derive model parameters. This identification technique when implemented, recursively generates the model parameters fast enough so that the leading edge of the step response is appropriately utilized.

1.2 Historical Background

There are three aspects of the problem considered in this thesis. These are detection of quick/saccadic eye movement in an eye movement record, the generation of slow phase responses, and the parameter identification of a model for the generation of slow phase response.

Despite the fact that the detection theory provides basis for dealing with many signal processing problems [38], to-date it has not

been used to process oculomotor response signals. An old analog technique due to Henriksson [16] is still very popular, since it is easy to use. This technique along with other detection and slow phase response generation methods is discussed in detail in chapter 3. The newer saccadic detection and slow phase response generation methods known as MITNYS and MITNYS-II are from a group working at MIT [2], [37]. These are computer-oriented techniques and provide a variety of signal waveforms for the understanding of oculomotor system. These techniques are reviewed in chapter 3. The detection processes in both these techniques are cumbersome and do not provide any mathematical basis for predicting their performance. A microprocessor-oriented oculomotor response analysis scheme was presented by Michaels et al [22] which is a step in the direction of portable instruments for this purpose. This technique, however, needs to be perfected to reduce the error-rate in the detection of saccades. In order to obtain eye velocity a number of differentiator algorithms are available [18], [20], [23], [34]. Most of these algorithms implement higher order transfer functions and therefore need large processing times. A simpler algorithm is needed to obtain slow phase eye velocity so that the detection and the slow phase eye velocity generation may be implemented in real-time.

In the area of parameter identification of a model for the slow phase generation in an OKN and OKAN response, work that is available is due to Raphan and Cohen [26], [8], [27]. In their work, the parameters are obtained manually and no on-line computer method has been developed to estimate parameters of the model. A number of on-line parameter identification techniques are available in the literature [17],

[6], [19], [35]. Most of these techniques apply only in cases where the input is rich enough to excite all the modes of a system. Traditionally, only the step response is available to estimate parameters of an OKN and OKAN model. Thus one must develop an on-line technique to estimate parameters from a given step response. The nonlinear structure of OKN and OKAN model has further constraints on an identification technique that can be used to yield a unique parameter set [13].

The next section outlines the dissertation organization and gives a brief description of the contents of subsequent chapters.

1.3 Organization of Dissertation

The presentation of this research effort is organized into 6 chapters described below:

Chapter 1 introduces the problem addressed and the motivation behind it. A brief historical background is given and the dissertation organization is described.

Chapter 2 is a study of essential response signals of an oculomotor system. These signals consist of periods of fixation, slow eye movements, and fast or saccadic eye movements. The laboratory techniques for the measurements of eye movements are described and evaluated. The quantitative characteristics of saccadic and slow eye movements are studied so as to formulate functional descriptions for them. Next, nystagmus along with its constituents slow and quick phase eye movements is defined. Two experimentally generated nystagmus waveforms, the vestibular nystagmus and optokinetic nystagmus are described and their

characteristics are studied. The study of properties of oculomotor control system signals is essential to the design of signal analysis algorighms and for the parameter identification of oculomotor control system models.

In chapter 3, the saccadic detection algorithm is derived based on 'Baye's likelihood ratio criterion'. The application of the detection alogorithm to an EOG waveform is discussed. In section 3.3 an expression for the probability of error is derived. The probability of error expression considers two types of detection errors - one due to the noise in signal and the other due to the finite window width which contributes to delay in the detection of on-coming movements. The detection algorithm is implemented on a PDP-8/E computer and is tested on simulated EOG-like waveforms. The chapter closes with application of the detection algorithm to real EOG waveforms that demonstrates its usefulness as a saccadic detector.

Chapter 4 describes algorithms which were developed to generate the signals related to the slow phase eye velocity. These include cumulative slow phase position (CSPP) and the slow phase velocity (SPV). The detector of chapter 3 is used to mark the beginning and the end of saccadic movements. Once saccades are detected, saccadic jump is subtracted and the slow phases are bridged together using extrapolated slow phase positions during saccades. The extrapolation and the CSPP generation algorithms are described and implemented. Next an algorithms for a simple digital differentiator based upon least squares straight line fit is described and implemented. The complete signal processing technique consisting of detection of saccades, generation of CSPP and

SPV along with input output routines is implemented on a PDP-8/E computer. Simulated EOG-like waveforms are tested to evaluate its applicability in real situations. The last section shows the performance of this scheme on real EOG waveforms and also compares the results with currently used analog technique.

In chapter 5, the parameter identification of the slow phase system of oculomotor system is considered. Practical constraints are described which influence the choice of an on-line identification technique. In this work, the identification technique is based on familiar 'least squares fit' over a finite data window which leads to simplicity in computation and works recursively to generate the model parameters. The technique is used to identify parameters of a slow phase model for optokinetic and optokinetic-after nystagmus (OKN and OKAN). The chapter ends with an evaluation of the parameter identification technique as applied to OKN and OKAN generation.

The last chapter gives a summary of research and discusses possible extensions to this work. The recommendations for future research include theoretical developments, implementation techniques and hardware realization of an instrument for automated analysis of oculomotor responses.

CHAPTER 2

THE OCULOMOTOR CONTROL SYSTEM

2.1 Introduction

The function of the oculomotor system is to move the eyes. The visual system and the vestibular system are the two primary inputs to this system. The vestibular system provides a compensatory mechanism to stabilize the environments during head movements. The visual system drives the oculomotor system to make compensatory eye movements when the visual field moves. In response to visual and vestibular stimuli all animals make combinations of two basic types of movements; quick or saccadic movements and slow or smooth pursuit movements. Saccades shift the gaze of the eye from one point to another and have peak velocities up to 600°/sec. in man and 1000°/sec. in monkey [30]. The rapid movements bring an image from the periphery of the retina to the forvea, the high resolution region of the retina which is in the center of the visual field. Smooth pursuit movements are continuous movements of the eye and can be elicited when a target moves smoothly over the retina. These movements are generally slower than the saccadic movements; their velocities usually being less than 45°/sec. in man [31] and 90°/sec. in monkey [8].

Nystagmus is a combination of the saccadic and the slow phase eye movements. It consists of slow phases interspersed with rapid movements in the opposite direction. Nystagmus can be induced by stimulation of either the vestibular system by head turning or the

visual system when the environment turns. These stimuli induce vestibular nystagmus and optokinetic nystagmus (OKN) respectively. Perception of visual information occurs during the slow phases.

This chapter will review how eye movements are measured (sec. 2.2) to define the properties of the signals (sec. 2.3) that will be used to identify and separate saccades from nystagmus. After the saccades have been removed, the slow phase velocity of the resulting waveform will be used to automatically identify a model for optokinetic nystagmus and optokinetic after-nystagmus (Raphan et al, 1979, Cohen et al, 1977).

2.2 Eye Movement Measurement Methods

The three most widely used methods for measuring eye movements are the corneal reflection, contact lens and electrooculography (EOG). All of these eye movement measuring techniques generate voltage proportional to eye position differing in sensitivity and in the range of the eye movements being measured. This section reviews these measurement techniques with particular emphasis on the EOG measurement technique since it is a common technique used in animal and human studies. A review of these and other techniques can be found in [42].

2.2.1 Corneal Reflection Method

A beam of light is reflected from the surface of the cornea to form a bright spot on a screen. The angle of reflected light depends upon the angle between the incident light and the normal to the reflecting (corneal) surface. The normal to the cornea changes as the eye

rotates during a movement resulting in a corresponding movement of the spot. The reflected beam is photographed on a moving film to produce an eye movement record.

The corneal reflection method is suitable for untrained subjects, since it does not interfere with normal eye movements. The limitations of this method are: first, the linear range of the method is restricted to about ± 12.5° [42] due to nonspherical corneal surface; second, lateral head movements affect the measurements to a great extent. For instance a lateral displacement of 0.1 mm. introduces an error of about 1° in the measured eye position [41].

2.2.2 Contact Lens Methods

Contact lens methods involve fitting special lenses over the cornea. A small plane mirror mounted on the lens reflects the image of a light source. The reflected image is then photographed on a moving film to obtain a record of the eye movements. A modified method involves placing a small lamp at the end of a short aluminum tube attached to the contact lens. As the eye moves, the amount of light passing through two knife edges and falling on the sensitive surface of a photomultiplier, changes. The output voltage variations indicate the variation in eye position.

A nonoptical contact lens measuring method was introduced by Robinson [29]. Two small thin wire coils, oriented orthogonal to each other and embedded in the contact lens, pick up an induced voltage from two large orthogonal electromagnetic coils surrounding the head. The induced voltage in each coil varies with the sine of the angle of gage relative to the magnetic field. Fuchs and Robinson [12] modified the

coil method for animal study by implanting the coil of wire on the globe under the insertion of extraocular recti muscles. This method measures both vertical and horizontal movements simultaneously, has a sensitivity of .25° and can measure very large movements.

The contact lens methods are the most sensitive eye movement measurement methods and yield good records of miniature eye movements down to 5 seconds of arc [42]. The accurate range of such methods is limited to about 5°, since the lens slippage becomes important for larger eye movements. The other disadvantage of these methods is the necessity of placing a foreign object on the eye and thereby interfering with normal eye movements. The fitting of contact lenses is an exacting task and can't be used on all subjects. To avoid lens slippage, it has to fit tightly which causes discomfort. The contact lens methods are the most appropriate for the precise measurements of eye movements less than 1°.

2.3.3 Electrooculography (EOG)

The position of the eye can be measured by placing electrodes around the eye and recording potential differences. There exists a standing potential between the cornea and the retina, setting up an electrostatic field which rotates with the eye. The cornea is approximately 1mV positive with respect to the retina. The potential difference detected by a pair of electrodes placed lateral to an eye is zero with the gaze directed forward and varies sinusoidally when the eye moves to the left or to the right. Similar potential difference can be detected by the electrodes placed above and below the eye when the eye moves vertically. the voltage versus gaze angle relationship is approximately

linear for eye movements less than 40°, since the difference between sinθ and θ is less than 10% for such movements. The recorded voltage falls in the range of 15-200uV with approximate sensitivity of 4uV/degree of movement [42].

The small potential difference corresponding to eye movement must be amplified by a DC amplifier in order to determine the eye position. The problem of drift in electrodes and DC amplifiers makes these recordings very difficult. Recent advances in skin electrodes such as silver-silver chloride electrodes coupled with high input impedance preamplifiers have eased the problem of drift. The electromagnetic pick ups can be reduced by using a high common-mode rejection ratio preamplifier close to the head, grounding through an ear electrode and using shielded cables. Fig. 2.1 shows the placement of electrodes when both horizontal and vertical recordings are performed. Conjugate horizontal eye movements are recorded between the electrodes at the outer canthi of the eyes. Separate recording of the horizontal movements of each eye can be performed by placing a third electrode over the bridge of the nose. The vertical eye movements are recorded from a set of 4-electrodes, the upper two and the lower two being tied together to reduce the coupling between horizontal and vertical movements. Surface electrodes are used for humans but suffer from problems such as muscle artifacts and drift.

The use of implanted, silver-silver chloride electrodes for animal recording [7] removes some of the problems with surface electrodes. These electrodes are permanently placed in holes in the bony orbit. The use of fine platinum needle electrodes in the skin around the orbit is also used for animal recording [42].

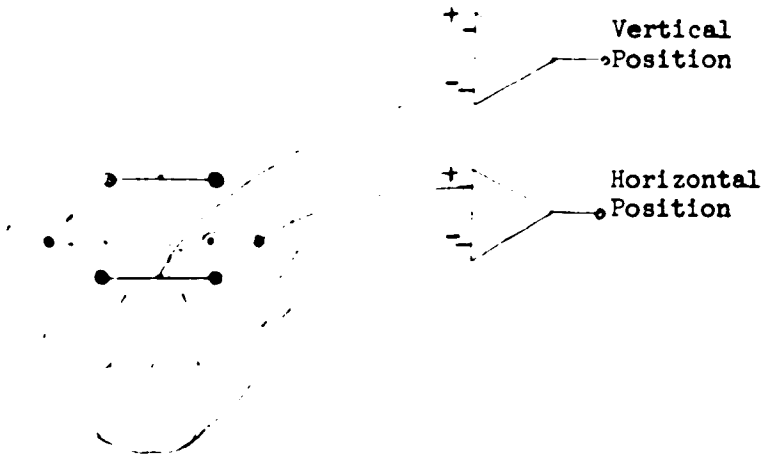

Fig. 2.1 Placement of skin electrodes in humans for the measurement of vertical and horizontal positions by electrooculography (From Young and Sheena [42])

The corneoretinal potential, the basis of EOG, tends to change with environmental and experimental changes, thereby affecting EOG gain. This may require frequent calibration to offset such changes [42].

Despite its limitations, electrooculography is a commonly used method to record eye position since it is easy to use especially for humans, has a wide range of eye movements that can be measured and has practically a linear relation for commonly occurring eye movements. Recordings using electrooculography are accurate to within 2° of eye movements [42] and therefore are suitable for measuring movements in the range of 5-50°. EOG is the technique used to obtain eye movement records analyzed in chapters 3, 4 and 5.

A detailed study of the properties of EOG noise has not been carried out. This is due to the many factors which contribute to the noise variations such as physiological changes, environmental changes and the specific instrumentation used in filtering, amplifying and recording signals. In order to facilitate the analysis in chapter 3, the noise in EOG will be assumed to be gaussian. Based on this assumption, a sufficient statistics is derived for the detection of rapid and slow eye movements. Other kinds of noise statistics should give different sufficient statistics and could be investigated as an extension of this thesis.

2.3 Properties of Eye Movements

The temporal characteristics distinguishing the two kinds of eye movements (the rapid and the slow movements) must be considered in the design of a technique for their separation. In this section, these

characteristics are studied. This leads to the formulation of a criterion for the detection of saccades in a record of eye movements.

2.3.1 Properties of Saccadic Eye Movements

Saccades are the rapid jumps by which we voluntarily divert our eyes from one fixation point to another. These are generally conjugate movements, i.e. both eyes move simultaneously in the same direction. Fig. 2.2A shows an electrooculogram (EOG) record of saccadic eye movements performed by a monkey looking around in an environment with no moving objects. When a monkey is presented with a random change in target position, his response typically starts after about 240msec [11]. The eye accelerates to a maximum speed, which is reached about midway in the total trajectory, and then decelerates to a stop (Fig. 2.2B). In response to target displacements greater than 25°, the eye often falls short of the target with its initial saccade, requiring a second saccade within about 250msec to correct the remaining error [11]. The duration of a saccadic eye movement depends upon its size and it is about 25msec for a saccade of 10°. The maximum velocity during a saccadic eye movement can be as high as 1000°/sec and depends upon the size of the saccade. The relations between the magnitude, duration and maximum eye velocity are shown in Fig. 2.3 (taken from Fuchs, 1967). The maximum saccadic velocity increases nonlinearly with the saccadic magnitude whereas the saccadic duration is approximately linearly related to the saccadic magnitude. The temporal (abduction) saccades have been found to be slightly slower than the nasal saccades. Duration vs magnitude plot has an approximate slope of 1msec/deg. for horizontal saccades.

Fig. 2.2. A. Horizontal saccadic eye movements of a monkey looking about the laboratory with no moving objects. B. Velocity corresponding to the eye movements in A. C. Time.

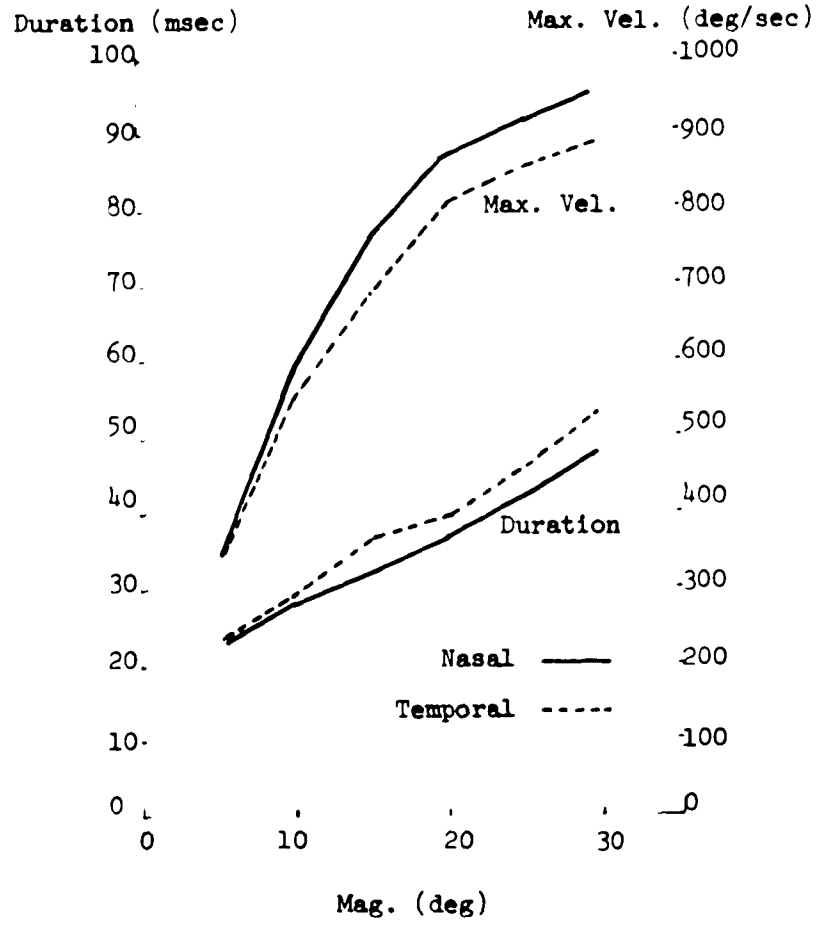

Fig. 2.3. Duration and maximum velocity of horizontal saccades of a monkey (taken from Fuchs [11])

Vertical saccadic response is qualitatively similar to the horizontal. Vertical saccades have an average latency of 235msec and duration vs magnitude plot is characterized by an approximate slope of 1.35msec/deg. [11].

The saccadic movements of a monkey are not qualitatively different from those of man. Monkeys execute their saccades more rapidly than humans. The duration vs magnitude and maximum velocity vs magnitude plots for the two primates are compared in Fig. 2.4. As is apparent from these plots, humans perform a 30° saccade in about double the time than monkeys. The maximum velocity reached in monkeys is about 400°/sec faster than in humans. The saccadic latency both in man and monkey has been reported to be the same [11]. The human saccades were analyzed by Baloh et at [5] and Bahill et al [3]. Quantitative analysis as done by Baloh et al [5] indicates that saccadic duration and amplitude are linearly related with a mean slope of 2.7sec/°, whereas amplitude and velocity have a nonlinear relationship that is best fit by an exponential equation of the form

$$EV = K\,(1 - \exp\,[-A/L])$$

where EV = eye velocity, A = saccade amplitude, K = 551 $\pm$ 65°/sec and L = 14.0 $\pm$ 1.7°.

The mathematical characterization of saccades is an important first step for detecting them in an eye movement record. The time behavior (position vs time) of saccades will be used in chapter 3 to design a technique for their detection and then their removal to study the slow eye movement characteristics. Since saccades occur in conjunction with slow eye movements, the properties of the slow eye movements are reviewed in the next section.

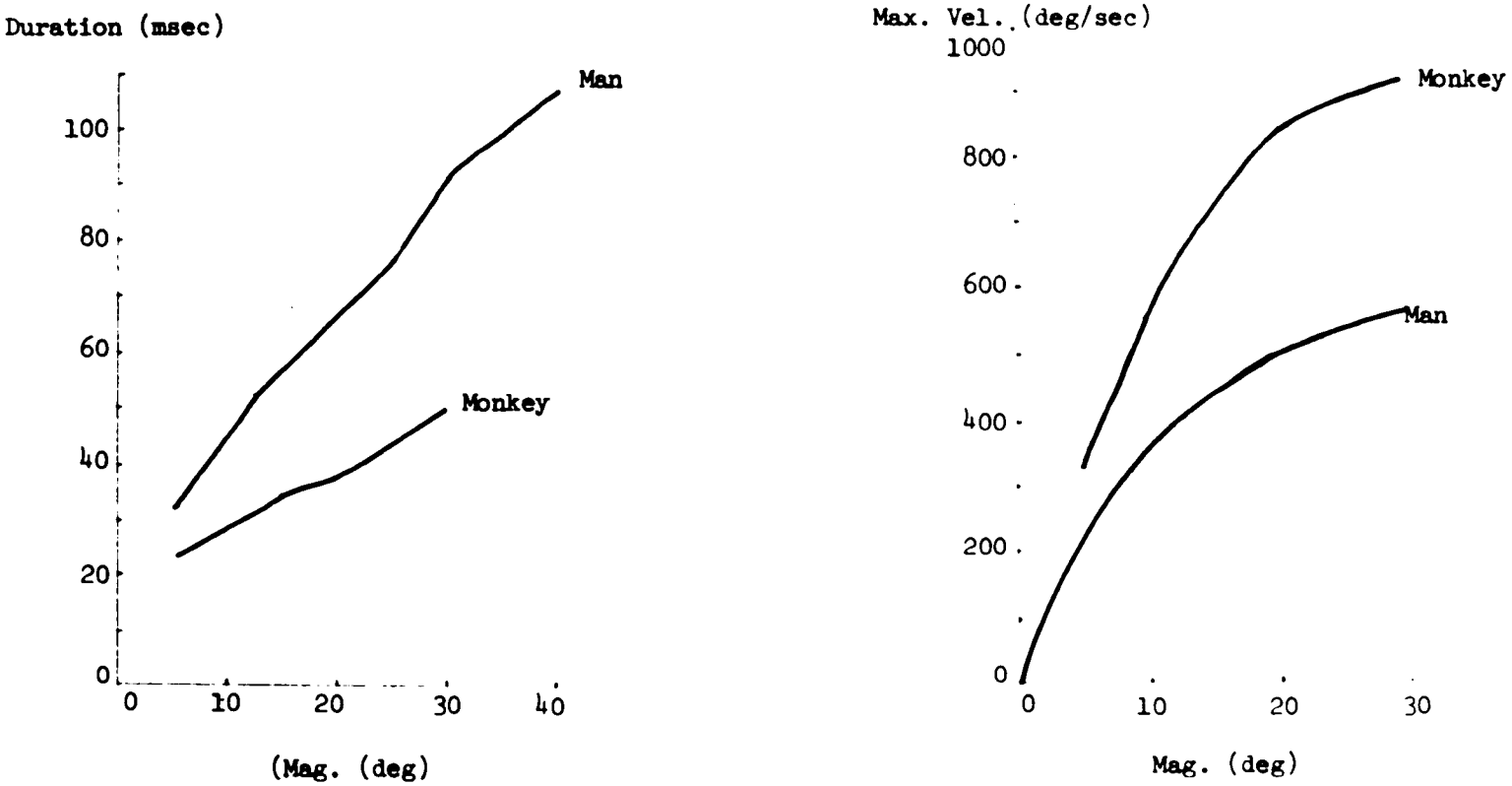

Fig. 2.4. Comparison of monkey and human saccadic eye movements (taken from Fuchs [11])

2.3.2 Slow Eye Movements

The eye performs slow tracking conjugate movements while following a slowly moving target or while compensating for movements of head or trunk. The function of compensatory and tracking eye movements is to stabilize the retinal image of an object during relative motion between the head and the object. These movements are characterized by low velocities relative to saccades and are presumed to be generated by different neuronal structure in the central nervous system (Raphan and Cohen, [25]). Fig. 2.5 shows a record of smooth pursuit eye movements of a monkey in response to moving objects in its field. It may be noted from Fig. 2.5 that the pure pursuit movements are difficult to excite; they are generally made in conjunction with saccades.

The characteristics of slow eye movements in man were studied by Robinson [31] and in monkey by Fuch [11]. Qualitatively the two primates perform similar smooth pursuit movements and are believed to possess similar mechanisms for their generation. Quantitatively, a monkey can attain a smooth pursuit velocity which is twice as fast as that of man. Fig. 2.6 shows the response of a monkey to ramp inputs from 10°/s to 40°/s. The response consists of a smooth component and a saccadic component. The latency in response varies with the target velocity and is approximately 174 msec for a 10°/s target velocity which is about 50msec more than in humans as reported by Robinson [31]. The saccadic component appears after about 250msec and the size of the saccade increases with the target velocity. After the saccade, the pursuit eye movement follows the target at its velocity for target velocities up to 25°/s. For higher target velocities, that is

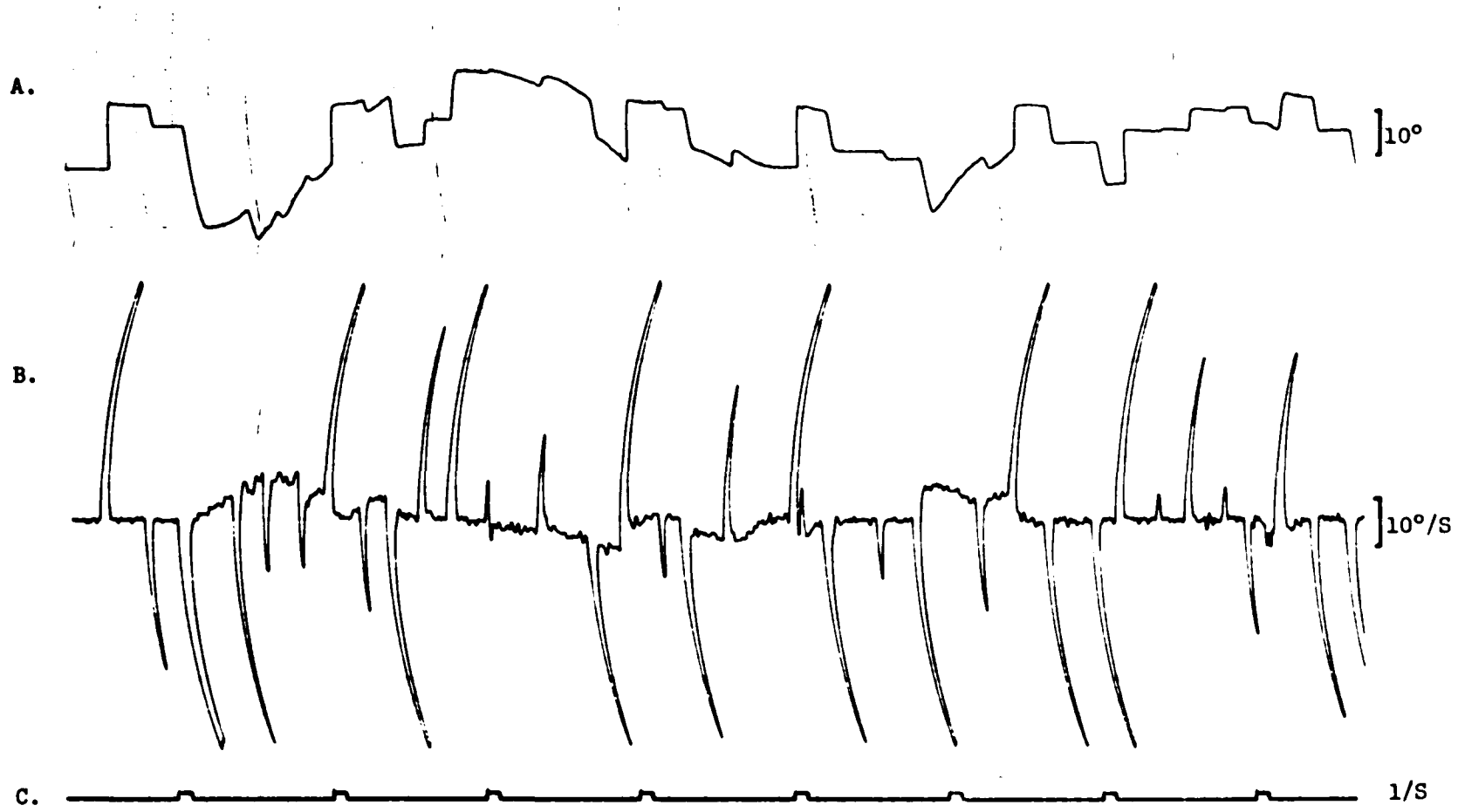

Fig. 2.5. A. Smooth pursuit eye movements of a monkey induced by moving objects in its environments. B. Velocity associated with the eye movements in A. C. Time

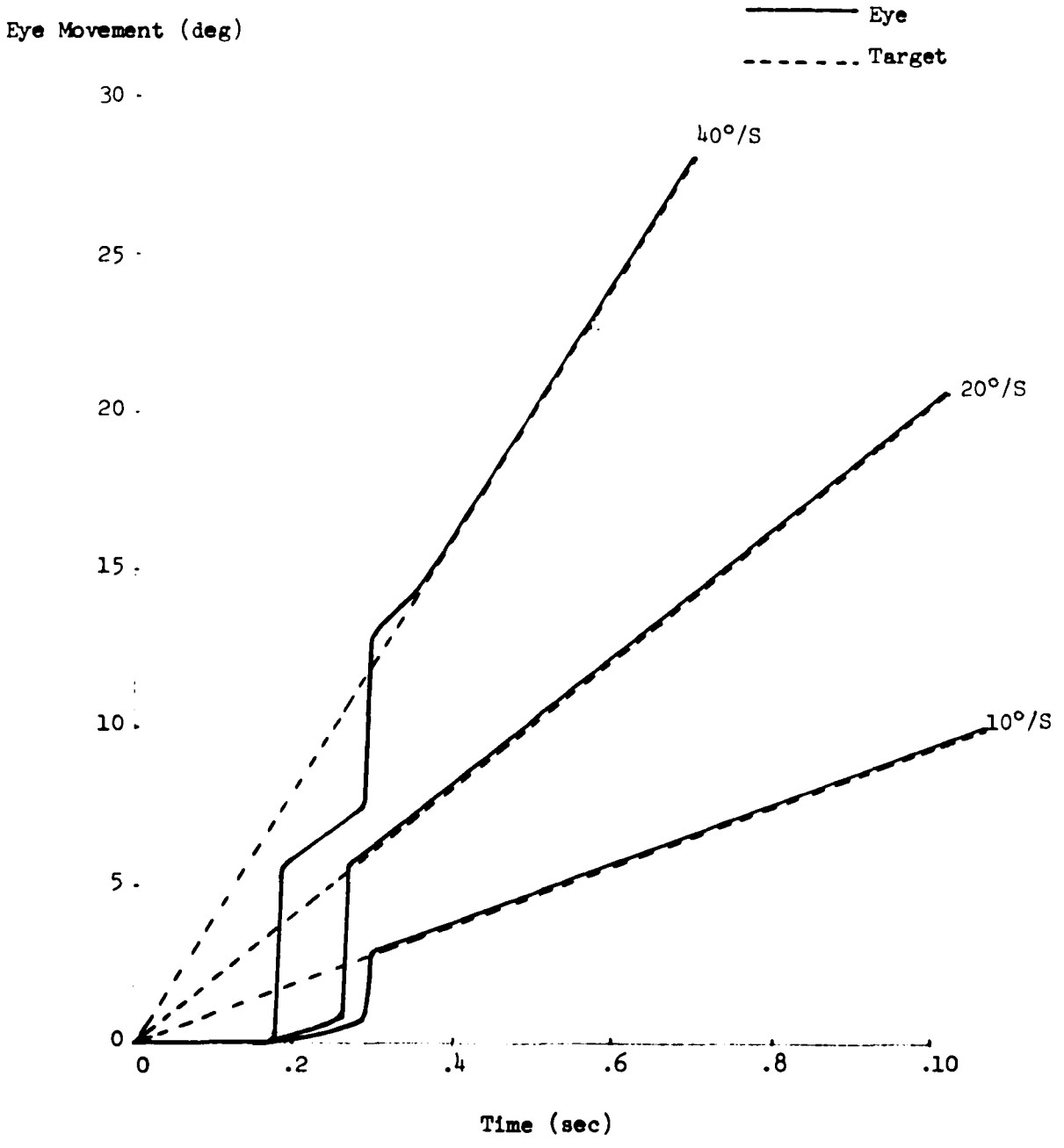

Fig. 2.6. Eye movement response of a monkey to target ramps (taken from Fuchs [11]).

velocities greater than 25°/s, the monkey displays many combinations of saccades and smooth pursuit movements. For instance to catch a target moving at 40°/s, the monkey makes two saccades (see Fig. 2.6). The second saccade is made either after about 250msec or earlier. The earlier saccades are generally accompanied by a small overshoot. Monkeys are capable of following target velocities up to about 90°/s [25] which is about twice the velocity that humans can turn their eyes to follow a ramp stimulus.

That the smooth component of the ramp response is elicited by the target velocity and not its position was demonstrated by Rashbash [28]. He presented a monkey with a step-ramp trajectory by first moving the target in one direction followed by a constant velocity in the opposite direction, after a delay, the response exhibits a smooth component which moves the eyes away from the target but in the direction of target motion. After one saccadic latency, the eye catches the target by performing a saccade in the opposite direction which shows the sample-data system nature of saccadic system.

The velocity attained by the eye during smooth pursuit movements is an important diagnostic tool [4] for brainstem dysfunction. In general, the smooth pursuit velocity decreases in patients having brainstem diseases [4]. The computation of smooth pursuit velocity from EOG records becomes a difficult task since the pursuit movements always have interspersed saccadic movements. One of the objects of this dissertation is to obtain pursuit eye velocity after removing saccadic movements from an EOG record.

The position vs time characteristics of slow eye movements are

required to design a detection scheme for saccadic movement. The performance of the detection scheme discussed in chapter 3 is a function of how accurately such characteristics are available.

2.4 Nystagmus

A class of eye movements of an oscillatory or unstable nature are known as nystagmus. The most common types of nystagmus are vestibular and optokinetic nystagmus. Vestibular nystagmus occurs when a subject undergoes angular acceleration, and consists of slow compensatory eye movements opposite to the acceleration and fast movements for resetting the eyes. Optokinetic nystagmus occurs whenever a nonhomogeneous visual field is moved past an observer; the eyes move conjugately with the field, as with normal pursuit movements, and then rapidly return to a central position so as to continue to follow the motion of the visual field. The optokinetic nystagmus characteristics are described in section 2.4.1 and in many respects are similar to the characteristics of vestibular nystagmus described in section 2.4.2. A nystagmus waveform is shown in Fig. 2.7. There are two components which characterize a nystagmus waveform, first, a component having a smaller eye velocity which is called the slow phase of nystagmus and second, a component with larger eye velocity and this component is called a quick or fast phase of nystagmus. The velocity characteristics of the slow and quick phases of a nystagmus resemble those of pursuit and saccadic eye movements respectively. The velocity waveform can be obtained by differentiating the nystagmus waveform. The quick phases are of much shorter duration and of higher

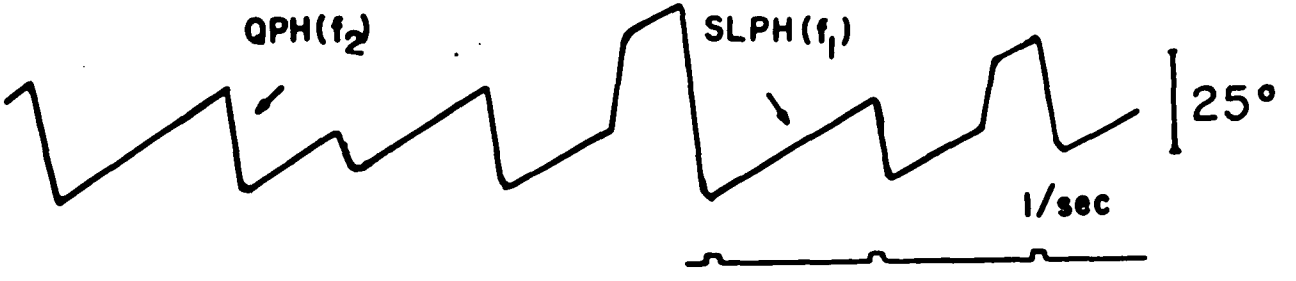

Fig. 2.7. A time-expanded view of a nystagmus waveform. The quick phase (QPH) and the slow phase (SLPH) movements can be described by functions f_2 and f_1 respectively. Note the relative durations and velocities associated with these eye movements.

eye velocities as compared to slow phases. Due to the shorter duration of a quick phase, the slow phase eye velocity just before and just after a quick phase is essentially the same. This fact will be used in chapter 4 to obtain slow phase eye velocity waveforms from EOG waveforms.

Thus, in both monkey and man, saccades and quick phases are approximately 2 to 3 times faster than normal slow phases or pursuit eye movements. It is these characteristics which will enable us to derive functional templates representations for these signals and derive a criterion for their separation.

The following sections describe the properties of Optokinetic nystagmus (OKN), optokinetic after-nystagmus (OKAN) and vestibular nystagmus. The waveforms are used as inputs to the detection program and to estimate parameters of the OKN and OKAN model.

2.4.1 Optokinetic Nystagmus and Optokinetic After-Nystagmus Characteristics

Optokinetic nystagmus (OKN) is the nystagmus induced by continuous movement of the visual field, and it lasts as long as the stimulus continues. When the stimulus is terminated, if the animal is in darkness, there is a persistent after-reponse, known as optokinetic after-nystagmus (OKAN). The significance of OKN is that it stabilizes the retinal image of a moving environment by matching eye velocity to the stimulus velocity. OKAN is a motor response to a prolonged central excitatory state which is produced simply by viewing a moving visual field. Both these responses characterize the slow phase sybsystem of the oculomotor system and are fundamental to modeling of this system.

Velocity characteristics of OKN and OKAN induced by constant velocity fill field rotation were studies by Cohen et al [8] and Raphan et al [27]. In their studies, OKN was induced by an internally lit, servo-controlled, rotating drum 90 cm in diameter and 60 cm high. It surrounded the monkey and filled the field of vision. The drum wall was made of opalescent white plastic with 3° black stripes at 45°. A mirror was placed under the monkey's chin to reflect stripes on the roof of the visual field. Such a stimulation is known as full field rotation, since not only the stripes but the textured background also contributes to the response. Electrooculography (EOG) was used to record eye movements. The EOG was differentiated and rectified to obtain the velocity of slow phases of nystagmus. The velocity characteristics of OKN and OKAN are summarized as follows:

1. Slow phase velocity of OKN in response to a step in stimulus velocity is composed of two components, a rapid rise, followed by a slower rise to a steady state value. A typical response to a stimulus velocity of 45°/sec is shown in Fig. 2.8. For stimulus velocities up to 90°/sec, the rapid rise is found to be about 60% of the final steady state eye velocity. The slower rise has a time constant in the range of 2.6 to 3.3 sec. The steady-state velocity has a gain of 1 to about 180°/sec stimulus. This gain drops with increased stimulus velocity and saturates at about 240°/sec in monkeys. The saturation velocity in the monkey is 2-3 times as great as in humans.

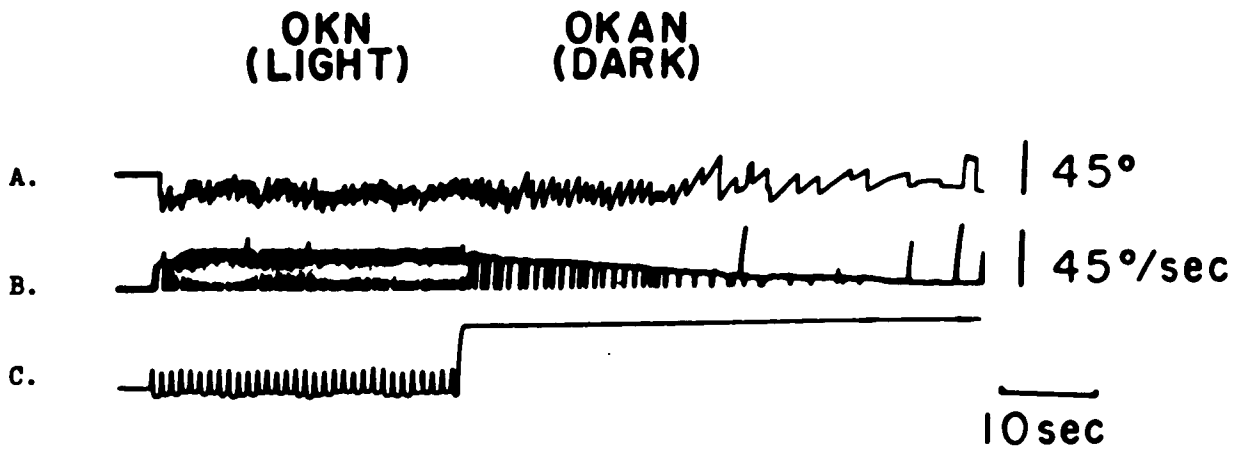

Fig. 2.8. A. The horizontal EOG during optokinetic and optokinetic-after-nystagmus of a monkey subjected to full field visual stimulation.

B. The eye velocity associated with the nystagmus in A.

C. The visual stimulus for the generation of OKN and OKAN.

2. At the onset of OKAN, slow phase velocity falls by about 10-20%, followed by a slower decline to zero. Peak OKAN velocities are linearly related to optokinetic stimulus velocities up to 90-120°/sec. Above 120°/sec OKAN slow phase velocity saturates. The optokinetic stimulus duration is important to the generation of OKAN, since if OKAN is initiated before reaching the steady state for OKN, the drop in the slow phase velocity is considerably larger than 10-20%. In other words, the system generating OKAN charges to its full value in about the same time that the OKN attains its steady state. The time constant for the slow decline ranges from 10 to 25 seconds and seems to depend upon the stimulus velocity; furthermore, it can be different for rightward and leftward beating nystagmus. Extended visual fixation (lights on) discharges the activity responsible for producing OKAN. Short fixations cause only partial discharge of OKAN mechanism. Following brief fixations, OKAN resumes but with decreased slow phase velocity.

A model which closely predicts the dominant characteristics of OKN and OKAN in normal monkeys was developed by Raphan (Cohen et al, 1977, Raphan et al, 1979). However, to relate the model parameters to pathological states associated with vestibular system lesions, automatic parameter identification techniques must be developed. This is the subject of chapter 5.

2.4.2 Vestibular Nystagmus Characteristics

Vestibular nystagmus is induced by head rotation. It is also a combination of rapid and slow eye movements whose relationship to stimulus velocity has been quantitatively described and modelled (Raphan et al, 1979). The relationship between stimulus velocity and peak eye velocity (of slow phases) during per and post-rotatory nystagmus is linear up to 240°/sec with a slope close to one. The per-rotatory nystagmus is the animal's response during rotation in darkness and the post-rotatory nystagmus is the response of the animal after the rotation is stopped. A typical vestibular nystagmus and the corresponding slow phase velocity response are shown in Fig. 2.9. The transient characteristics of vestibular nystagmus can be summarized as follows:

1. At the onset of stimulation slow phase velocity rises abruptly, peak velocity is maintained for several seconds and then it declines to zero with a dominant time constant of 15-28 sec. For higher stimulus velocities, peak velocity is held for a shorter time and the decline in slow phase velocity is more rapid.
2. The post-rotatory nystagmus slow phase velocity is set to zero after per-rotatory nystagmus has entirely disappeared, the characteristics of the per and post-rotatory nystagmus are approximately similar with opposite velocity sign.

The slow phase velocity characteristics of nystagmus are used in mathematical modeling of the neuronal structures responsible for their production. Such models are considered in chapter 5.

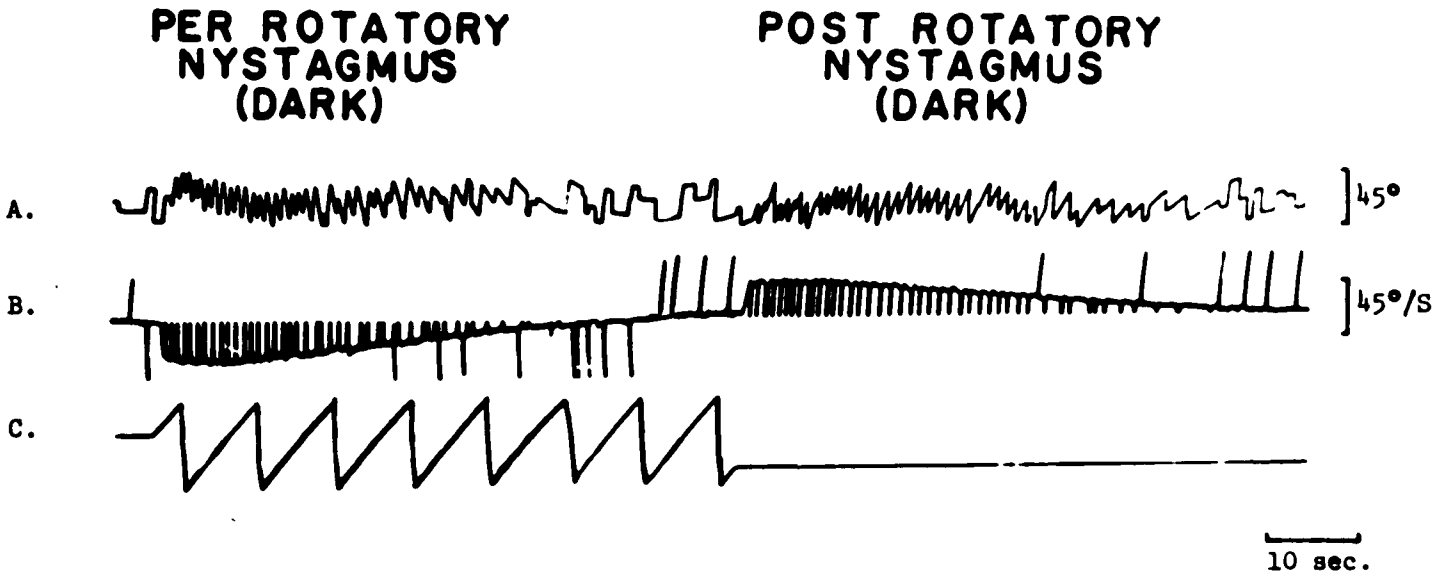

Fig. 2.9. A. The horizontal EOG during a per and post rotatory nystagmus.

B. The eye velocity associated with the nystagmus waveform in A.

C. The vestibular input to generate the vestibular nystagmus in A.

CHAPTER 3

AN ON-LINE SACCADE DETECTION PROGRAM

3.1 Introduction

Eye movement records in the form of electrooculographs (EOG) are analyzed [22] to extract diagnostically important information such as the relationships between the slow eye velocity characteristics and head velocity and surround velocity. Another important purpose of this analysis is to understand the brain mechanism responsible for generating various types of eye movements. The information usually needed includes time, duration and frequency of occurrence of quick phases and the velocity associated with slow phase eye movements.

Analog differentiators have been used and are still being used to detect quick phases in an EOG record [16]. However, an analog differentiating scheme introduces delay and performs poorly when operating on noisy data (see next chapter, section 4.2.2). For these reasons, in recent years, several researchers have developed computer programs to process EOG waveform on-line and generate the required information [37] [2]. These techniques involve cumbersome algorithms for the detection of quick phases and therefore are inappropriate for microprocessor implementation. A more recent technique based upon an acceleration sensitive detector [22] seems to be a step in the direction of dedicated portable instruments for the analysis of nystagmus. This technique is basically an implementation of a differentiating type digital filter and therefore is noise sensitive and has high detection errors [22]. Thus,

there is a need of a detection scheme which should be relatively immune to noise and implementable at microprocessor level to design portable diagnostic instruments.

The new technique presented in this chapter is based upon a 'likelihood ratio detector' [38]. A decision function is computed, the value of which reflects to the origin of the data used to compute it, i.e., whether the sample taken belongs to a slow phase or a quick phase. Once a quick phase is detected it can be suppressed to generate slow phase waveform. The technique to generate slow phase waveform is discussed in the next chapter. The detection technique is mathematically simple and is implementable using a microprocessor for on-line processing of EOG records.

Since a central problem to be treated is the on-line detection of quick phases, we first review the existing analysis techniques from this view point in section 3.2 and then the new technique is presented in section 3.3. The performance of the 'likelihood ratio detector technique' is studied in section 3.4 by computer simulations and by on-line processing of experimentally obtained eye movement records. This technique will be utilized in the next chapter to generate some diagnostically important waveforms, such as the slow phase velocity and the cumulative slow phase position waveforms.

3.2 The Current Status of Saccade Detection Methods

There has been appreciable interest in the processing of EOG waveform so that the nystagmus parameters could be used to understand the oculomotor control system and relate eye movement disorders to the

neuronal activity. The complication in the analysis procedures arises due to the presence of quick phases whose occurrence is random in both magnitude and time. Another problem arises due to the fact that one of the requirements of analysis [2] is to generate slow phase eye velocity which involves differentiation in noisy environments. Thus the techniques of analysis developed so far differ in the manner in which the quick phases are detected or in the manner in which the slow phases are differentiated to generate slow phase eye movement velocity.

The first on-line technique is due to Henriksson [16]. This technique is shown in Fig. 3.1 and involves differentiating the EOG waveform using an analog differentiator of the form S/(S+K). The differentiated waveform is passed through a positive or a negative halfwave rectifier to extract positive or negative slow phase velocities respectively. Fig. 3.2 shows the results of processing an EOG waveform by Henriksson's method. The quick phases are indicated by large magnitude jumps and the rest of the waveform is that of slow phase velocity. This method though limited in information is used due to easier implementation. The analog differentiator used in the analysis introduces considerable time delay and therefore renders this method inappropriate for further on-line work.

The first attempt to use a computer for the process of on-line nystagmus analysis was made at MIT by Tole and Young [37]. They developed a hybrid technique : MITNYS, for on-line analysis of nystagmus. The algorithm used to detect quick phases depended upon the relative magnitude and the sign of the velocity associated with EOG waveform. The forward quick phases were detected due to the change in velocity magnitude and the reverse quick phases were detected due to the change in velocity sign or both. This technique had a number of limitations [2]

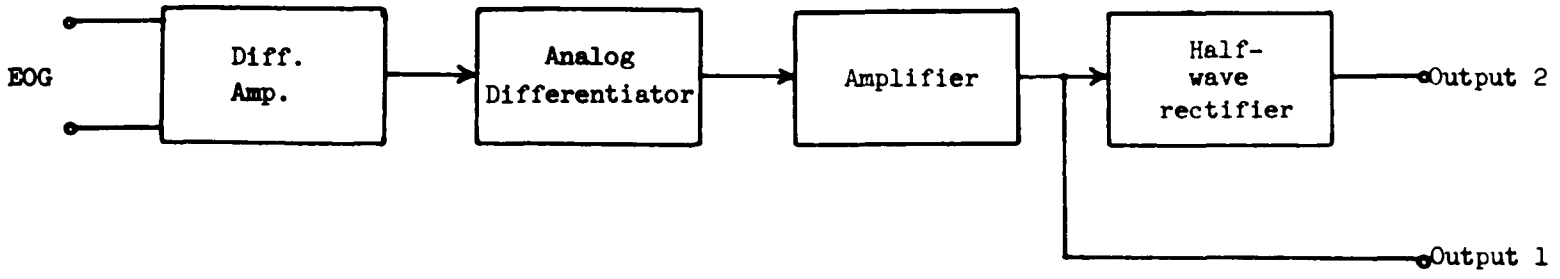

Fig. 3.1. Block diagram of Henriksson's method of EOG record analysis

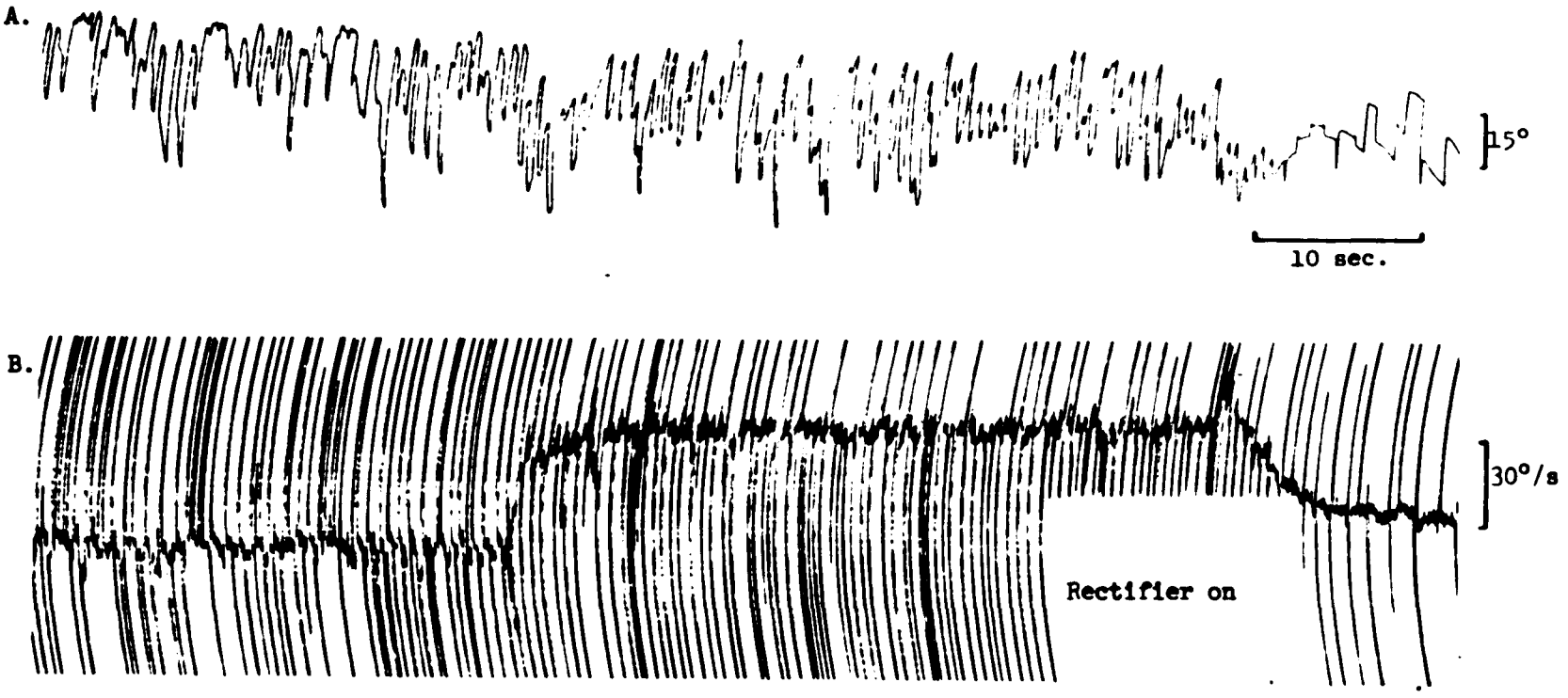

Fig. 3.2 A. EOG waveform. B. Differentiated EOG waveform. Note that the spikes in the differentiated waveform indicate saccades and trend of the waveform indicates slow phase eye velocity.

including high error rate in quick phase detection and limited stimulus frequency bandwidth. Low pass analog filters of the form K/S+τ) were used to smooth differentiator noise. The time constant 'τ' of these filters ran in seconds and therefore the technique was incapable of reproducing faithfully the transitions in EOG velocity.

Some of the problems of MITNYS were overcome by MITNYS-II, an all-digital program developed by Alum, Tole and Weiss [2]. Their technique of saccade detection involved three tests i.e., velocity test, slope-sense test and the minimum velocity test were used to mark quick (fast) phases. If the eye velocity magnitude as calculated by subtracting two successive eye position samples exceeded the estimated fast phase velocity (FPV), the fast phase was said to have occurred. FPV was estimated using fast phase estimator which was developed after studying the relation between slow phase velocity (SPV) obtained from a 33 point digital differentiator operating upon pieced together slow phase segments of eye position called cumulative slow phase position, and the FPV. The slope sense test involved estimating the SPV sign. The SPV sign was taken to be that of the slow phase velocity averaged over 9 samples ($\overline{SPV}$) provided the SPV was greater than $3^\circ/s$. If SPV was $< 3^\circ/s$, the sign of slow phase velocity averaged over 80 samples (Ave SPV) was used as the estimate of SPV sign. In both cases |Ave SPV| must be $> 2^\circ/s$ and |SPV| $< 3^\circ/s$ for more than 0.3 seconds. If SPV criterion was not met, the test was not used. Estimated sign of SPV thus obtained was compared to the eye velocity sign provided the eye velocity was $> 30^\circ/s$ and unequal signs indicated a fast phase. In the event the minimum SPV criterion was met, FPV was assumed to be at $20^\circ/s$ and the minimum velocity test was applied. The

minimum velocity test involved using three successive eye positions and computing two successive velocities. If the magnitude of both of these velocities exceeded 20°/s, a fast phase was indicated. In the event two successive velocities of opposite signs were detected, the test was ignored. MITNYS-II though useful is simply too complex to be implemented at the microprocessor level [22]. Secondly the program uses so much smoothing that it is suitable only for very slow running nystagmus and is not capable of reproducing sharp transitions in the slow phase velocity.

The most recent technique of analysis has been developed by Michaels and Tole [22]. It involves convolving the EOG waveform with a finite impulse response digital filter of the type:

$$d(k) = -x(k-4) - x(k-3) + x(k-1) + 2x(k) + x(k+1) - x(k+3) - x(k+4)$$

where d(k) is the output of the filter and x(k) is the input. The important characteristic of this digital filter is its sensitivity to acceleration. The output after convolution contains peaks corresponding to quick phases and therefore can be detected using a threshold detector. This technique is simple and microprocessor implementable, but suffers from a high percentage of errors in quick phase detection. This technique when applied to EOG samples taken 16.7 ms apart on a filtered waveform which ensures high filter gain and reliable detection, still has an error of 3% in saccade detection [22]. These results were obtained by using the technique in conjunction with a spike elimination routine, because the filter itself is very sensitive to these spikes and produces false detections. In spite of its limitations this technique is a step in the direction of portable instruments for nystagmus analysis.

3.3 Likelihood Ratio Detector

Consider received data which has been produced by one of two subprocesses of a system. The outputs of these subprocesses are denoted by $f_1(t)$ and $f_2(t)$. Let the corresponding hypotheses be denoted by H_1 and H_2 respectively, i.e. H_j denotes the hypothesis that the data is produced by subprocess $f_j(t)$; $j = 1,2$. For the analysis of nystagmus waveforms, $f_1(t)$ will denote the slow phase subsystem response and $f_2(t)$ the response of the quick phase generating subsystem.

The received data is scaled before processing. The scaling is done with respect to the first sample in the window of samples considered before making a decision. The scaled samples then are used to compute a scalar function called 'decision function'. The value of the 'decision function' leads to the assignment of the latest sample to either $f_1(t)$ or $f_2(t)$. The 'decision function' evolves from the process of minimizing a probability of error, based upon the window of samples.

The input being noisy, there is a finite probability of error associated with each decision. Another kind of error which occurs during transitions from $f_1(t)$ to $f_2(t)$ or vice versa, arises since the decision concerning the latest sample is based upon all the samples in a window. A window comprising a large number of samples can reduce the probability of error when the decision is based on all the received samples, but a large window introduces detection delay during transitions. These are the topics considered in sections 3.3.3 and 3.3.4.

The theoretical background is based upon the Bayes likelihood ratio test [38]. In section 3.3.1 we consider 'the decision rule' for the detection process. The application of 'the decision rule' to EOG waveform analysis is considered in section 3.3.2 followed by the derivation

of the probability-of-error equation in section 3.3.3. The results of these sections are applied to a simulated EOG waveform in section 3.3.4. In section 3.4 laboratory results are presented for various types of simulated waveforms and experimentally obtained nystagmus waveforms.

3.3.1 The Decision Rule

In this section, the Bayes likelihood ratio test is used to derive an inequality which can be used to assign received data samples to one of two possible processes. The decision rule is optimum in the sense that the probability of error is minimized. A moving window of N samples is used to arrive at a decision. The fact that the received samples are noise contaminated is the motivation for using a window of samples to smooth out the effect of noise. Let N data samples be denoted by a vector R and the outputs of two processes by vectors F_1 and F_2, i.e.

$$R = [r(1) \quad r(2) \quad r(3) \text{ ---------- } r(N)]'$$

$$F_j = [f_j(1) \quad f_j(2) \quad f_j(3) \text{---------- } f_j(N)]' \; ; \; j = 1,2$$

where

$$r(i) = f_j(i)+n(i) \text{ for } i = 1,2,3\text{----}N \text{ and } j = 1,2 \qquad (3.3.1)$$

n(i) being the noise component of the received sample r(i). Equation (3.3.1) assumes all samples come from either F_1 or F_2. The noise samples n(i) are assumed to be zero mean Gaussian with variance σ_n^2. In other words, the probability density function of n(i) is given by

$$p_n(n(i)) = \frac{1}{\sqrt{2\pi}\,\sigma_n} \exp\left(-n(i)^2/2\sigma_n^2\right) \qquad (3.3.2)$$

Let H_j be used to denote the hypothesis that the received data R is due to F_j ; j = 1,2. The conditional probability density functions over the entire window, in the case of independent noise samples are given by

$$p(R/H_1) = \prod_{i=1}^{N} p(r(i)\,|\,f_1(i)) \tag{3.3.3}$$

and

$$p(R/H_2) = \prod_{i=1}^{N} p(r(i)\,|\,f_2(i)) \tag{3.3.4}$$

According to Bayes likelihood ratio test [38] (which minimizes the probability of error), H_1 or H_2 are accepted to be true as per the following inequality

$$\frac{\prod_{i=1}^{N} p(r(i)\,|\,f_1(i))}{\prod_{i=1}^{N} p(r(i)\,|\,f_2(i))} \underset{H_2}{\overset{H_1}{\gtrless}} \frac{P_2}{P_1} \tag{3.3.5}$$

where P_1 and P_2 are the a-priori probabilities associated with F_1 and F_2 respectively.

For acase of Gaussian noise we have

$$p(r(i)\,|\,f_j(i)) = \frac{1}{\sqrt{2\pi}\,\sigma_n} \cdot \exp\left(-(r(i)-f_j(i))^2/2\sigma_n^2\right) \tag{3.3.6}$$

Substituting (3.3.6) in (3.3.5) yields

$$\prod_{i=1}^{N} \exp\left[\frac{(r(i)-f_2(i))^2}{2\,\sigma_n^2} - \frac{(r(i)-f_1(i))^2}{2\,\sigma_n^2}\right] \underset{H_2}{\overset{H_1}{\gtrless}} \frac{P_2}{P_1} \tag{3.3.7}$$

Alternatively, taking logarithms, we get

$$\sum_{i=1}^{N} \left[[r(i) - f_2(i)]^2 - [r(i) - f_1(i)]^2\right] \underset{H_2}{\overset{H_1}{\gtrless}} 2\,\sigma_n^2 \ln \frac{P_2}{P_1}$$

or

$$\sum_{i=1}^{N} (2r(i)-f_2(i)-f_1(i))(f_1(i)-f_2(i)) \underset{H_2}{\overset{H_1}{\gtrless}} 2\sigma_n^2 \ln \frac{P_2}{P_1} \qquad (3.3.8)$$

or

$$\sum_{i=1}^{N} r(i)(f_1(i)-f_2(i)) \underset{H_2}{\overset{H_1}{\gtrless}} \frac{1}{2} \sum_{i=1}^{N} (f_1^2(i)-f_2^2(i)) + \sigma_n^2 \ln \frac{P_2}{P_1}$$

In vector form (3.3.8) can be written as

$$(F_1-F_2)'R \underset{H_2}{\overset{H_1}{\gtrless}} \frac{1}{2}\|F_1\|^2 - \frac{1}{2}\|F_2\|^2 + \sigma_n^2 \ln \frac{P_2}{P_1} \qquad (3.3.9)$$

Inequality (3.3.8) or (3.3.9) can be used to determine if the received data samples R belong to F_1 or F_2, the known vectors.

Now defining:

$$\Delta f_{12}(i) = f_1(i) - f_2(i) \qquad (3.3.10)$$

and

$$\frac{1}{2} \sum_{i=1}^{N} (f_1^2(i) - f_2^2(i)) + \sigma_n^2 \ln \frac{P_2}{P_1} = K \qquad (3.3.11)$$

(3.3.8) can be rewritten as

$$\sum_{i=1}^{N} r(i)\Delta f_{12}(i) \underset{H_2}{\overset{H_1}{\gtrless}} K \qquad (3.3.12)$$

This decision rule is illustrated by Fig. 3.3. The threshold K is a function of noise and processes' statistics. By increasing N, K can be made less dependent on σ_n (Eqn. (3.3.11)) which demonstrates the smoothing property of the decision rule.

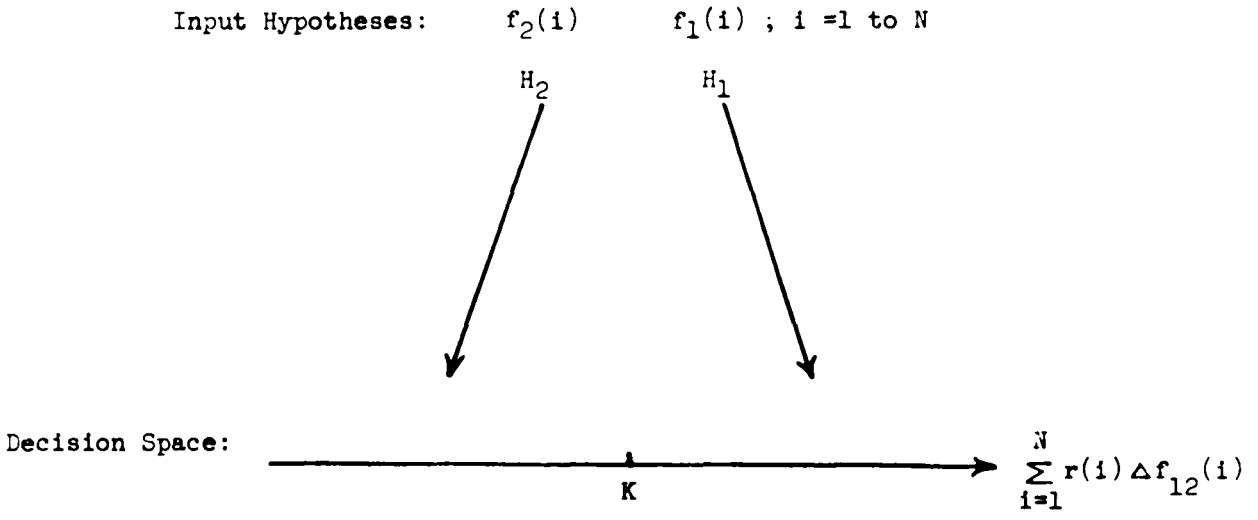

$$K = \frac{1}{2} \sum_{i=1}^{N} (f_1^2(i) - f_2^2(i) + \sigma_n^2 \ln \frac{P_2}{P_1}$$

Fig. 3.3. Decision regions as determined by the decision rule of section 3.3.1.

3.3.2 The Decision Rule as applied to Nystagmus Waveform

A nystagmus waveform consists basically of two types of eye movements, the slow phase movements and the quick phase movements. For the purpose of their detection, these movements can be defined by vectors F_1 and F_2. In general these vectors will not define the total time span of these movements, but will only be representative of the time functions defining them. With respect to a moving data window of (N+1) samples, where the first sample is subtracted from the rest of the samples, the vectors F_1 and F_2 are defined in Fig. 3.4.

In an on-line EOG data processing scheme one would like to associate each received sample to one of the two possible eye movements. If the decision rule of section 3.3.1 is used, the decision will be statistically correct if all the components of the received vector are due to either F_1 or F_2. The decision may not be correct if the data window (or vector R) is due partly to F_1 and partly to F_2. Such is the case at the time of transition from F_1 to F_2 or F_2 to F_1. This is illustrated in Fig. 3.5. for a window of 5 samples and will be pursued further in section 3.3.3.

The implementation of (3.3.8) or (3.3.9) requires the knowledge of P_1 and P_2, which in the case of a nystagmus waveform, can be obtained as follows. Consider a typical cycle of nystagmus shown in Fig. 3.6, P_1 and P_2 are estimated by

$$P_1 = T_1/(T_1 + T_2) \tag{3.3.13}$$

$$P_2 = T_2/(T_1 + T_2) \tag{3.3.14}$$

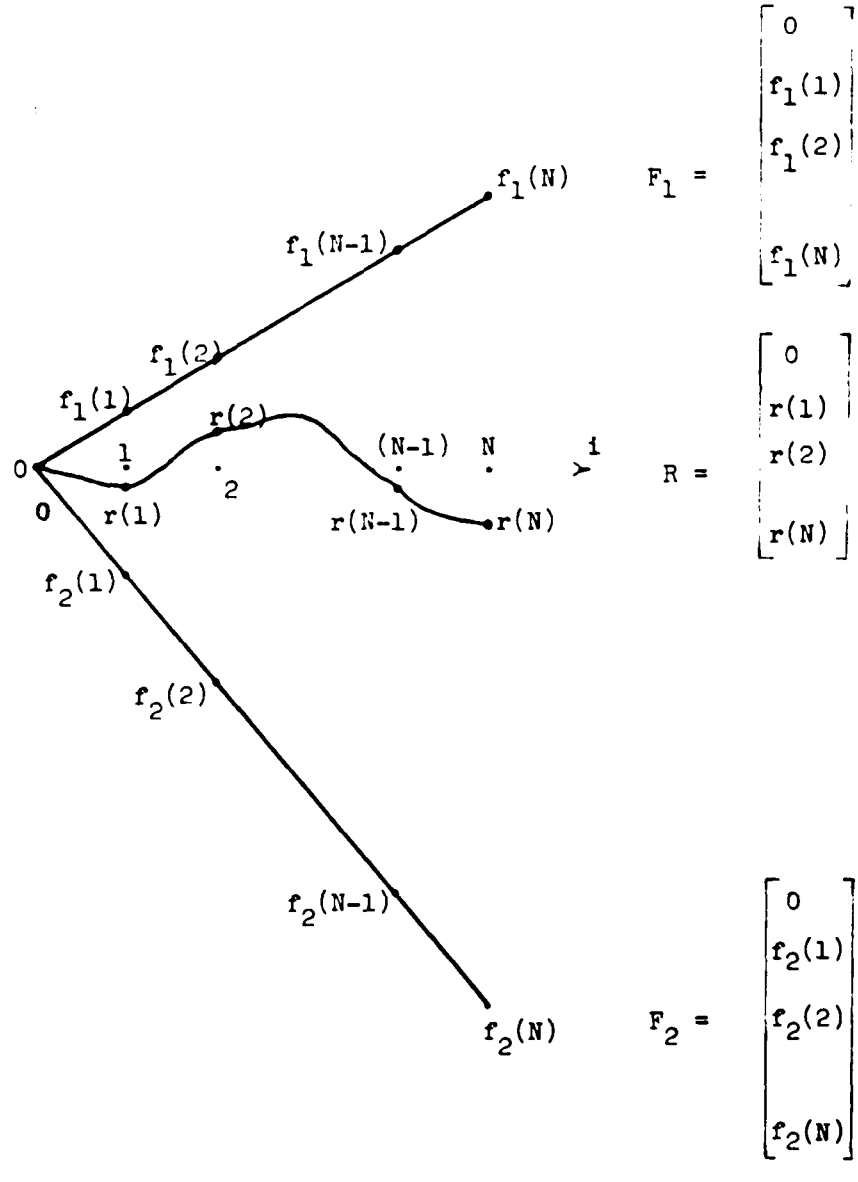

Fig. 3.4. Definitions of vectors F_1 and F_2 and the received data vector R.

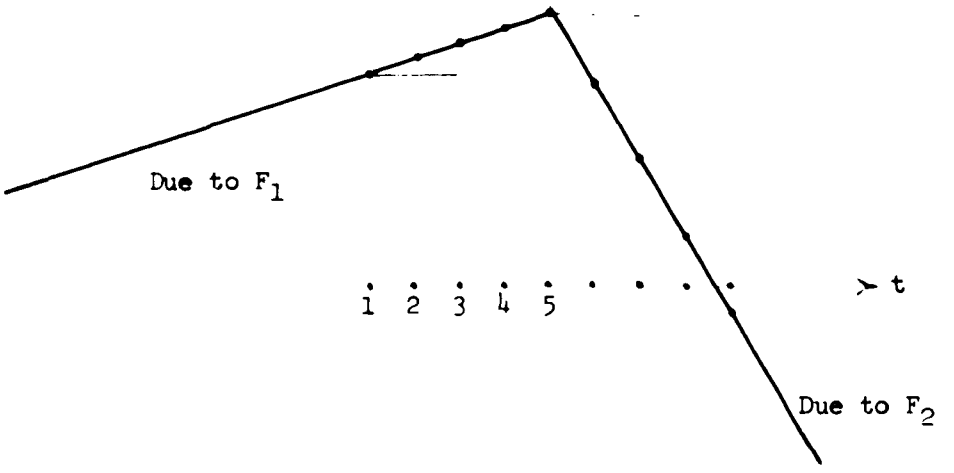

Window Starting Time

t	Samples
1	$0, f_1(1), f_1(2), f_1(3), f_1(4) \triangleq F_1$
2	$0, f_1(1), f_1(2), f_1(3), f_1(3) + f_2(1)$
3	$0, f_1(1), f_1(2), f_1(2) + f_2(1), f_1(2) + f_2(2)$
4	$0, f_1(1), f_1(1) + f_2(1), f_1(1) + f_2(2), f_1(1) + f_2(3)$
5	$0, f_2(1), f_2(2), f_2(3), f_2(4) \triangleq F_2$

Fig. 3.5. **For a moving window of 5 samples, the sample sequences during transition from F_1 to F_2. Noise is assumed to be zero. Similar sequences arise during the transition from F_2 to F_1.**

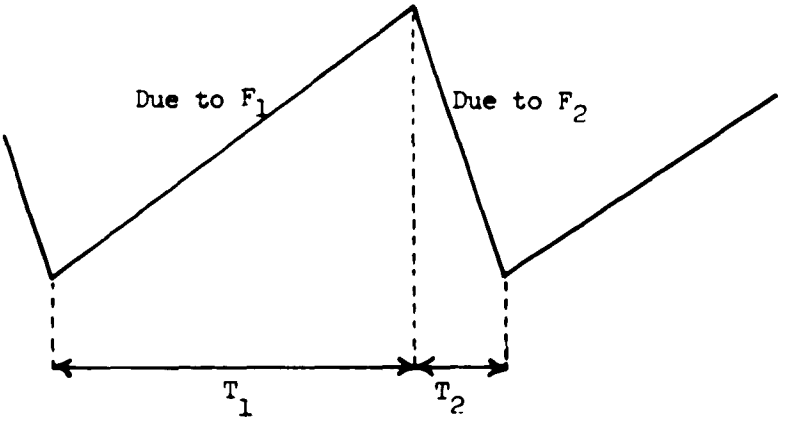

Fig. 3.6. A-priori probabilities P_1 and P_2 calculations use T_1 and T_2 intervals for a typical cycle of nystagmus.

A simplifying assumption that F_1 and F_2 represent two straight lines with different slopes will be made in the analysis. It is assumed that the slopes of these lines are correct enough to represent the entire spans of two types of eye movements. The justification of this assumption is that, within the window span the EOG is practically a straight line and over the entire span of one type of movement the slope change is small enough not to introduce any gross detection error.

3.3.3 The Probability of Error of the Detection Process

Each incoming data sample must either be assigned to $f_1(i)$ or to $f_2(i)$. The decision rule of section 3.3.1 uses all the sample points in a window. Therefore, if at an instant, all the sample points received up to that time are due to one or the other process, the only error in the decision may be due to noise. In another case where the window samples are partly due to $f_1(i)$ and partly due to $f_2(i)$, the decision about the latest sample is influenced by the samples before it. Here, we will derive expressions for the probability of error associated with the decision process where the decision rule of (3.3.12) is used and at each time the decision is either $f_1(i)$ or $f_2(i)$.

The value of the expression $\sum_{i=1}^{N} r(i)\Delta f_{12}(i)$ depends upon the data samples $r(i)$ which may all be due to $f_1(i)$ or all due to $f_2(i)$ or partly due to $f_1(i)$ and partly due to $f_2(i)$. Let us use the

following variables to denote the value of $\sum_{i=1}^{N} r(i)\Delta f_{12}(i)$ for these different data sets:

$$\sum_{i=1}^{N} r(i)\Delta f_{12}(i) = Z_{11N} \text{ when all (N+1) samples are due to } f_1(i)$$

$$= Z_{22N} \text{ when all (N+1) samples are due to } f_2(i)$$

$$= Z_{12x} \text{ when the last 'x' samples are due to } f_2(i) \text{ and the rest are due to } f_1(i)$$

$$= Z_{21x} \text{ when the last 'x' samples are due to } f_1(i) \text{ and the rest are due to } f_2(i) \qquad (3.3.15)$$

In terms of $f_1(i)$ and $f_2(i)$ (3.3.15) can be written as

$$Z_{11N} = \sum_{i=1}^{N} (f_1(i)+n(i)-n(0))\Delta f_{12}(i) \qquad (3.3.16)$$

$$Z_{22N} = \sum_{i=1}^{N} (f_2(i)+n(i)-n(0))\Delta f_{12}(i) \qquad (3.3.17)$$

$$Z_{12x} = \sum_{i=1}^{N-x} (f_1(i)+n(i)-n(0))\Delta f_{12}(i) + \sum_{i=N-x+1}^{N} (f_1(N-x)+ f_2(i-N+x)+n(i)-n(0))\Delta f_{12}(i) \qquad (3.3.18)$$

$$Z_{21x} = \sum_{i=1}^{N-x} (f_2(i)+n(i)-n(0))\Delta f_{12}(i) + \sum_{i=N-x+1}^{N} (f_2(N-x)+ f_1(i-N+x)+n(i)-n(0)\Delta f_{12}(i) \qquad (3.3.19)$$

where n(0) is the noise term with the reference sample r(0).

Now an error in the decision will be made if $Z_{11N} < K$ or $Z_{21x} < K$ for all x or $Z_{22N} > K$ or $Z_{12x} > K$ for all x. The a-priori probabilities associated with the cases generating Z_{12x} and Z_{21x} depend upon the sampling interval and the average frequency of transitions in the

waveform. These will, though, be the same for all cases and let us denote them by P_t. P_1 and P_2 will also be slightly different from (3.3.13) and (3.3.14) if the window interval is accounted in calculations. Ignoring these minor differences, the probability of error is given by

$$P(E) = P_1 P(Z_{11N} < K) + P_2 P(Z_{22N} > K) + P_t \sum_{x=1}^{N-1} P(Z_{21x} < K) + P_t \sum_{x=1}^{N-1} P(Z_{12x} > K) \quad (3.3.20)$$

To compute P(E), we need to determine the statistics of Z_{11N}, Z_{22N}, Z_{21x} and Z_{12x} for $1 \leq x \leq N-1$. For normally distributed noise, these are also normally distributed random variables with the following means and variances.

$$\bar{Z}_{11N} = \sum_{i=1}^{N} f_1(i) \Delta f_{12}(i) \quad (3.3.21)$$

$$\bar{Z}_{22N} = \sum_{i=1}^{N} f_2(i) \Delta f_{12}(i) \quad (3.3.22)$$

$$\bar{Z}_{21x} = \sum_{i=1}^{N-x} f_2(i) \Delta f_{12}(i) + \sum_{i=N-x+1}^{N} (f_2(N-x) + f_1(i-N+x). \Delta f_{12}(i) \quad (3.3.23)$$

$$\bar{Z}_{12x} = \sum_{1=1}^{N-x} f_1(i) \Delta f_{12}(i) + \sum_{i=N-x+1}^{N} (f_1(N-x) + f_2(i-N+x). \Delta f_{12}(i) \quad (3.3.24)$$

$$\sigma_{11N}^2 = \sigma_{22N}^2 = \sigma_{12x}^2 = \sigma_{21x}^2 = \sigma_n^2 . \sum_{i=1}^{N} (\Delta f_{12}(i))^2 \quad (3.3.25)$$

These equations lead to the probability density functions as follows

$$P_{11N}(X) = \frac{1}{\sqrt{2\pi}\,\sigma_{11N}} \cdot \exp \frac{-(X - \bar{Z}_{11N})^2}{2\,\sigma_{11N}^2} \qquad (3.3.26)$$

$$P_{22N}(X) = \frac{1}{\sqrt{2\pi}\,\sigma_{22N}} \cdot \exp \frac{-(X - \bar{Z}_{11N})^2}{2\,\sigma_{22N}^2} \qquad (3.3.27)$$

$$P_{21x}(X) = \frac{1}{\sqrt{2\pi}\,\sigma_{21x}} \cdot \exp \frac{-(X - \bar{Z}_{21x})^2}{2\,\sigma_{21x}^2} \qquad (3.3.28)$$

$$P_{12x}(X) = \frac{1}{\sqrt{2\pi}\,\sigma_{12x}} \cdot \exp \frac{-(X - \bar{Z}_{12x})^2}{2\,\sigma_{12x}^2} \qquad (3.3.29)$$

Eqn. (3.3.20) when rewritten in terms of probability density functions is given by

$$P(E) = P_1 \cdot \int_{-\infty}^{K} P_{11N}(X)dX + P_2 \cdot \int_{K}^{\infty} P_{22N}(X)dX + P_t \cdot \sum_{x=1}^{N-1} \left[\int_{-\infty}^{K} P_{21x}(X)dX \right] + P_t \cdot \sum_{x=1}^{N-1} \left[\int_{K}^{\infty} P_{12x}(X)dX \right] \qquad (3.3.30)$$

Substituting (3.3.26) - (3.3.29) in (3.3.30) and further simplification yields

$$P(E) = \frac{P_1}{2} \cdot \operatorname{erf}\left(\frac{K - \bar{Z}_{11N}}{\sqrt{2}\,\sigma_{11N}}\right) + 1 + \frac{P_2}{2} \cdot \operatorname{erfc}\left(\frac{K - \bar{Z}_{22N}}{\sqrt{2}\,\sigma_{22N}}\right) + \frac{P_t}{2} \cdot \sum_{x=1}^{N-1} \left(\operatorname{erf}\left(\frac{K - \bar{Z}_{21x}}{\sqrt{2}\,\sigma_{21x}}\right) + 1\right) + \frac{P_t}{2} \cdot \sum_{x=1}^{N-1} \operatorname{erfc}\left(\frac{K - \bar{Z}_{12x}}{\sqrt{2}\,\sigma_{12x}}\right) \qquad (3.3.31)$$

In most practical cases $P_t \ll P_1$ and P_2. Thus (3.3.31) can be approximated by

$$P(E) \approx \frac{P_1}{2}\left[\operatorname{erf}\left(\frac{K - \bar{Z}_{11N}}{\sqrt{2}\,\sigma_{11N}}\right)+1\right] + \frac{P_2}{2} \cdot \operatorname{erfc}\left(\frac{K - \bar{Z}_{22N}}{\sqrt{2}\,\sigma_{22N}}\right)$$

for small N (3.3.32)

In (3.3.31) and (3.3.32), error function and complementary error function are defined as

$$\operatorname{erf}(Z) = \frac{2}{\sqrt{\pi}} \int_0^Z e^{-t^2}\, dt \qquad (3.3.33)$$

and $\operatorname{erfc}(Z) = 1 - \operatorname{erf}(Z)$

The results of this section are illustrated in the next section by application to a simulation example.

3.3.4 A Simulation Example

Let us construct an artifical example to illustrate the theory of section 3.3.3. Consider a case where $f_1(t)$ and $f_2(t)$ are given by

$$f_1(t) = .2t \qquad (3.3.34)$$

$$f_2(t) = -1.6t \qquad (3.3.35)$$

The associated a-priori probabilities are computed based upon the assumption that average time period for $f_1(t)$ is 900 msec(T_1) and for $f_2(t)$ is 100 msec(T_2). Let the sampling period be 2msec(T). The a-priori probabilities are obtained as follows:

$$P_1 = \frac{T_1 - (N-1).T}{T_1 + T_2} \approx \frac{T_1}{T_1 + T_2} = .9 \qquad (3.3.36)$$

$$P_2 = \frac{T_2 - (N-1).T}{T_1 + T_2} \approx \frac{T_2}{T_1 + T_2} = .1 \qquad (3.3.37)$$

$$P_t = \frac{T}{T_1 + T_2} = .002 \qquad (3.3.38)$$

Where (N=1) are the number of samples in a window. Approximation in (3.3.36) and (3.3.37) assumes that the window width is relatively much smaller than T_1 and T_2.

Substituting (3.3.36) - (3.3.38) in (3.3.31) and (3.3.32) yields

$$P(E) = .45\left[\operatorname{erf}\left(\frac{K - \bar{Z}_{11N}}{\sqrt{2}\,\sigma_{11N}}\right)+1\right] + .05\operatorname{erfc}\left(\frac{K - \bar{Z}_{22N}}{\sqrt{2}\,\sigma_{22N}}\right) + .001\sum_{X=1}^{N-1}$$

$$\left(\operatorname{erf}\left(\frac{K - \bar{Z}_{21x}}{\sqrt{2}\,\sigma_{21x}}\right)+1\right) + .001\sum_{x=1}^{N-1}\left(\operatorname{erfc}\left(\frac{K - \bar{Z}_{12x}}{\sqrt{2}\,\sigma_{12x}}\right)\right. \qquad (3.3.39)$$

and

$$P(E) \approx .45\left[\operatorname{erf}\left(\frac{K - \bar{Z}_{11N}}{\sqrt{2}\,\sigma_{11N}}\right)+1\right] + .05\operatorname{erfc}\left(\frac{K - \bar{Z}_{22N}}{\sqrt{2}\,\sigma_{22N}}\right) \text{ for small } N$$

(3.3.40)

Probabilities of error as obtained from (3.3.39) and (3.3.40) are plotted in Fig. 3.7 for N=2, 4 and 6 ; and σ_n = 0.0 to 3.5. Observe that for small N (say N=2), equations (3.3.39) and (3.3.40) yield about the same probability of error and it increases with σ_n. For larger values of N (say N=6), the error probability is mainly due to the transitional error and is approximately constant for small σ_n (<2.5). For larger σ_n values, the error probability is due to both the transition and the noise and it increases with σ_n.

The probability of error conditioned on the latest sample during the transition from $f_1(t)$ to $f_2(t)$ varies from

$$\left[\text{erf}\ \left(\frac{K-\bar{Z}_{11N}}{\sqrt{2}\ \sigma_{11N}}\right)+1\right]\ \text{to}\ \left[\text{erfc}\ \left(\frac{K-\bar{Z}_{12x}}{\sqrt{2}\ \sigma_{12x}}\right)\ ,\ x=1\ \text{to}\ (N-1)\right]$$

$$\left[\text{to}\ \ \text{erfc}\ \left(\frac{K-\bar{Z}_{22N}}{\sqrt{2}\ \sigma_{22N}}\right)\right].$$

Similarly for the transition from $f_2(t)$ to $f_1(t)$ it varies from

$$\left[\text{erfc}\ \left(\frac{K-\bar{Z}_{22N}}{\sqrt{2}\ \sigma_{22N}}\right)\right]\text{to}\quad\left[\text{erf}\ \left(\frac{K-\bar{Z}_{21X}}{\sqrt{2}\ \sigma_{21X}}\right)+1\ ,\ x=1\ \text{to}\ (N-1)\right]$$

$$\text{to}\ \left[\text{erf}\ \ \left(\frac{K-\bar{Z}_{11N}}{\sqrt{2}\ \sigma_{11N}}\right)+1\right].$$

The probability of error conditioned on each new received sample during the transition from $f_1(t)$ to $f_2(t)$ is plotted in Fig. 3.8a. Observe that as the number of samples in a window are increased, a larger number of samples are needed from $f_2(t)$ before it can be detected. For instance for N=4, we must receive at least 3 samples from $f_2(t)$ before it is detected. Similar results are plotted for the transition from $f_2(t)$ to $f_1(t)$ in Fig. 3.8b. The plots of Fig. 3.8a and 3.8b lead to the conclusion that there is a definite amount of delay in the detection of an on-coming process and it depends upon the window width.

In Fig. 3.8c, the error probability associated with each sample for the transition $f_1(t)$ to $f_2(t)$ for N=6 is plotted for various σ_n values. Observe that increasing σ_n increases the error probability when a larger number of samples are contributed by the on-coming process. However, this probability of error is decreased for smaller number of samples contributed by the on-coming process. Similar results are shown for the transition $f_2(t)$ to $f_1(t)$ in Fig. 3.8d. The two transitions are compared in Fig. 3.8e for a case of $\sigma_n = 3.0$

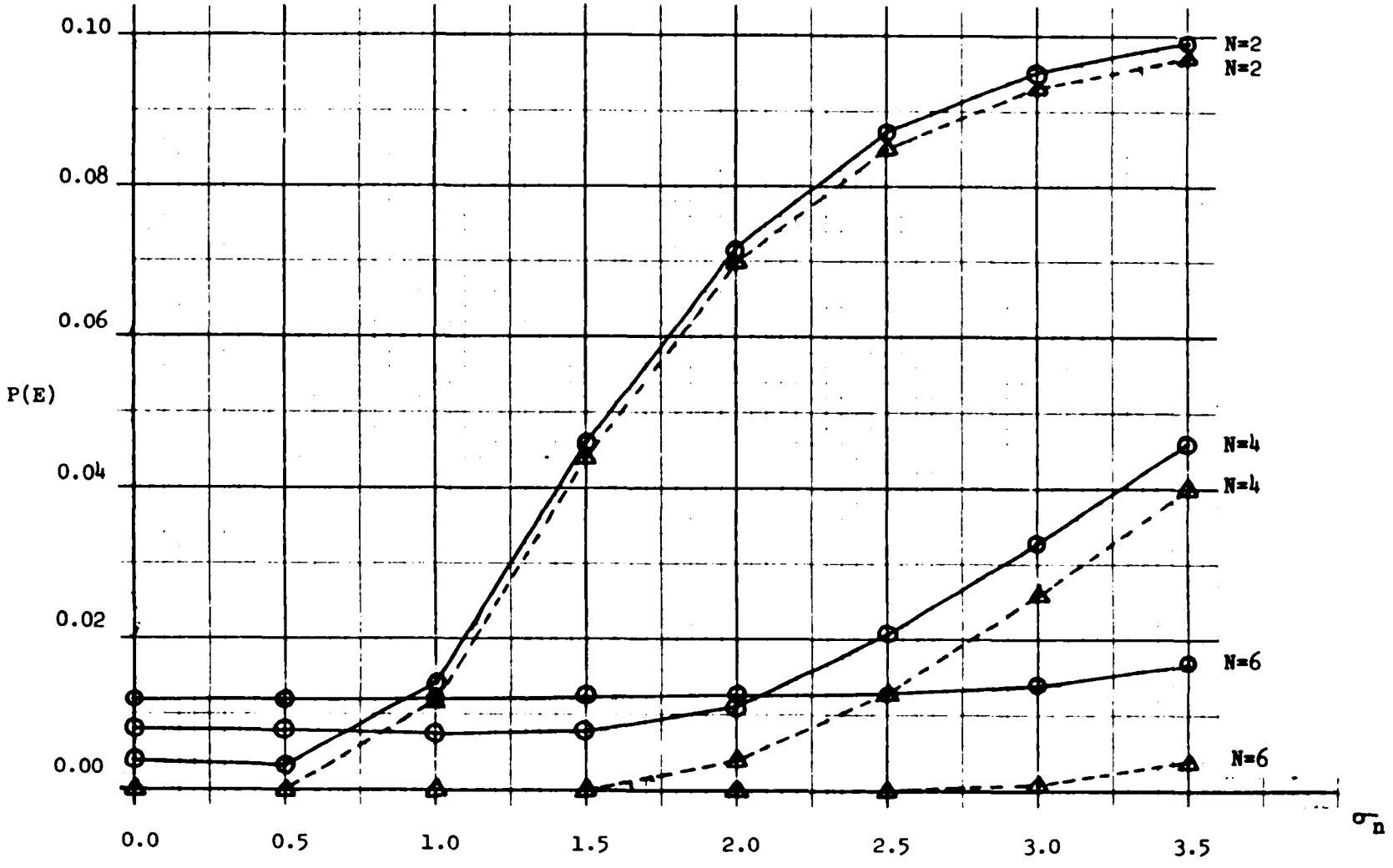

Fig. 3.7 . Total probability of error for the detection of example in section 3.3.4.
0——0 Eqn. 3.3.39, △--------△ Eqn. 3.3.40.

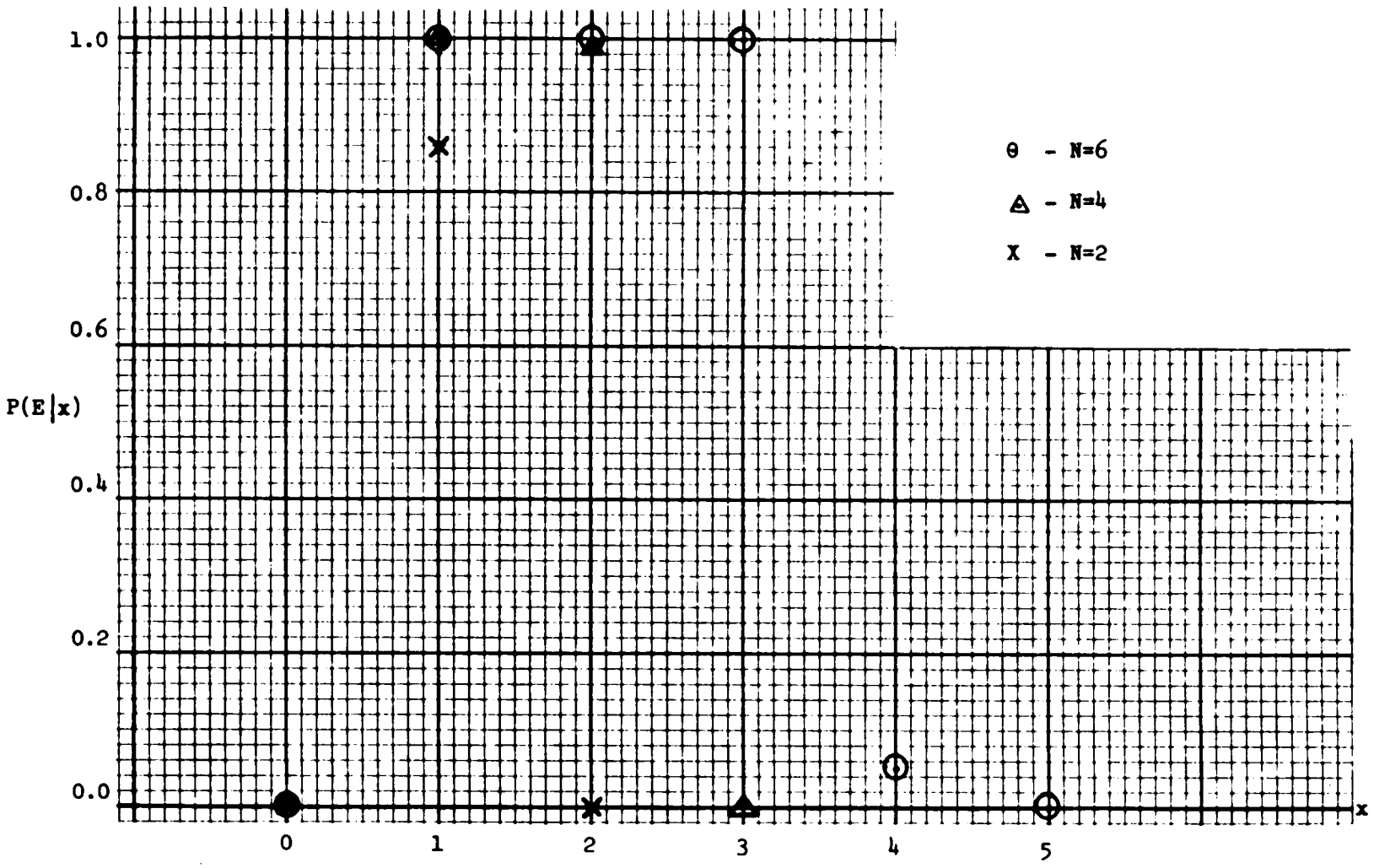

Fig. 3.8a. Conditional probability of error during the transition from $f_1(t)$ to $f_2(t)$. $\sigma_n = 0.5$ for all the cases.

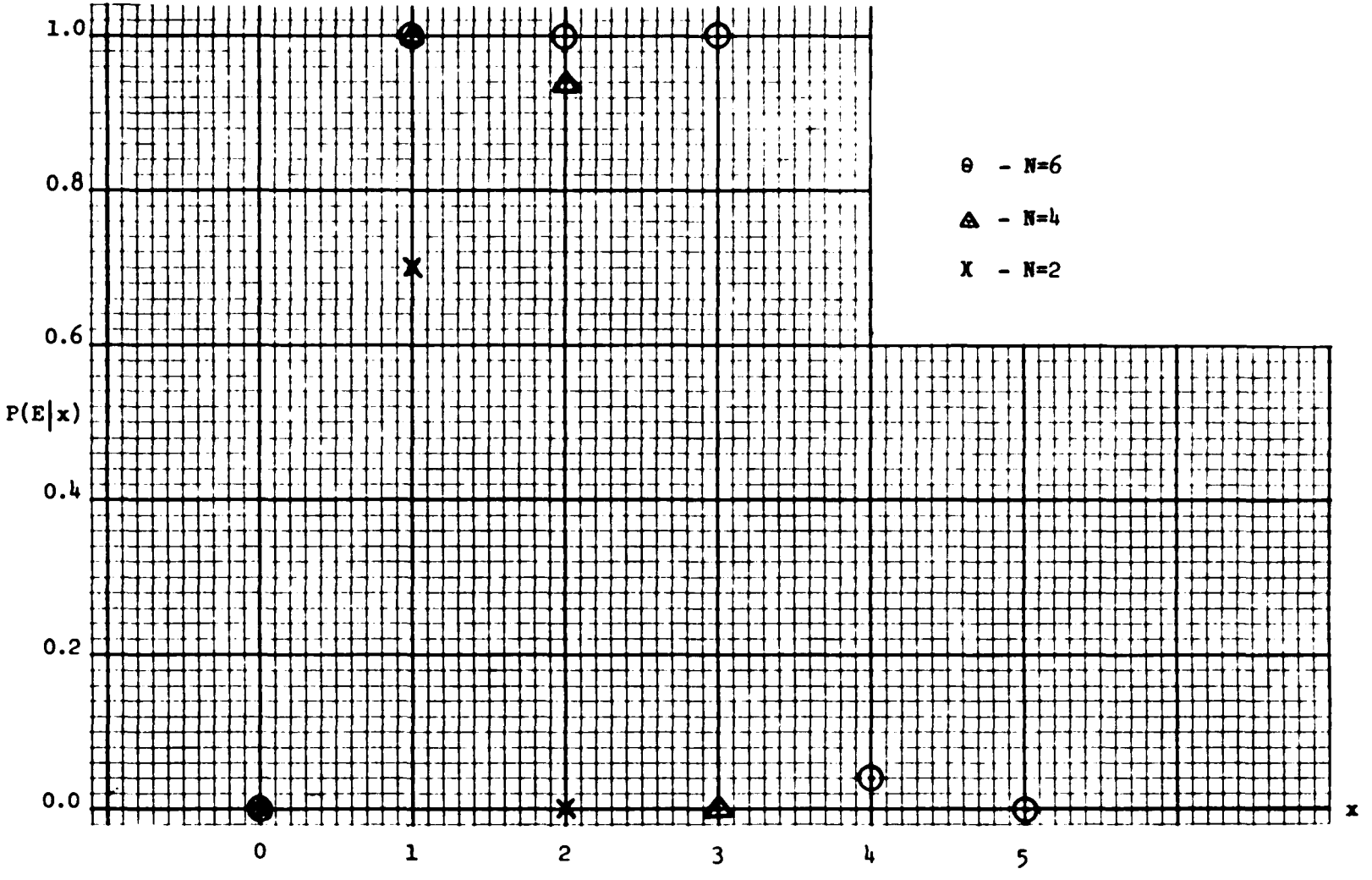

Fig. 3.8b. Conditional probability of error during the transition from $f_2(t)$ to $f_1(t)$. $\sigma_n = 0.5$ for all the cases.

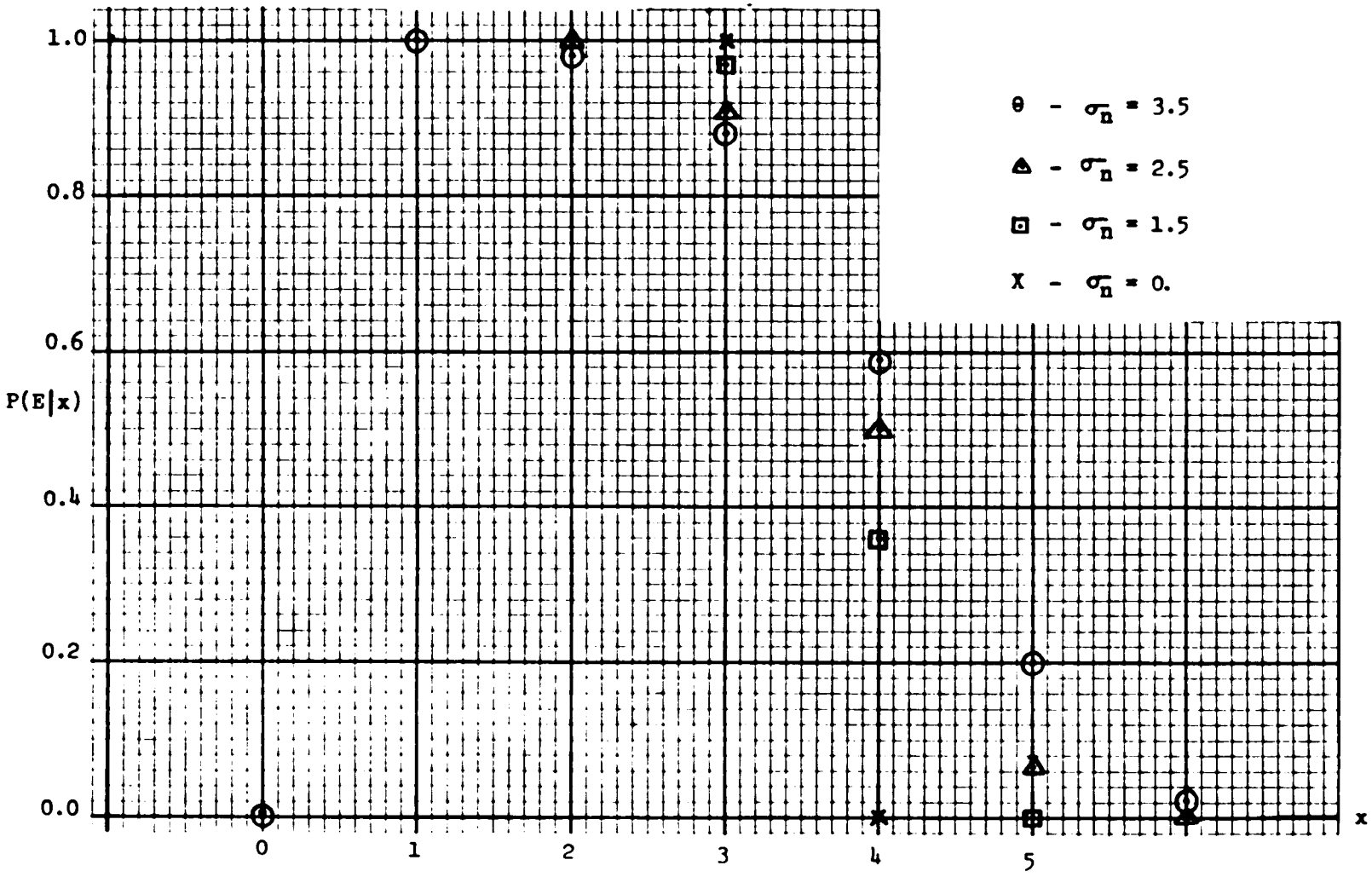

Fig. 3.8c. Conditional probability of error for the transition from $f_1(t)$ to $f_2(t)$ for N=6 and σ_n = 0.0, 1.5, 2.5 and 3.5.

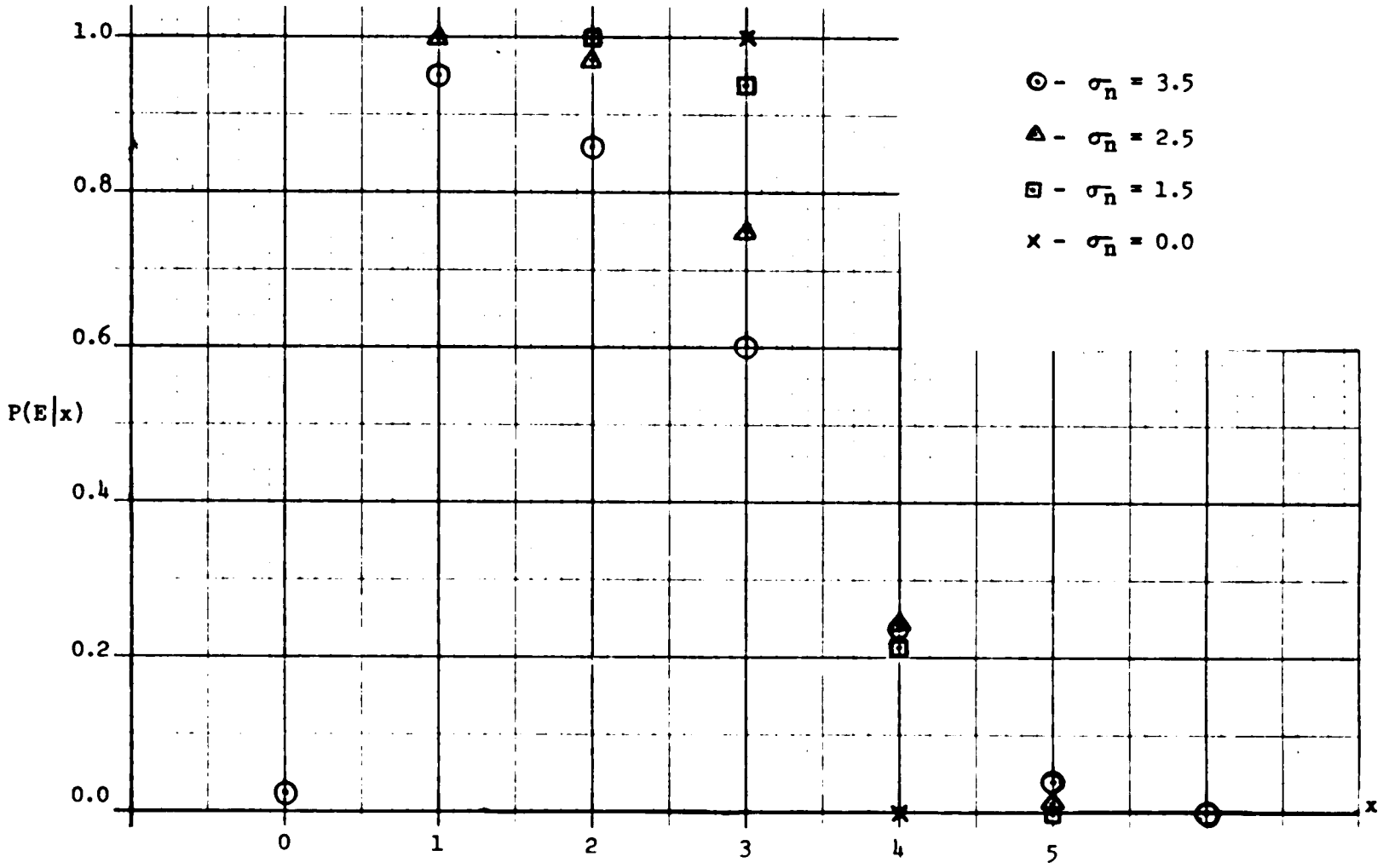

Fig. 3.8d. Conditional probability of error for the transition from $f_2(t)$ to $f_1(t)$ for N=6 and σ_n = 0.0, 1.5, 2.5 and 3.5.

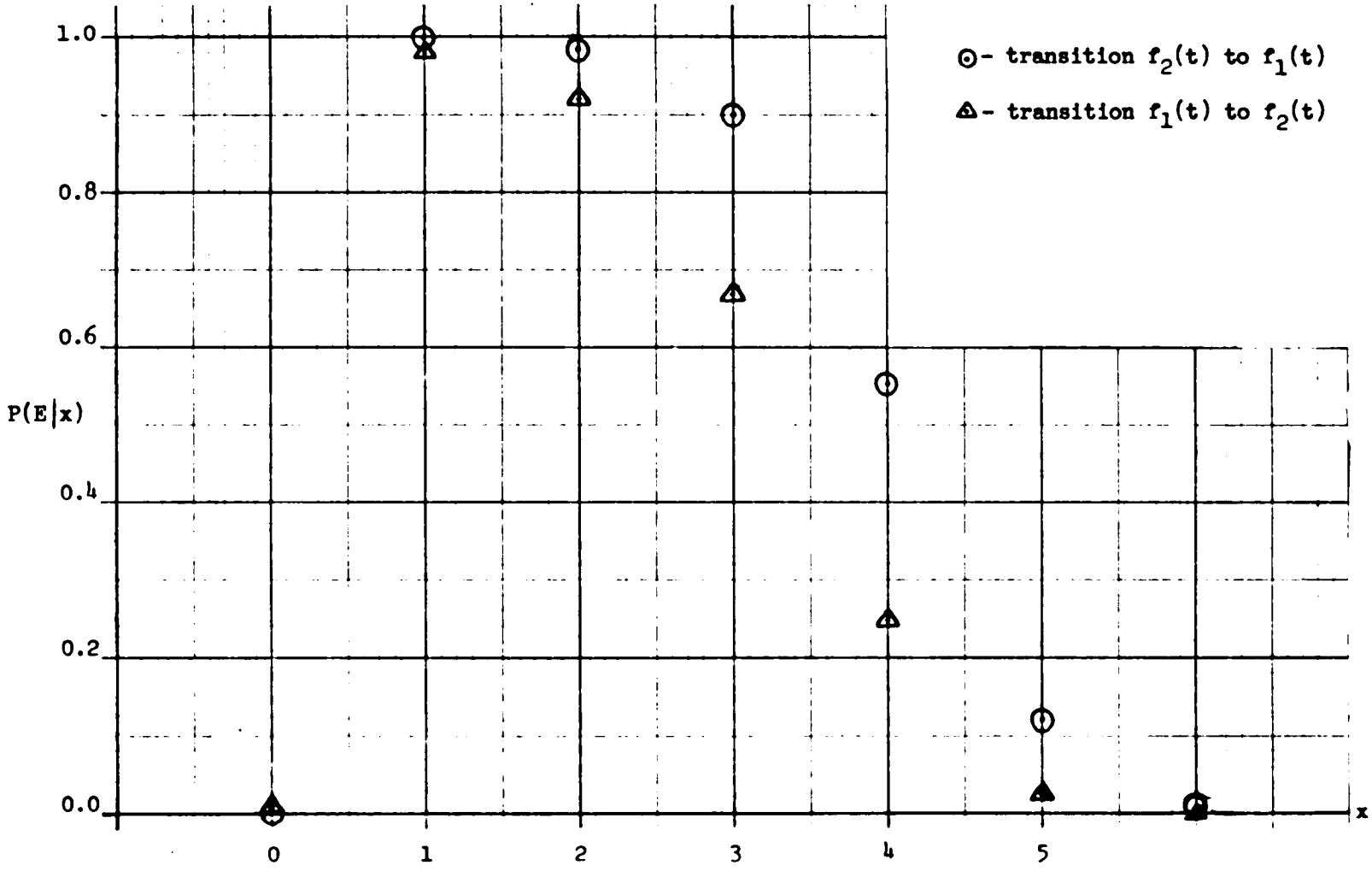

Fig. 3.8c. Conditional probability of error comparison for the two transitions $f_1(t)$ to $f_2(t)$ and $f_2(t)$ to $f_1(t)$.

and N=6. Observe that the transition $f_1(t)$ to $f_2(t)$ is accompanied by larger error probability as compared to the transition $f_2(t)$ to $f_1(t)$. When all the samples belong to one or the other process, the error associated with $f_2(t)$ is larger than the error associated with $f_1(t)$.

The program used to obtain the results of Fig. 3.7 & Fig. 3.8 is in Appendix A.

3.4 Experimental Results

The theory presented in the previous sections was tested in the laboratory on simulated and real data. The following sections are organized to present the experimental hardware configuration, software implementation, the simulation results, and the real EOG saccade detection results.

3.4.1 EOG Data Processing Hardware Configuration

Fig. 3.9 is a simplified block diagram of EOG data processing system as used in our laboratory. Eye movements are recorded by electrooculography using implanted Ag-Agcl electrodes [7]. The EOG so obtained is filtered and amplified. For later processing it can be stored on FM magnetic tape. For on-line processing it is fed directly into the computer system.

A 10-bit successive approximation type analog to digital converter AD8-EA [10] with sample and hold circuits, conversion circuits, an input buffer, and control logic is used to convert analog EOG to

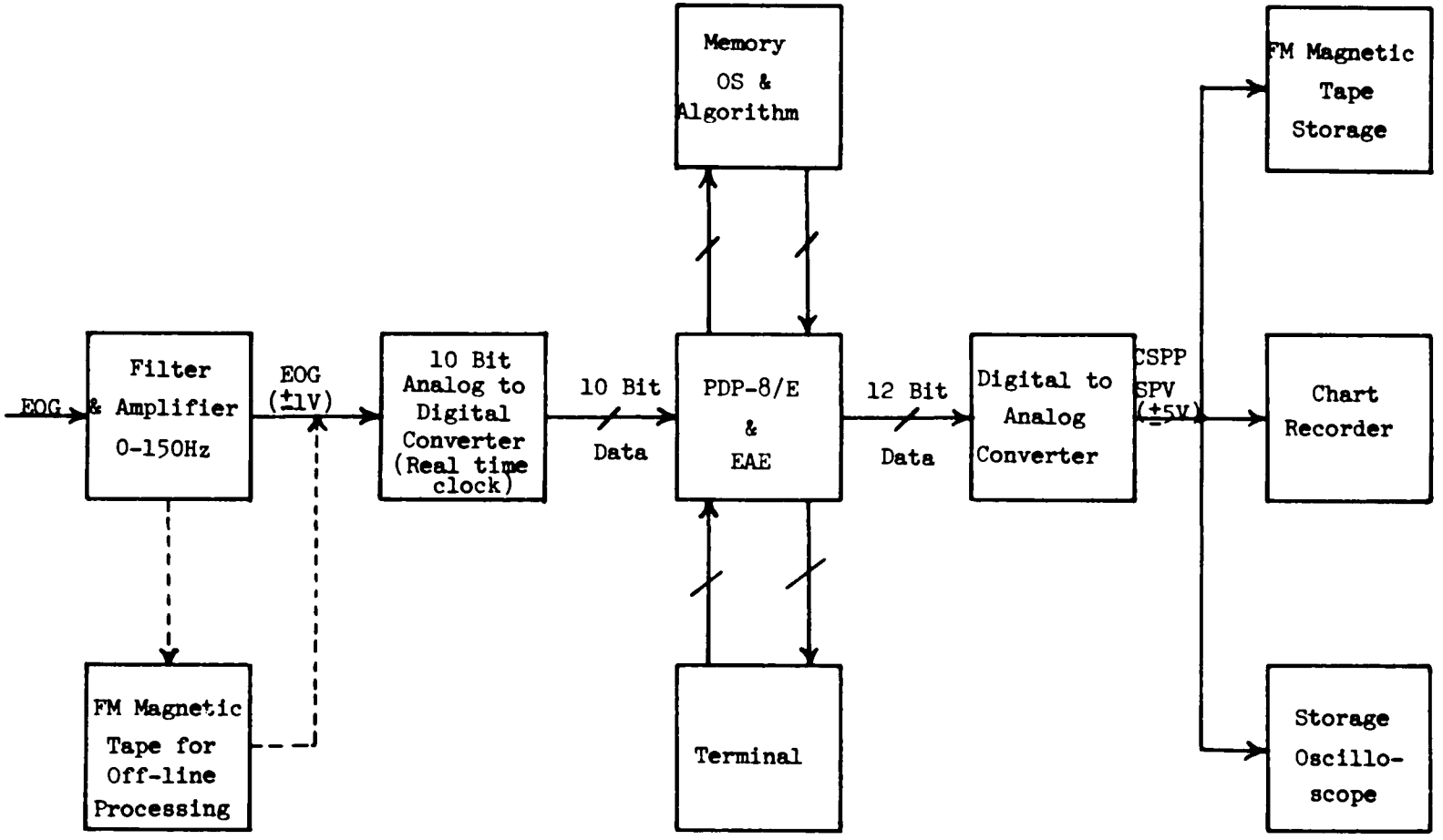

Fig. 3.9. A simplified block diagram of EOG data processing system as used in this study.

digital signal. The analog EOG must be limited between ±1 volt to avoid overdriving the converter. The conversion is initiated by the Real Time Clock DK8-EP [10]. When the conversion is complete, A/D Done Flag is set. This is sensed by the processor and the 10-bit digital word is transferred to 10 least significant bits of the accumulator. Since the 10-bit word is in two's complement form, the sign bit is extended to the two most significant bits of the accumulator. Thus all further processing can be done on 12-bit words. The data so gathered is stored in the memory.

The computer used to process the data is the Digital Equipment Corporation's PDP-8/E a 12-bit machine [10]. It is a single-address, fixed word length, parallel transfer computer using two's complement arithmetic. It has a cycle time of 1.2/1.4 usec. Apart from a 12-bit accumulator (AC) it also has another 12-bit register called multiplier-quotient (MQ) register. MQ acts as an extension of the AC during extended arithmetic operations. For extended operations a KE8-E Extended Arithmetic Element (EAE) is installed [10]. EAE allows implementation of 24-bit arithmetic operation for more accuracy. The computer used in this study is equipped with 28K memory. The memory is divided into fields each of 4K for addressing purposes. Each field is further subdivided into 32 pages each page having space for 128 12-bit words.

The processed digital data is converted back to an analog signal by a digital to analog (D-A) converter. The D-A converter used has 12-bits equivalent to ±5 volts. Thus the computed information can be directly fed to the D-A converter without any modification. The analog waveforms obtained from the converter can be displayed on a storage

oscilloscope or recorded on a chart recorder or stored on a magnetic tape for further processing at a later time.

3.4.2 EOG Saccade Detection Algorithm

The 'Likelihood Ratio Detector' of the last section is implemented on the PDP-8/E computer for the detection of saccades in an EOG waveform. The functional description of saccades and slow phases was obtained by examining records of typical EOG waveforms. Then tables were prepared describing their time vs. functional value plots. If $f_1(t)$ designates slow phase and $f_2(t)$ designates quick phase, then further tables of $f_1(t) + f_2(t)$ and $f_1(t) - f_2(t)$ were prepared to be used in the implementation of the left side of inequality (3.3.8). The right side of (3.3.8) was evaluated examining previously obtained EOG records and in most cases it turned out to be a very small number in comparison with the left side.

Actual implementation of the left side in (3.3.8) is shown in Fig. 3.10. In the flow chart 'DFN', the decision function is the negative of the left hand side of inequality (3.3.8). A decision window width of 'N+1' is assumed which may be increased to reduce noise effect but must be decreased to detect the transitions appropriately and at the right time. A value of N=5 was found to be a compromise for the detection of transitions and in minimizing false detections due to noise. In order to detect both left going and right going saccades, the absolute value of the scaled signal is used in the computation of 'DFN'. The value of 'DFN' calculated leads to the origin of the data, i.e. whether the received signal is

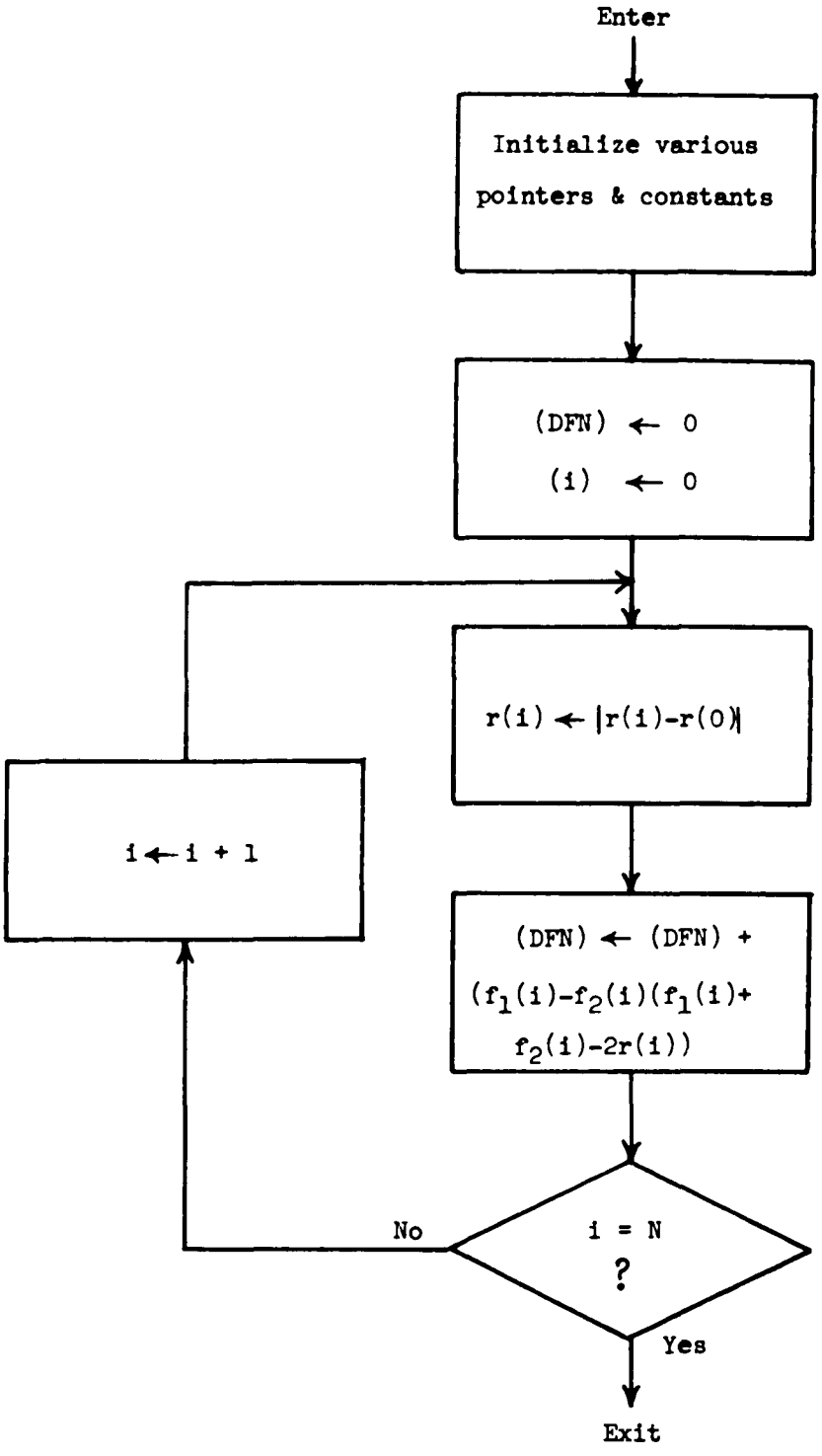

Fig. 3.10. Flow chart of DETECT subroutine for computing a decision function (DFN). Window width = N+1.

from saccadic process or from the slow phase system. The following criterion was used to detect saccades in the EOG waveform

$$DFN > 2\ \sigma_n^2 \ln (P_2/P_1) \text{ implies saccade}$$

and $$DFN < 2\ \sigma_n^2 \ln (P_2/P_1) \text{ implies slow phase}$$

The program for the implementation of saccade detection algorithm appears in Appendix B along with the rest of the program used in Chapter 4. The saccadic detection part of that program is tested in the next section on simulated and experimentally obtained EOG waveforms.

3.4.3 Simulated and Real Saccadic Detection Examples

The saccadic detection algorithm of the last section was used to compute the decision function for an EOG-like waveform. The result is shown in Fig. 3.11. It is obvious from the 'DFN' waveform that 'DFN' changes in accordance with the slope of the simulated EOG waveform. To indicate saccades, an appropriate threshold function may be used. In Fig. 3.12a and 3.12b, the saccade indications are obtained from the sign of 'DFN' (which is equivalent to ignoring $2\ \sigma_n^2 \ln (P_2/P_1)$), positive value of 'DFN' indicates a saccade and a negative value indicates a slow phase. Various types of saccade-like waveforms are processed to generate saccade indication waveform. There is no miss or false detection indication in the case of the simulated waveforms.

In Fig. 3.13, an experimentally obtained EOG waveform is used to generate the corresponding 'DFN' waveform. The threshold value to

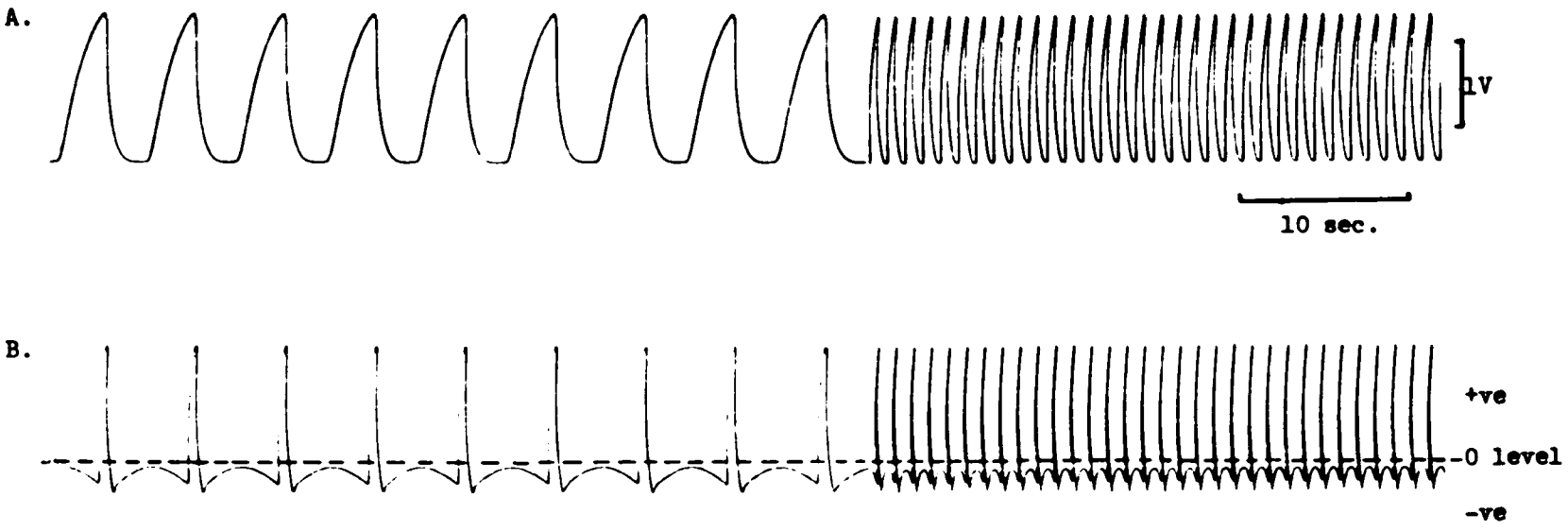

Fig. 3.11. Simulated EOG and its decision function. A. Simulated EOG. B. Decision function as computed by 'likelihood ratio detector' subroutine.

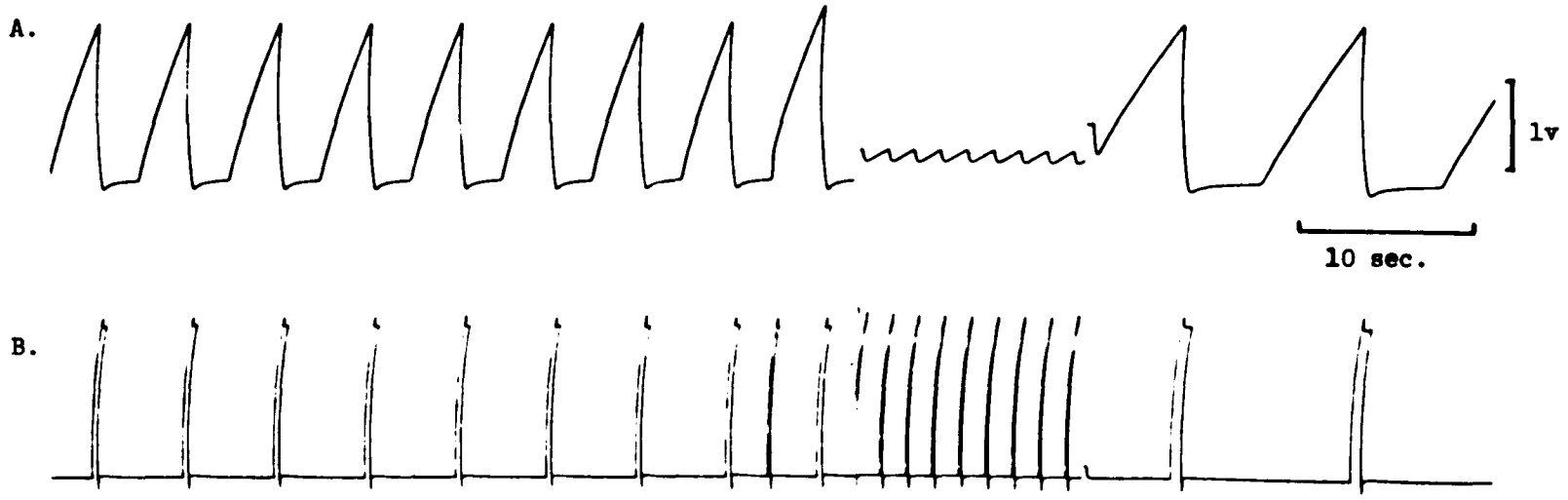

Fig. 3.12a. Saccade indications for simulated EOG waveforms. A. Simulated EOG waveforms. B. Saccade indication as determined by 'likelihood ratio detector' subroutine.

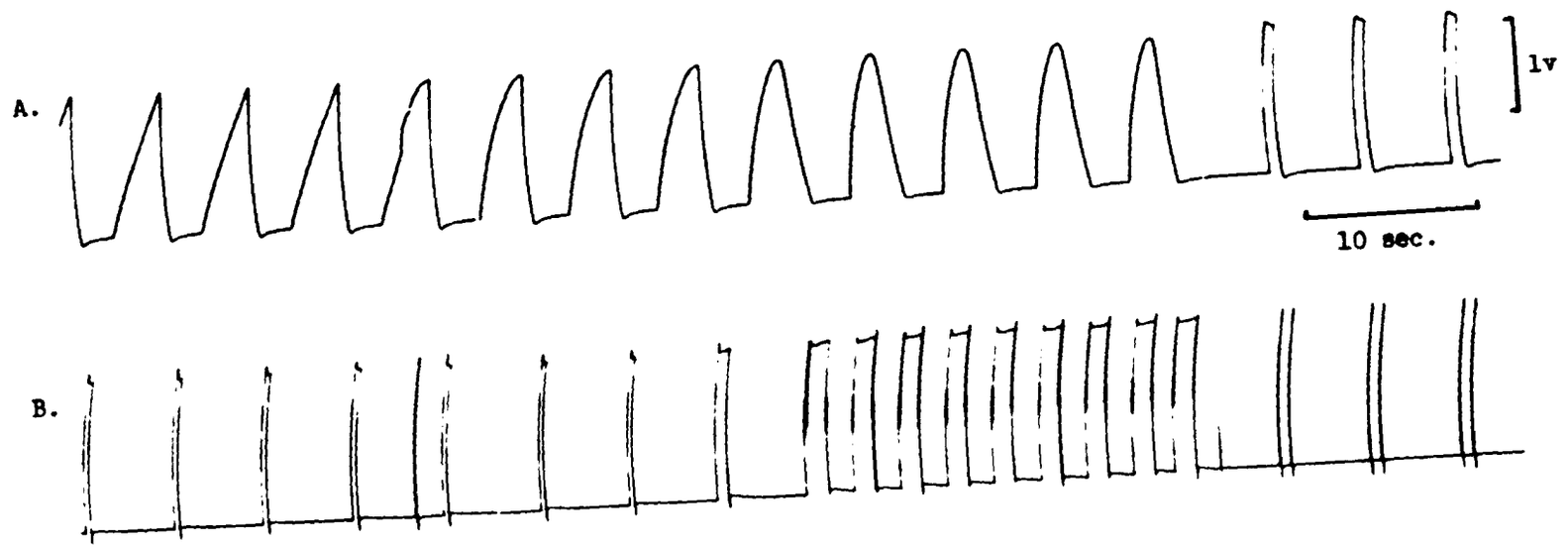

Fig. 3.12b. Saccade indications for various shapes of simulated EOG waveforms. A. Various simulated EOG shapes. B. Saccade indication as determined by 'likelihood ratio detector' subroutine.

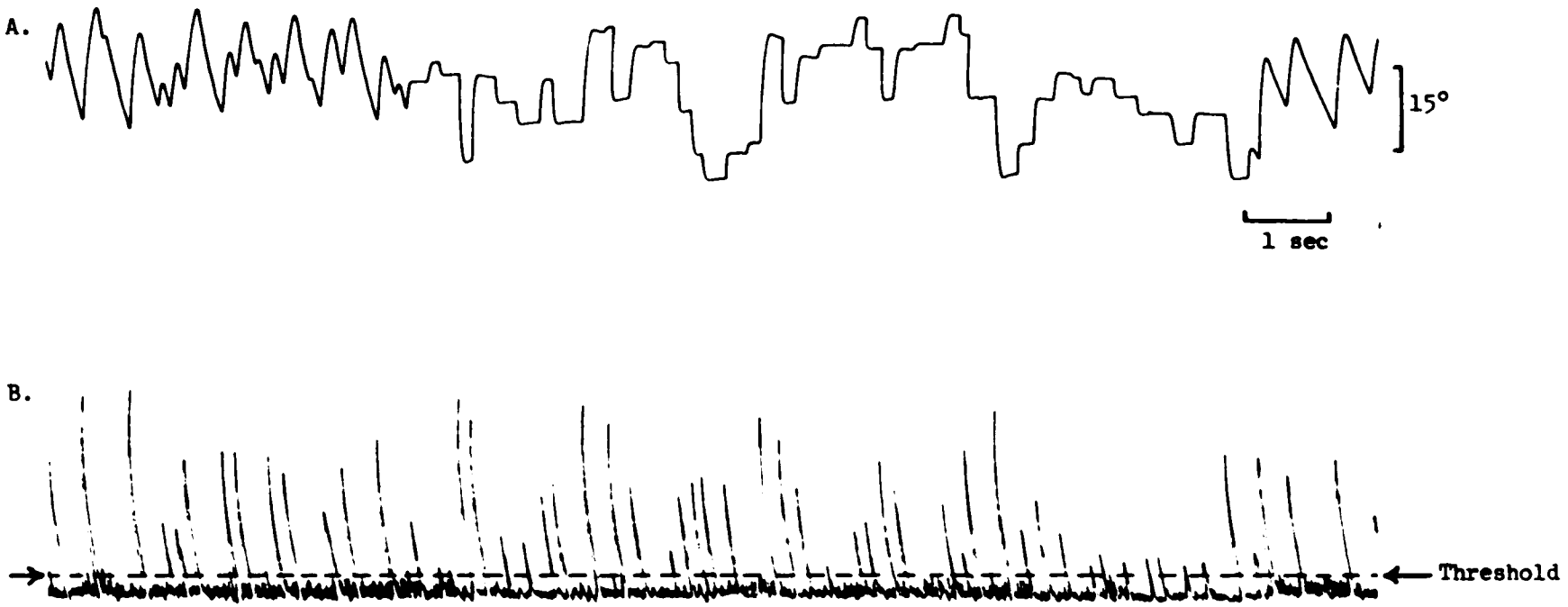

Fig. 3.13. Experimentally obtained EOG and its decision function.
A. Experimentally obtained EOG waveform containing nystagmus.
B. Decision function computed by 'likelihood ratio detector' technique.

make distinction between a saccade and a slow phase might be crucial not to miss saccade or not to produce false detections. In Fig. 3.14, the saccade indications are derived using the same rule as in the case of simulated waveforms, i.e., positive value of 'DFN' implies saccade and a negative value implies a slow phase. The result obtained seems to be acceptable as only a few tiny saccades have been missed. The analysis of Fig. 3.14 yields that less than 10% saccades were missed and no false detection occurred. The missed saccades are circled in A. of Fig. 3.14. Now if threshold is changed to include the noise term (the right hand side of (3.3.8)), the new threshold being shown by two arrows in B. of Fig. 3.13, the indication analysis yields missed saccades $<1\%$ and false detection $<.5\%$. Obviously it is possible to bias the saccade detection to reduce misses to as low as possible by lowering the threshold, but it would mean accepting some false detections. Increasing the number of samples will lower the false detections but will increase misses of tiny saccades. These misses may be avoided by using a smaller sampling interval. The detection scheme allows sampling intervals as small as 1 msec which are adequate for many kinds of saccades.

Functional descriptions for the slow and the quick phases is very crucial to the process of detection. A set of function templates that is optimal for a specific nystagmus velocity may not be suitable for another nystagmus velocity. However, it was discovered by experimentation that for a sampling interval of 2 msec, the detection scheme

optimized for a specific nystagmus velocity works well (with no added misses) over an approximate range of 75% to 125% of that velocity. Since straight-line function templates were used in the implementation, the slopes of these lines were supplied to the program from a switch register. This gave a convenient control for optimization of the detection process for various nystagmus velocities.

The saccade detection of this chapter will be utilized in the next chapter to generate slow phase system responses.

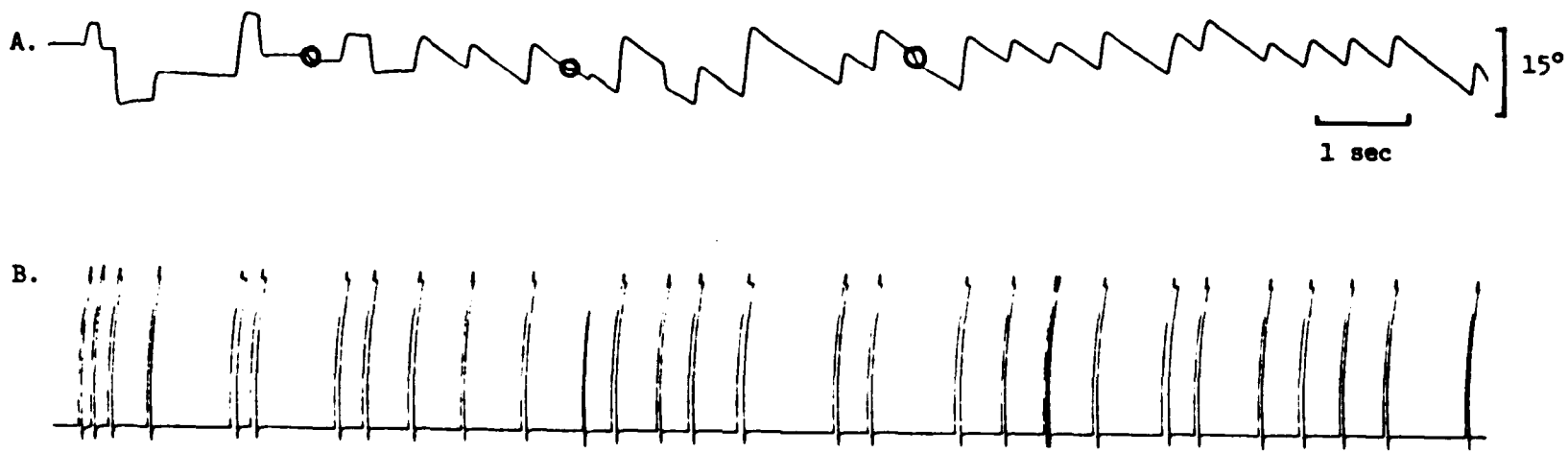

Fig. 3.14. Saccade indications for an experimentally obtained EOG waveform.
A. Experimentally obtained EOG waveform.
B. Saccade indications as determined by 'likelihood ratio detector' technique. Note the missed saccades due to low gain on EOG waveform. The saccade indications waveform was obtained using the same threshold and slow and quick phase definitions as for Fig. 3.13 where the EOG gain is relatively higher.

CHAPTER 4

ON-LINE ANALYSIS OF SLOW PHASE GENERATING SYSTEM RESPONSES

4.1 Introduction

The electrooculograph representing response of the oculomotor control system to optokinetic or vestibular inputs, consists of two types of responses - the saccadic eye movements and the slow phase eye movements. In the last chapter, an on-line saccade detection scheme was described. The present chapter deals with the problem of obtaining slow phase system response characteristics. The characterization of the slow phase system response leads to mathematical modeling of the slow phase system. The slow phase system modeling is the subject of the next chapter.

The basic assumption of analysis done in this chapter is that the two types of eye movements are generated internally by two separate systems - the saccadic system and the slow phase system [25]. A further assumption used in the design of the on-line data reduction technique is that the slow phase system velocity response remains essentially the same during a saccade. This assumption is validated by the fact that the saccadic eye movements are much faster and of smaller duration compared to slow phase eye movements. The experimental results further support this assumption [8].

The saccadic detection technique of the last chapter marks the beginning and the end of a saccade. Once a saccade is detected, it is suppressed in the on-line processing program by subtracting the saccadic

jump from the original position waveform. The slow phase movements are then pieced together to generate cumulative slow phase position (CSPP) waveform. The cumulative slow phase position when differentiated yields slow phase velocity (SPV) waveform. The slow phase velocity is the primary output of the slow phase system and therefore it will be utilized in the next chapter to identify parameters of this system. The slow phase velocity is also a diagnostically important response of the slow phase system [9].

The next section describes the fundamental components of the EOG data processing algorithm which is described in the subsequent section. The results of the algorithm are demonstrated by applying it to the simulated and the experimentally obtained EOG waveforms.

4.2 Components of EOG Data Processing Algorithm

The EOG data processing algorithm has three fundamental components: first the extrapolation, which computes the slow phase eye position during saccadic eye movements; second the differentiator, which computes slow phase velocity from cumulative slow phase position; and third the data smoothing routine, which can be used to smooth or low pass filter the EOG waveform, the cumulative slow phase position waveform and/or the slow phase velocity waveform. These components are described in the next three sections. The performance of each is studied on simulated and experimentally obtained EOG waveforms.

4.2.1 The Approximate Cumulative Slow Phase Position During a Saccade (Extrapolation)

The slow phase velocity during a saccade is assumed to be the velocity just prior to the beginning of a saccade. The truth of this assumption lies in the fact that the saccadic duration is relatively small and the slow phase system remains practically in the same state during a saccade. This fact is used here to derive an equation to be used to extrapolate cumulative slow phase position during a saccade.

Consider a window of (2n+1) EOG position samples $y_0, y_1, y_2,$------, y_{2n} all of which are assumed to be from slow phase movement (see Fig. 4.1). Passing a least square error straight line through these points and calculating its slope to represent slow phase velocity at the nth time, we obtain (see section 4.2.2)

$$u_n = n(y_{2n}-y_0) + (n-1)\,(y_{2n-1}-y_1) + (n-2)\,(y_{2n-2}-y_2) + \text{-------} + 2\,(y_{n+2}-y_{n-2}) + (y_{n+1}-y_{n-1}) \qquad (4.2.1)$$

where u_n denotes the slow phase velocity at the nth time. Assume that the next sample y_{2n+1} at (2n+1)th time belongs to a saccade. At this point we need to extrapolate the slow phase position. Let $\hat{y}_{2n+1}$ denote the extrapolated slow phase position. To keep the window width constant at (2n+1) samples, we will drop y_0 to include $\hat{y}_{2n+1}$. The slow phase velocity computed from this new window using the least square error straight line fit is given by

$$u_{n+1} = n(\hat{y}_{2n+1}-y_1) + (n-1)\,(y_{2n}-y_2) + (n-2)\,(y_{2n-1}-y_3) + \text{-------} + 2\,(y_{n+3}-y_{n-1}) + (y_{n+2}-y_n) \qquad (4.2.2)$$

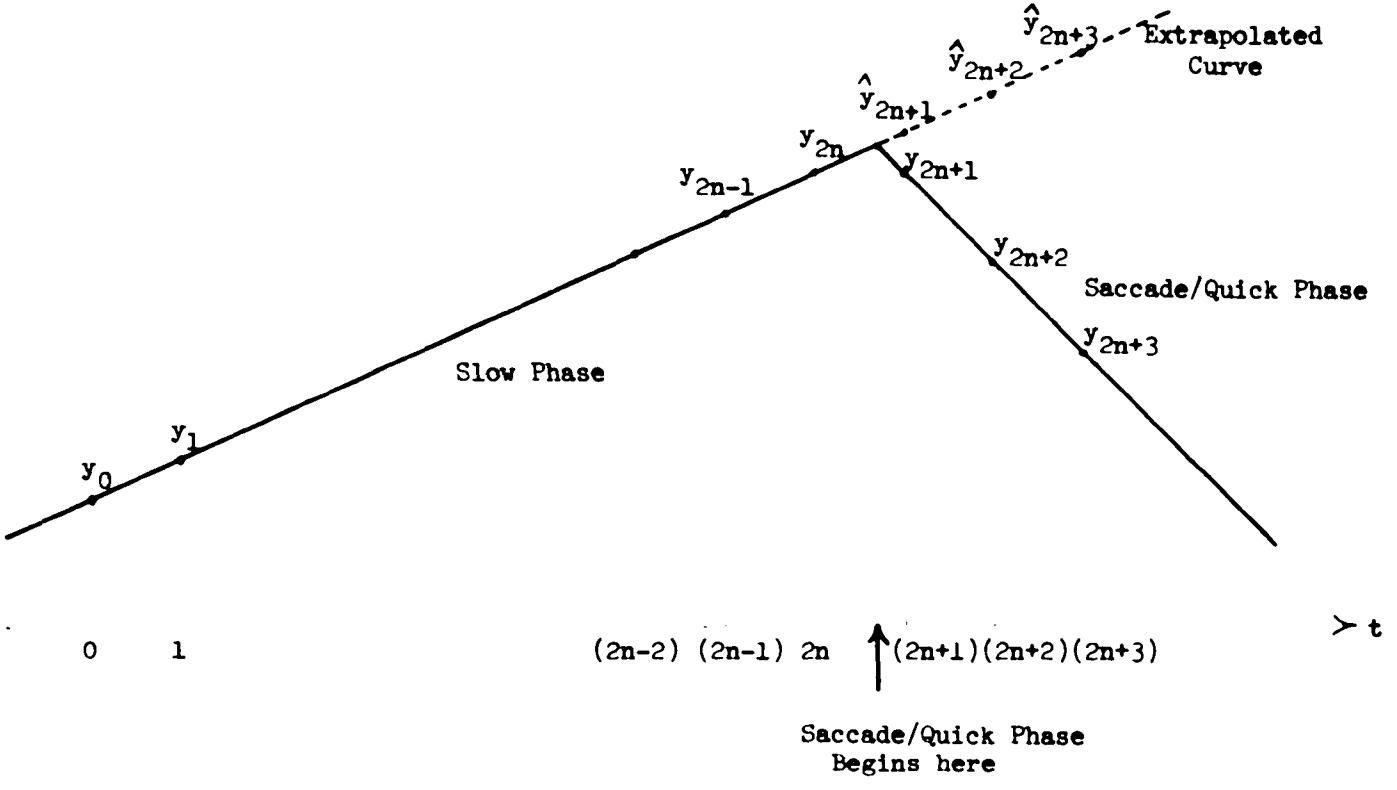

Fig. 4.1. Extrapolation of slow phase position during a saccade/quick phase.

By assumption as stated above, we have

$$u_{n+1} = u_n \tag{4.2.3}$$

From (4.2.1), (4.2.2) and (4.2.3), one can obtain

$$\hat{y}_{2n+1} = \frac{1}{n} \sum_{i=1}^{2n} y_i - y_0 \tag{4.2.4}$$

To estimate $\hat{y}_{2n+2}$, the already computed $\hat{y}_{2n+1}$ is used to give

$$\hat{y}_{2n+2} = \frac{1}{n} \left(\sum_{i=2}^{2n} y_i + \hat{y}_{2n+1} \right) - y_1 \tag{4.2.5}$$

Similarly $\hat{y}_{2n+3}$ is estimated using previous estimates $\hat{y}_{2n+2}$ and $\hat{y}_{2n+1}$ as follows

$$\hat{y}_{2n+3} = \frac{1}{n} \left(\sum_{i=3}^{2n} y_i + \sum_{j=2n+1}^{2n+2} \hat{y}_j \right) - y_2 \tag{4.2.6}$$

or in general we can write

$$\hat{y}_{2n+k} = \frac{1}{n} \left(\sum_{i=k}^{2n} y_i + \sum_{j=2n+1}^{2n+k-1} \hat{y}_j \right) - y_{k-1} \quad \text{for } k \leq 2n$$

$$= \frac{1}{n} \sum_{j=k}^{2n+k-1} \hat{y}_j - \hat{y}_{k-1} \quad \text{for } k > 2n+1 \tag{4.2.7}$$

The equations (4.2.4) and (4.2.5) can also be used to derive recursive formula as follows: substituting (4.2.4) in (4.2.5) and simplifying, we will get

$$\hat{y}_{2n+2} = \hat{y}_{2n+1} + \frac{1}{n} (\hat{y}_{2n+1} - y_1) + (y_0 - y_1) \tag{4.2.8}$$

or in general we can write

$$\hat{y}_{2n+k} = \hat{y}_{2n+k-1} + \frac{1}{n} (\hat{y}_{2n+k-1} - y_{k-1}) + (y_{k-2} - y_{k-1}) \quad \text{for } k \leq 2n+1$$

$$= \hat{y}_{2n+k-1} + \frac{1}{n} (\hat{y}_{2n+k-1} - \hat{y}_{k-1}) + (y_{k-2} - \hat{y}_{k-1}) \quad \text{for } k = 2n+2$$

$$= \hat{y}_{2n+k-1} + \frac{1}{n}(\hat{y}_{2n+k-1} - \hat{y}_{k-1}) + (\hat{y}_{k-2} - \hat{y}_{k-1}) \text{ for } k > 2n+2 \tag{4.2.9}$$

If an equation for $\hat{y}_{2n+1}$ is written using (4.2.8), it involves $\hat{y}_{2n}$, y_0 and y_{-1}. Now if (2n+1) represents the first time in the quick phase, y_{2n} is available in place of $\hat{y}_{2n}$. Thus using y_{2n} for $\hat{y}_{2n}$, the equation for $\hat{y}_{2n+1}$ is written as

$$\hat{y}_{2n+1} = y_{2n} + \frac{1}{n}(y_{2n} - y_0) + (-y_0 + y_{-1}) \tag{4.2.10}$$

Now let us define $\Delta = \frac{1}{n}(y_{2n} - y_0) + (-y_0 + y_{-1})$ (4.2.11)

where 'Δ' represents the change in position from the time 2n to the time 2n+1, and the position samples prior to the beginning of a quick phase determine its value. In view of (4.2.11), (4.2.10) can be written as

$$\hat{y}_{2n+1} = y_{2n} + \Delta \tag{4.2.12}$$

Now if Δ is used to estimate each position sample during a quick phase, i.e.

$$\hat{y}_{2n+j} = \hat{y}_{2n+j-1} + \Delta \tag{4.2.13}$$

then we are basing all our estimates $\hat{y}_{2n+1}$, $\hat{y}_{2n+2}$ ----- etc. on just three positions y_0, y_{-1} and y_{2n} used to calculate Δ. It gives us a computational advantage, but introduces inaccuracy by the amount the samples prior to the quick phase define other than a perfect straight line. The implementation of (4.2.9) was compared with this simplified implementation and no difference was found for extrapolation window width of 100 msec or less. Thus this simplified extrapolation will be used in the subsequent sections unless the window width is increased over this limit.

4.2.2 A Least Square Error Digital Differentiator

A digital differentiator is needed in order to generate velocity from position samples. A number of algorithms [1], [20], [23], [34] have been developed primarily for use on general-purpose computers. The complexity and timing requirement of these algorithms inhibits their use on microprocessor-based systems. In this section a simple digital differentiator algorithm is derived on the basis of using a least-squares approach to fit a straight line to the data. The frequency response of such a differentiator is studied to evaluate its performance when used on EOG signals.

Let us consider (2n+1) position samples y_0, y_1, y_2 -----, y_{2n}. Assume that these samples are uniformly spaced at Δt intervals of time. Let the straight line used to represent this data be given by

$$y(t) = \hat{a} + \hat{b}t \tag{4.2.14}$$

so that

$$u(t) = \frac{dy}{dt} = \hat{b} \tag{4.2.15}$$

$u(t)$ or $\hat{b}$ will be estimated by minimizing

$$I = \sum_{i=0}^{2n} (a + bt_i - y_i)^2 \tag{4.2.16}$$

where $t_i = i.\Delta t$

To minimize I we set its partial derivatives with respect to $\hat{a}$ and $\hat{b}$ = 0. That is

$$\frac{\partial I}{\partial \hat{a}} = 2 \sum_{i=0}^{2n} (\hat{a} + \hat{b}t_i - y_i) = 0 \tag{4.2.17}$$

$$\frac{\partial I}{\partial \hat{b}} = 2 \sum_{i=0}^{2n} (\hat{a} + \hat{b}t_i - y_i)\, t_i = 0 \tag{4.2.18}$$

Rewriting (4.2.17) and (4.2.18) in matrix form yields

$$\begin{bmatrix} \sum_{i=0}^{2n} 1 & \sum_{i=0}^{2n} t_i \\ \sum_{i=0}^{2n} t_i & \sum_{i=0}^{2n} t_i^2 \end{bmatrix} \begin{bmatrix} \hat{a} \\ \hat{b} \end{bmatrix} = \begin{bmatrix} \sum_{i=0}^{2n} y_i \\ \sum_{i=0}^{2n} y_i t_i \end{bmatrix} \qquad (4.2.19)$$

solving (4.2.19) for $\hat{b}$ yields

$$\hat{b} = \frac{\sum_{i=0}^{2n} 1 \sum_{i=0}^{2n} y_i t_i - \sum_{i=0}^{2n} t_i \sum_{i=0}^{2n} y_i}{\sum_{i=0}^{2n} 1 \sum_{i=0}^{2n} t_i^2 - \sum_{i=0}^{2n} t_i \sum_{i=0}^{2n} t_i} \qquad (4.2.20)$$

Using summation formulae, it can be shown that

$$\sum_{i=0}^{2n} 1 = (2n+1) \qquad (4.2.21)$$

$$\sum_{i=0}^{2n} t_i = n(2n+1)\,\Delta t \qquad (4.2.22)$$

$$\sum_{i=0}^{2n} t_i^2 = \frac{1}{3} n(2n+1)(4n+1)(\Delta t)^2 \qquad (4.2.23)$$

Substituting (4.2.21), (4.2.22) and (4.2.23) in (4.2.20) and subsequent simplification yields

$$\hat{b} = \frac{3 \sum_{i=0}^{n-1} (n-i)(y_{2n-i} - y_i)}{n(n+1)(2n+1).\,\Delta t} \qquad (4.2.24)$$

The $\hat{b}$ in (4.2.24) represents the velocity associated with the straight line fit to samples y_0, y_1, y_2, -----, y_{2n}. In order to give equal emphasis to the points around the point for which the velocity is being estimated, $\hat{b}$ will be assigned to be the velocity at the midpoint of the data window. Thus

$$u_n = \frac{3 \sum_{i=0}^{n-1} (n-i)(y_{2n-i}-y_i)}{n(n+1)(2n+1).\Delta t} \qquad (4.2.25)$$

or

$$u_n = K(n, \Delta t) \sum_{i=0}^{n-1} (n-i)(y_{2n-i}-y_i) \qquad (4.2.26)$$

where

$$K(n,\Delta t) = \frac{3}{n(n+1)(2n+1)\ \Delta t} \qquad (4.2.27)$$

As an example let us consider a window width of 9 so that n=4. From (4.2.25) and (4.2.24) we get

$$K(4,\Delta t) = \frac{3}{4.5.9.\ \Delta t} = \frac{1}{60\ \Delta t} \qquad (4.2.28)$$

and

$$u_4 = \frac{1}{60\ \Delta t} \sum_{i=0}^{3} (4-i)(y_{8-i} - y_i) \qquad (4.2.29)$$

or

$$u_4 = \frac{1}{60\ \Delta t}\left[4(y_8 - y_0) + 3\ (y_7 - y_1) + 2\ (y_6 - y_2) + (y_5 - y_3)\right] \qquad (4.2.30)$$

When (4.2.26) is applied to a window of samples y_{-n}, y_{-n+1}, y_{-n+2}, ----, y_0, y_1, ----, y_{n-1}, y_n so that the midpoint sample is y_0, the associated velocity is given by

$$u_0 = K(n,\Delta t)\left[\sum_{i=1}^{n} i\ (y_i - y_{-i})\right] \qquad (4.2.31)$$

For $y_i = e^{jwi\Delta t}$ where $j = \sqrt{-1}$, u_0 becomes the transfer function of the differentiator. Denoting the transfer function by H(w), we have

$$H(w) = K(n,\Delta t)\ .\ 2j \sum_{i=1}^{n} i \sin i\, w\Delta t \qquad (4.2.32)$$

For n=4, we get

$$H(w) = \frac{j}{30\,\Delta t}\left[4 \sin 4w\Delta t + 3 \sin 3w\Delta t + 2 \sin 2w\Delta t + \sin w\Delta t\right] \quad (4.2.33)$$

The non-recursive differentiator of equation (4.2.26) can be realized as recursive filter as follows: the velocities u_n, u_{n+1} and u_{n+2} as determined from (4.2.26) are given by

$$u_n = K(n,\Delta t) \sum_{i=0}^{n-1} (n-i)\,(y_{2n-i} - y_i) \quad (4.2.34)$$

$$u_{n+1} = K(n,\Delta t) \sum_{i=1}^{n} (n+1-i)\,(y_{2n+2-i} - y_i) \quad (4.2.35)$$

$$u_{n+2} = K(n,\Delta t) \sum_{i=2}^{n+1} (n+2-i)\,(y_{2n+4-i} - y_i) \quad (4.2.36)$$

Combining (4.2.34) and (4.2.35) we can obtain

$$u_{n+1} = u_n + K(n,\Delta t)\left[n(y_{2n+1} + y_0) - \sum_{i=1}^{2n} y_i\right] \quad (4.2.37)$$

Similarly combining (4.2.35) and (4.2.36) we can obtain

$$u_{n+2} = u_{n+1} + K(n,\Delta t)\left[n(y_{2n+2} + y_1) - \sum_{i=2}^{2n+1} y_i\right] \quad (4.2.38)$$

and now we can combine (4.2.37) and (4.2.38) to give

$$u_{n+2} = 2u_{n+1} - u_n + K(n,\Delta t)\left[n(y_{2n+2} - y_{2n+1}) + n(y_1 - y_0) + (y_1 - y_{2n+1})\right] \quad (4.2.39)$$

Equation (4.2.39) can be realized as a second order digital filter [15], [18]. It may be noted that the output of such a filter lags the latest input by n sampling intervals for a differentiator based on (2n+1) data samples.

The frequency response of the above differentiator is plotted in Fig. 4.2 for n = 2,3 and 4. It is obvious from these plots that as the number of samples are increased, the response approximates a differentiator frequency response. The cut-off frequency though decreases for the same sampling interval. This will not pose any problem for processing slow phase EOG data as its frequency spectrum is less than 1 Hz [25]. Fig. 4.3 shows the pass band of a 17 point (i.e. n=8) digital differentiator operating on a waveform sampled at 1 msec. sampling interval. The plot in Fig. 4.3 was obtained by applying a constant sinusoidal input to the differentiator and recording its output as the frequency was varied from 0Hz to 50Hz. When compared with an ideal differentiator, this response fairly matches with the latter.

In order to evaluate the performance of the digital differentiator with an analog differentiator, a simulated EOG waveform was applied simultaneously to these devices and their outputs are shown in Fig. 4.4. The digital device seems to have about the same performance as the analog one. To obtain a closer view of this, Fig. 4.5 shows the outputs of two differentiators on an expanded time scale. It is obvious from this figure that a digital differentiator response is superior to that of an analog one. There is not only shape distortion, but definite time delay in the response of analog device. This problem may be serious when observing exact transitions in EOG velocity waveforms. The fact that analog differentiator's output is delayed is further demonstrated by studying the phase relationship between the two outputs. The two outputs are shown for a 10Hz sine wave input and it can be seen from Fig. 4.6

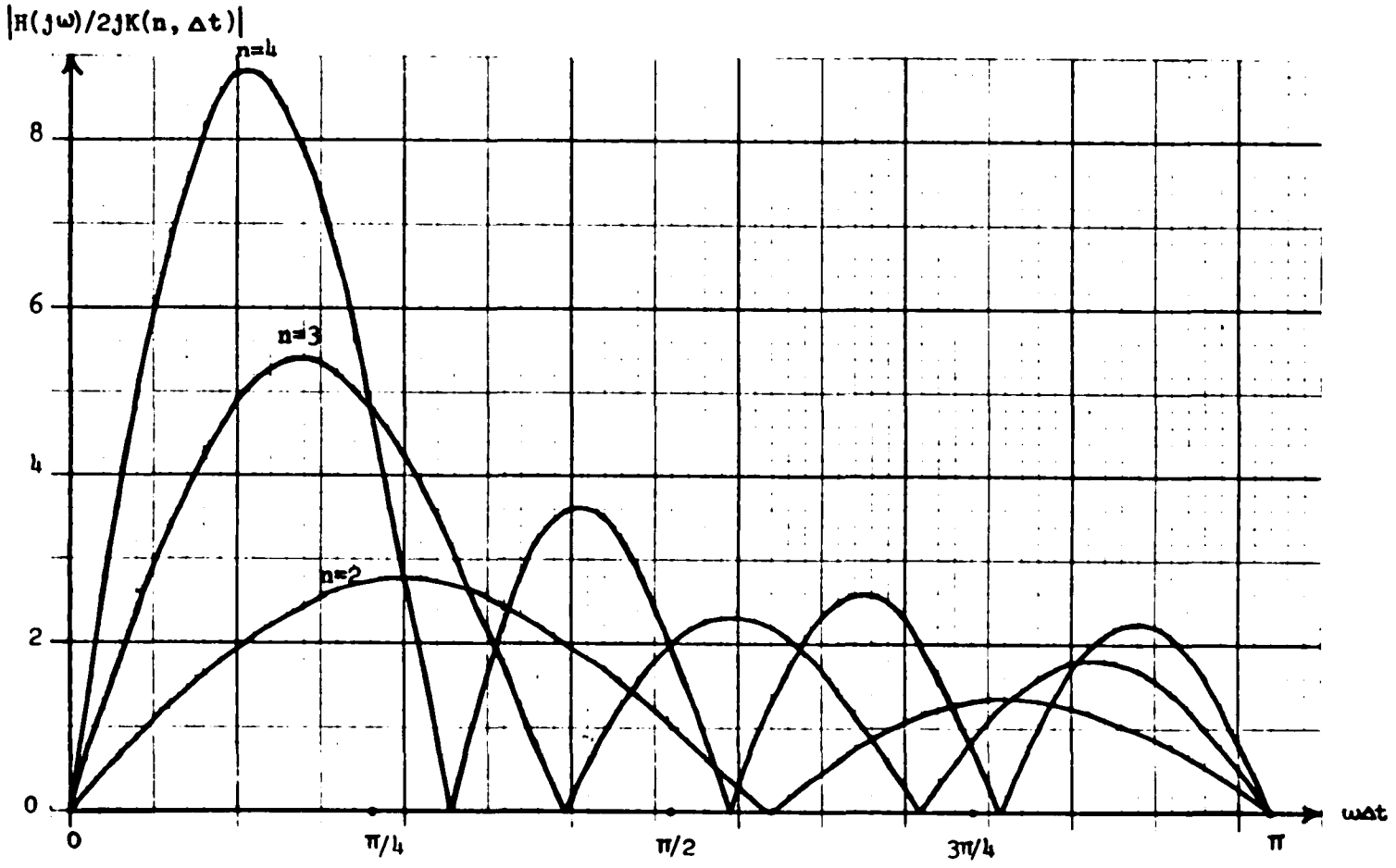

Fig. 4.2. Frequency response of the digital differentiators designed by least squares error straight line fit.

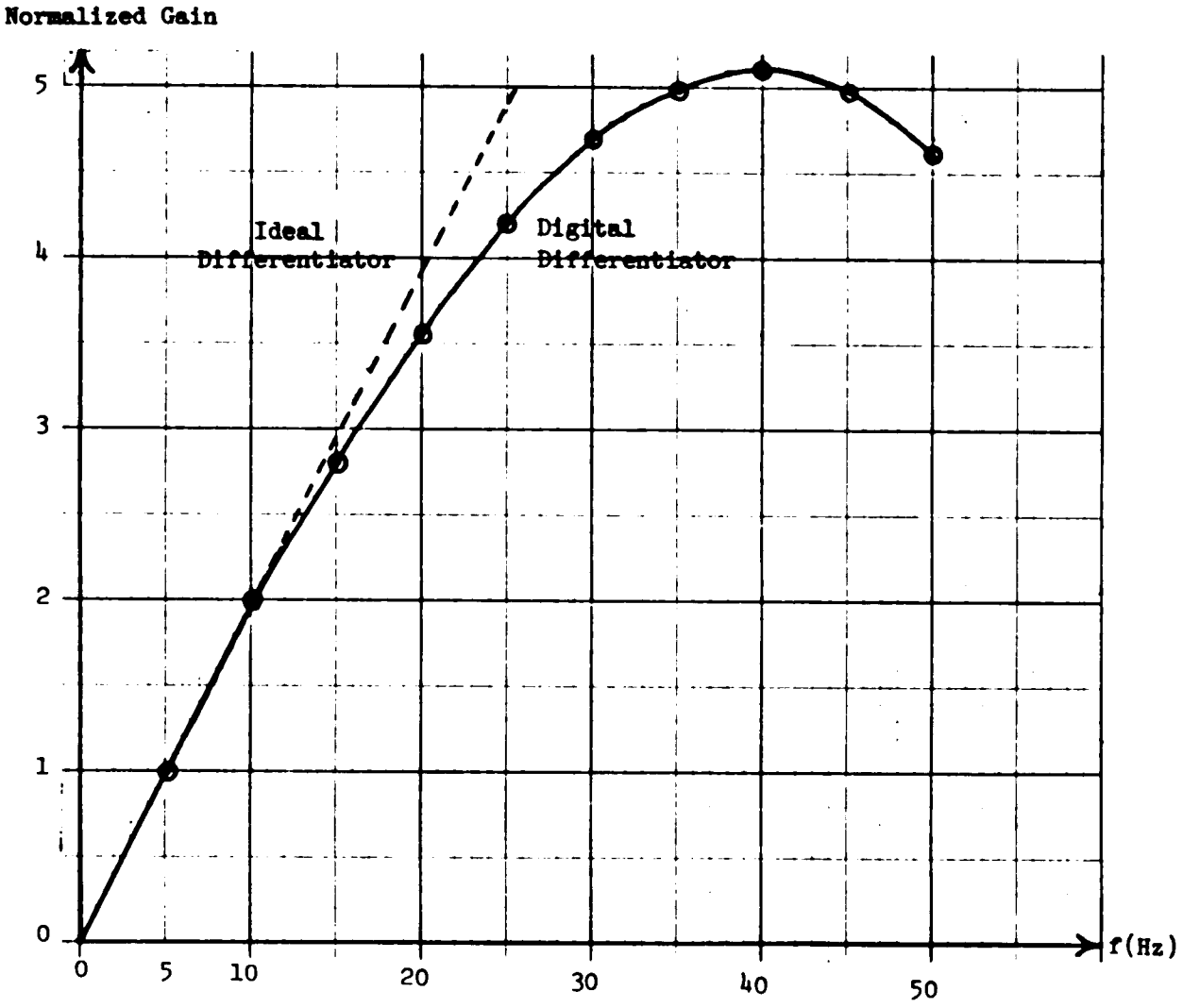

Fig. 4.3. Pass band of a 17-point digital differentiator. Input was sampled at 1 msec interval.

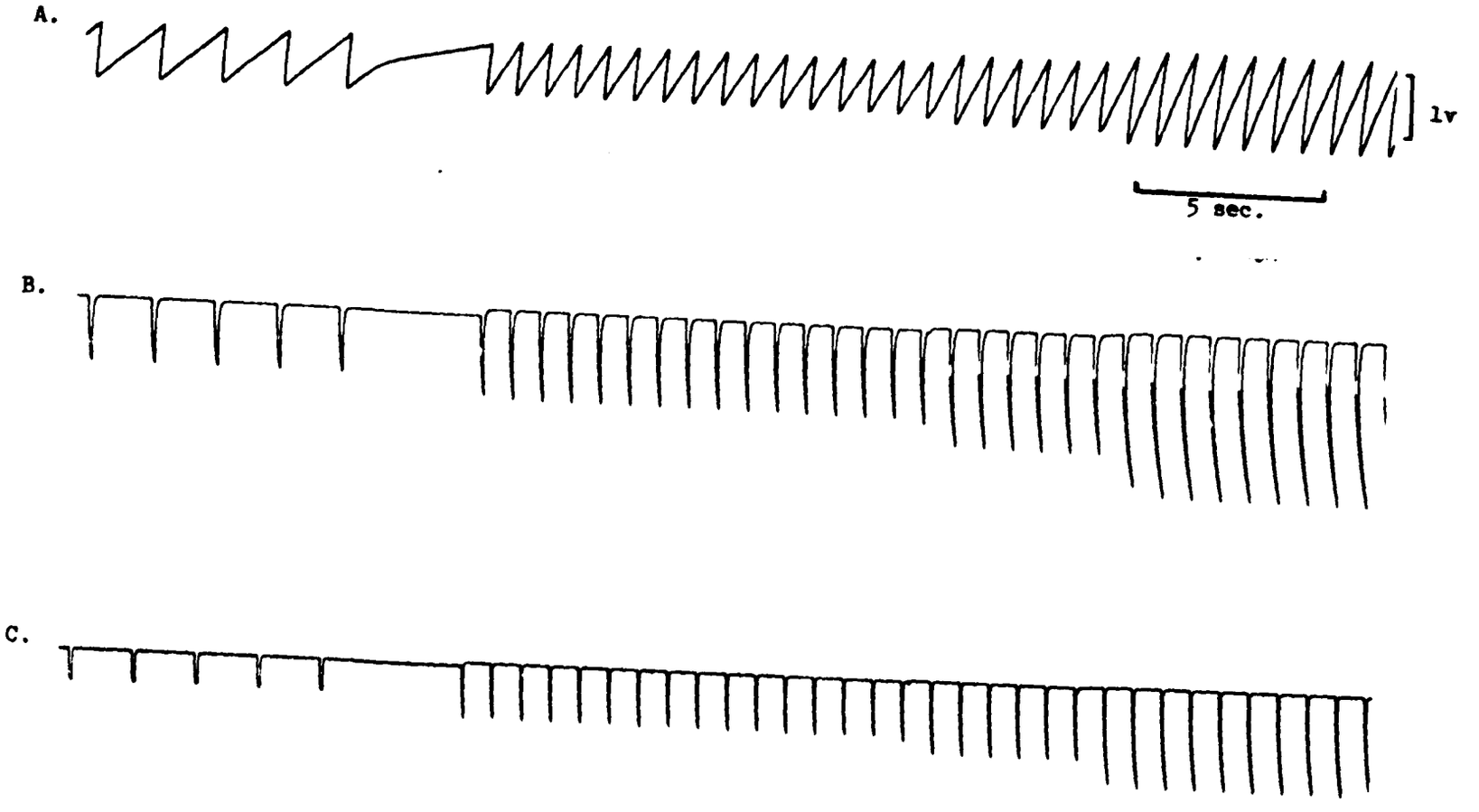

Fig. 4.4. Analog vs. digital differentiation of simulated data. A. Simulated waveform. B. Analog differentiation. C. Digital differentiation.

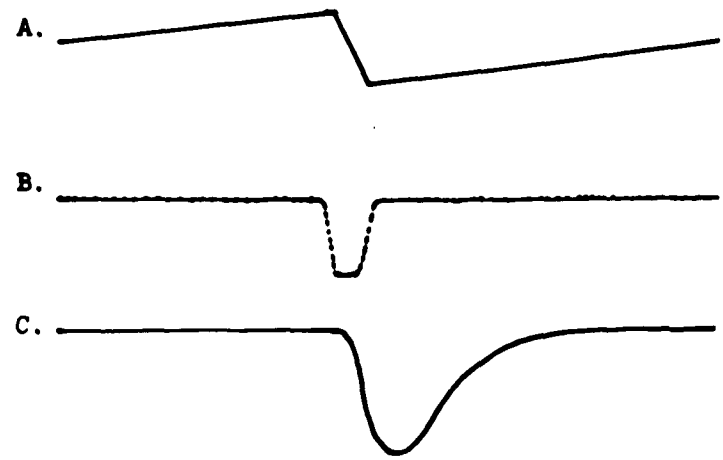

Fig. 4.5. Shape distortion in analog differentiation. A. Simulated waveform. B. Digital differentiation (1 msec. sampling). C. Analog differentiation

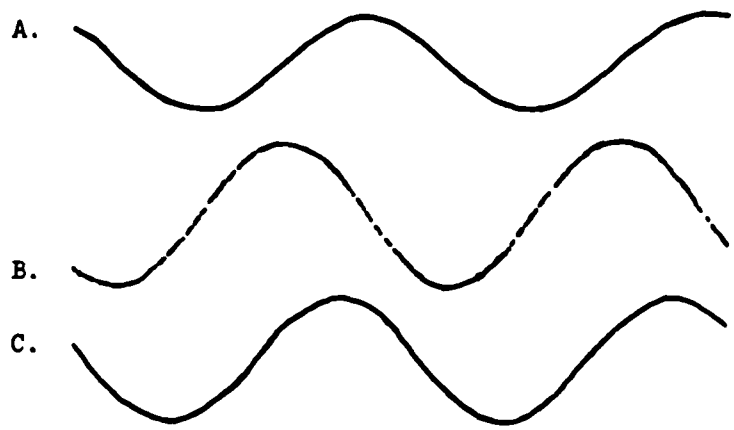

Fig. 4.6 Phase distortion in analog differentiation. A. Simulated waveform (10Hz). B. Digital differentiation (1 msec. sampling). C. Analog differentiation.

that the analog output is delayed by as much as 70°.

In the laboratory processing of EOG data, a differentiator is commonly used to obtain slow phase velocity waveform. Fig. 4.7 compares the performance of digital and analog differentiators as they operate upon an experimentally obtained EOG waveform. The differentiated outputs are just about the same from both devices. The only difference seems that the digital differentiator is noisier compared to an analog differentiator. This is even more obvious from Fig. 4.8C where a digital differentiator of 17 point window length was used to differentiate. This is really not a problem as a digital differentiator can produce smoother response when larger number of points are used. Thus, a digital differentiator response is easily controllable and does not suffer from the problem of delay in response.

4.2.3 Digital Filters for EOG Waveforms

The banwidth of nystagmus may be well over 100Hz, but most of the spectral power has been reported to be below 30Hz for most applications [22]. The noise above this frequency may be filtered before any processing is done. The processed waveforms may also need to be filtered. This can be done by employing appropriate analog or digital filters. To design an all digital processing scheme running in real time, appropriate digital filters should be considered. In this section, we consider two approaches, one which is based upon the least square error straight line fit of the last section and the

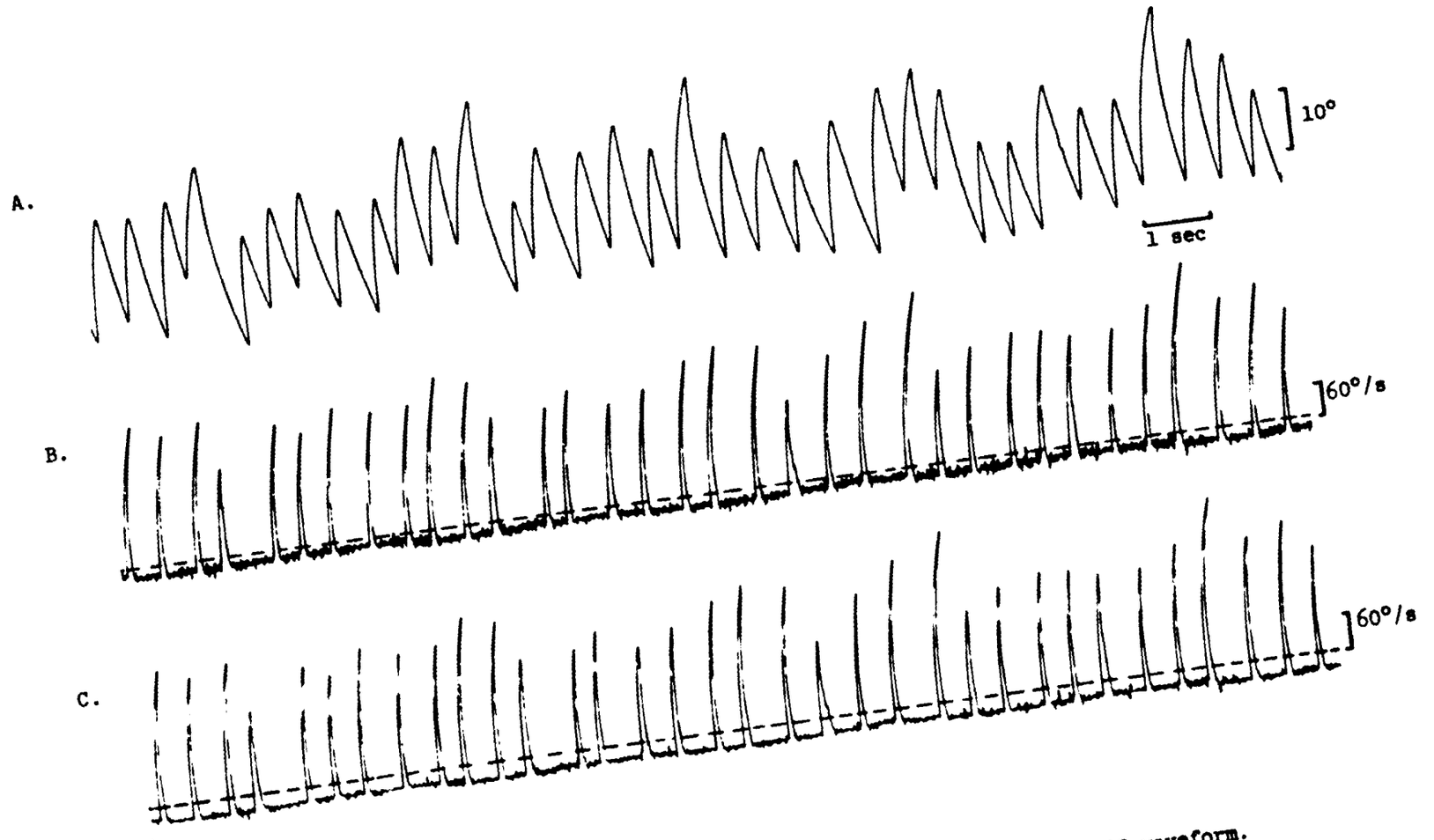

Fig. 4.7. Digital vs. analog differentiation of an EOG waveform. A. An EOG waveform. B. Digitally differentiated EOG waveform. C. Analog differentiation of EOG waveform.

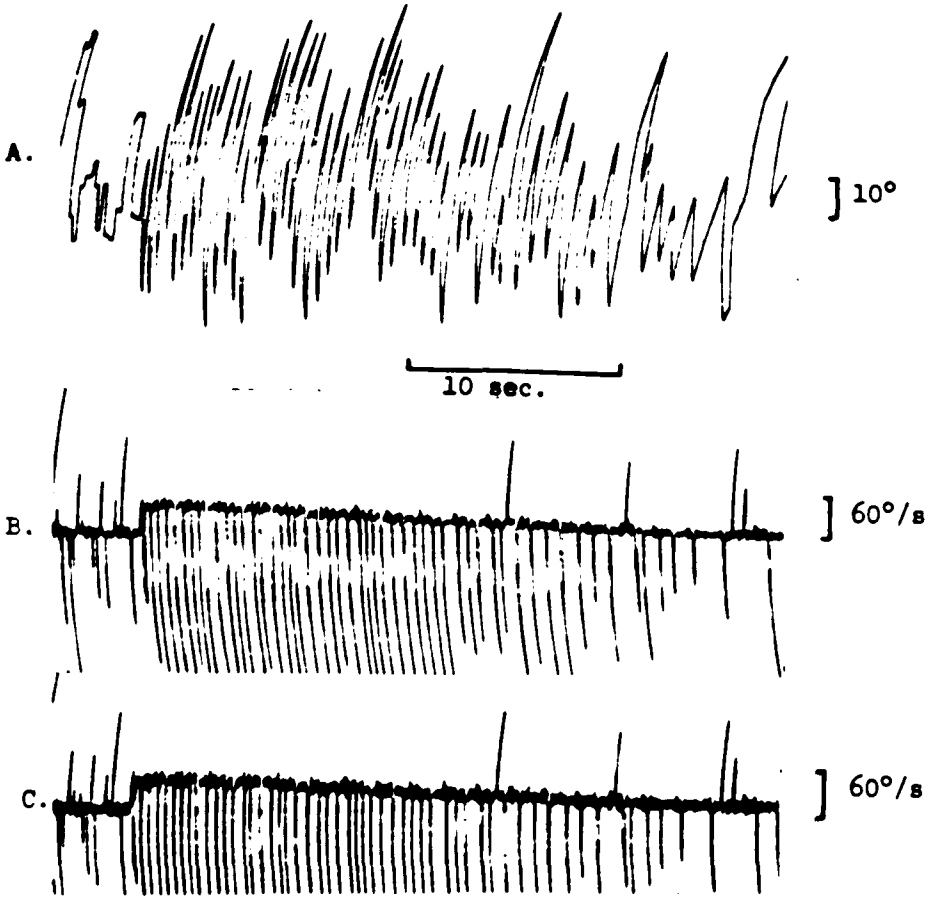

Fig. 4.8. Analog vs digital differentiation.
A. EOG waveform. B. Slow phase velocity from analog differentiator. C. Slow phase velocity from digital differentiator.

other based upon the idea of 'median' of a window of data.

If a least square error straight line $\hat{a} + \hat{b}t$ is fitted to $(2n+1)$ data points y_{-n}, y_{-n+1}, -------- y_0, ------ y_{n-1}, y_n and the estimated $\hat{a}$ is used to represent the smoothed value of y_0 denoted by $\hat{y}_0$, then it is given by [14]

$$\hat{y}_0 = \frac{1}{(2n+1)} \sum_{i=-n}^{n} y_{n+i} \qquad (4.2.40)$$

the corresponding transfer function being [14]

$$H(w) = \frac{\sin (n+\frac{1}{2})w\Delta t}{(2n+1)\sin(w\Delta t/2)} \qquad (4.2.41)$$

The well-known problem with this filter is that a single point in error affects all the subsequent points within the range of smoothing window width. Thus this filter is suitable where high frequency spikes are non-existent such as cumulative slow phase position.

The 'spiky' data such as the slow phase velocity may be better filtered by a 'median filter'. A median filter considers the median of a window of data to represent the middle point in the window, thereby ignoring points in gross error. This type of filter was found to be a slightly better filter when used on slow phase velocity waveform. However, there is no direct way to compare the two filters, since a smoothing filter is a linear device and a median filter is a non-linear device.

4.3 Cumulative Slow Phase Position (CSPP) and Slow Phase Velocity (SPV) Algorithm

The saccadic detection of the last chapter, the extrapolation and differentiation of the previous section are put together to design an

algorithm which generates the cumulative slow phase position and the slow phase velocity along with other useful waveforms. The hardware configuration is exactly the same as of saccadic detection of the last chapter, i.e., the PDP-8/E computer is interfaced to the experimental process producing data and also to the monitoring devices to generate resulting waveforms. The algorithm is described in this section and the experimental results are the subject of section 4.4.

The experimentally generated EOG waveform is sampled and the samples are stored in a buffer. The conversion is done by a 10-bit analog to digital converter. The sampling interval can be controlled from a programmable real-time clock. The 10-bit digital word is sign extended to adapt to the 12-bit accumulator of PDP-8/E computer. The data processing of the experimentally generated position data is described in flow chart of Fig. 4.9 and in software block diagram of Fig. 4.10.

The first step of processing is to detect the presence of saccades. The 'likelihood ratio detector' of the last chapter is used for this purpose. The saccadic detection program generates a value for a function called the decision function (DFN). The sign of DFN is used to indicate the origin of sampled data point. The positive sign of DFN indicates the presence of a saccade and the negative sign indicates the absence of one. This way the beginning and the end of a saccadic movement is marked.

The second step of processing involves generating cumulative slow phase position. Fig. 4.11 shows the schematic for the generation of the cumulative slow phase position waveform. When a first saccade is

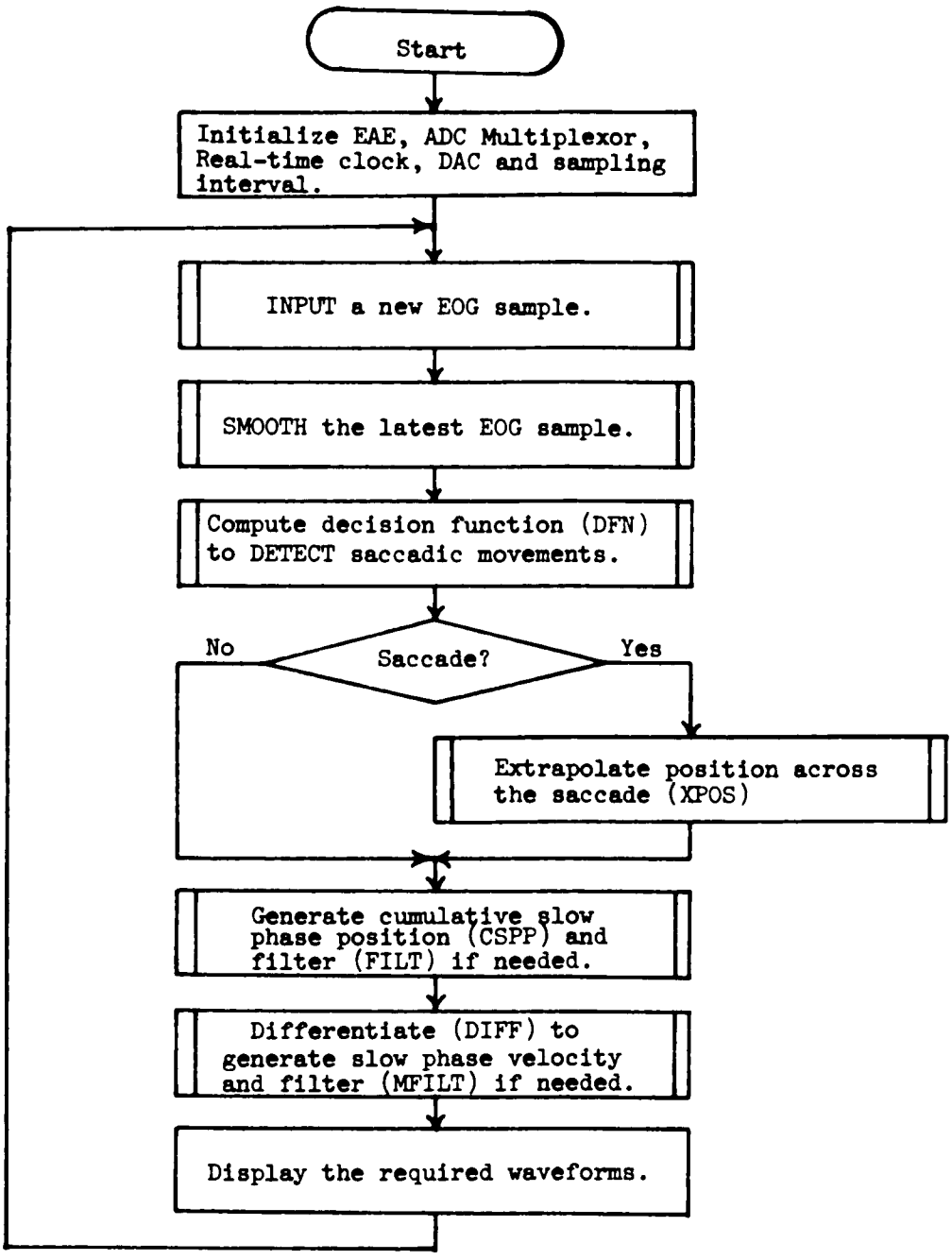

Fig. 4.9. Main program flow chart of EOG data processing for saccadic detection and slow phase velocity generation.

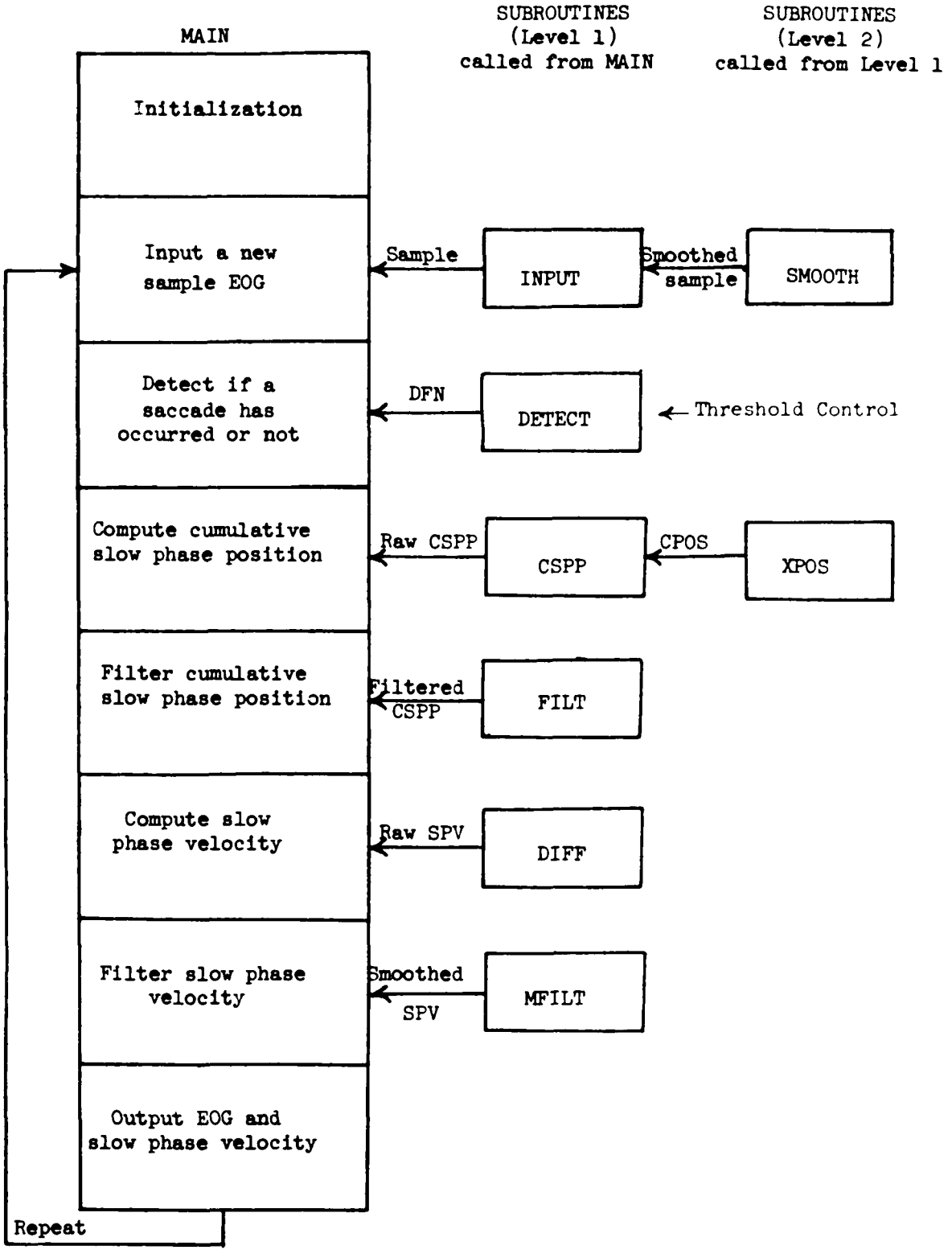

Fig. 4.10. Software components of saccadic detection and slow phase velocity and cumulative position generation program.

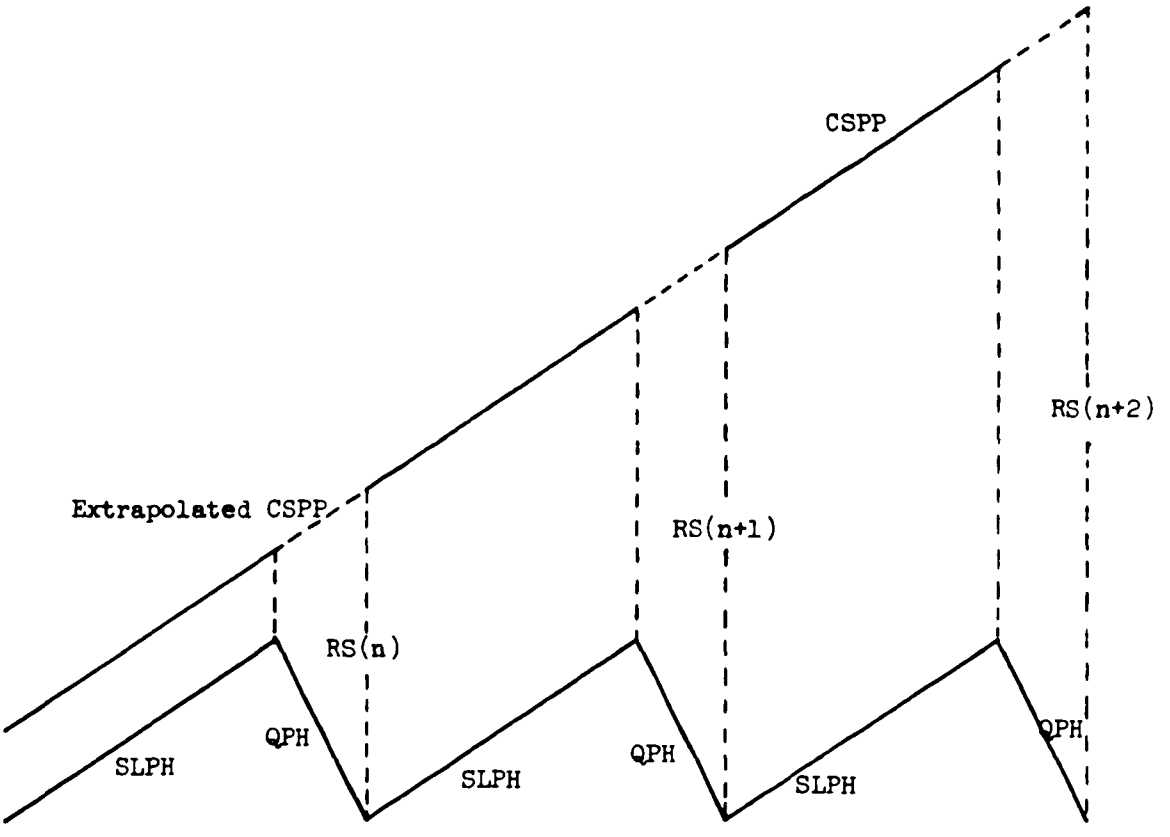

Fig. 4.11. Cumulative slow phase position (CSPP) generation schematic.

first detected, a few samples (2 or 3 for a window of 5 samples) before the first detected saccadic point are replaced by the extrapolated points. This is done to overcome any detection-delay, since a quick phase is not detected unless the detection window consists of sufficient points from the oncoming quick phase to turn DFN positive (see Chapter 3 for details). The extrapolation is done using EOG samples before the points to be replaced which belong to the slow phase eye movement. During the saccadic movement, the extrapolation is continuously repeated on the previously extrapolated and the actual slow phase points to generate new extrapolated positions (see section 4.2.1 for details). This way, the slow phase waveform is extended through the saccade using a line with the same slope as the slope at the end of the slow phase. When an end of the quick phase is detected, the saccadic jump for the immediate past saccade is computed by subtracting the measured EOG value from the extrapolated value. The negative of the saccadic jump is added to all the points on the oncoming slow phase movement. This process removes the saccadic movement and pieces together the two slow phase movement, generating a cumulative slow phase position (CSPP) waveform. For the next saccade, the extrapolation is done using the points on the CSPP waveform preceding it. Now when the next saccadic jump is computed using the extrapolated position at the end of the saccade and the first measured slow phase position from the on-coming slow phase it is representative of accumulated sum of the past two saccades. This sum is called the running sum denoted by RS in Fig. 4.11. RS(n) in the figure is the running sum generated by all the previous 'n'

saccades and is the amount by which the points on the on-coming slow phase, after having encountered n saccades, are offset to compute the corresponding cumulative slow phase position.

It is obvious that the above process of generating cumulative slow phase position can generate values which cannot be accommodated by the 12-bit arithmetic capability of the machine. This does not pose any problem as long as only addition of RS is done to slow phase positions to generate CSPP. However when the extrapolation itself involves points after the 12-bit overflow along with some points before it, the process of extrapolation runs into arithmetic overflow problem. This problem can be overcome by extrapolating only on the EOG slow phase position waveform which precedes the saccade. However, overflow may still occur due to the uncertainty of the type of eye movement preceding the saccade. A solution to this problem is to reformulate the extrapolation process so as to avoid arithmetic overflow condition by scaling the numbers whenever operating near ends and rescaling the results.

The details of marking the beginning and the end of a saccade, extending the saccadic interval on both sides to overcome detection errors, computing the cumulative slow phase position waveform are all described in a flow chart of Fig. 4.12. The flow chart is based upon the assumption that the extrapolation is done only once and its information used for all saccadic points. The symbols used in the flow chart are described below it.

The cumulative slow phase position thus obtained may be filtered if needed. The filtering can be done by an averaging type of smoothing

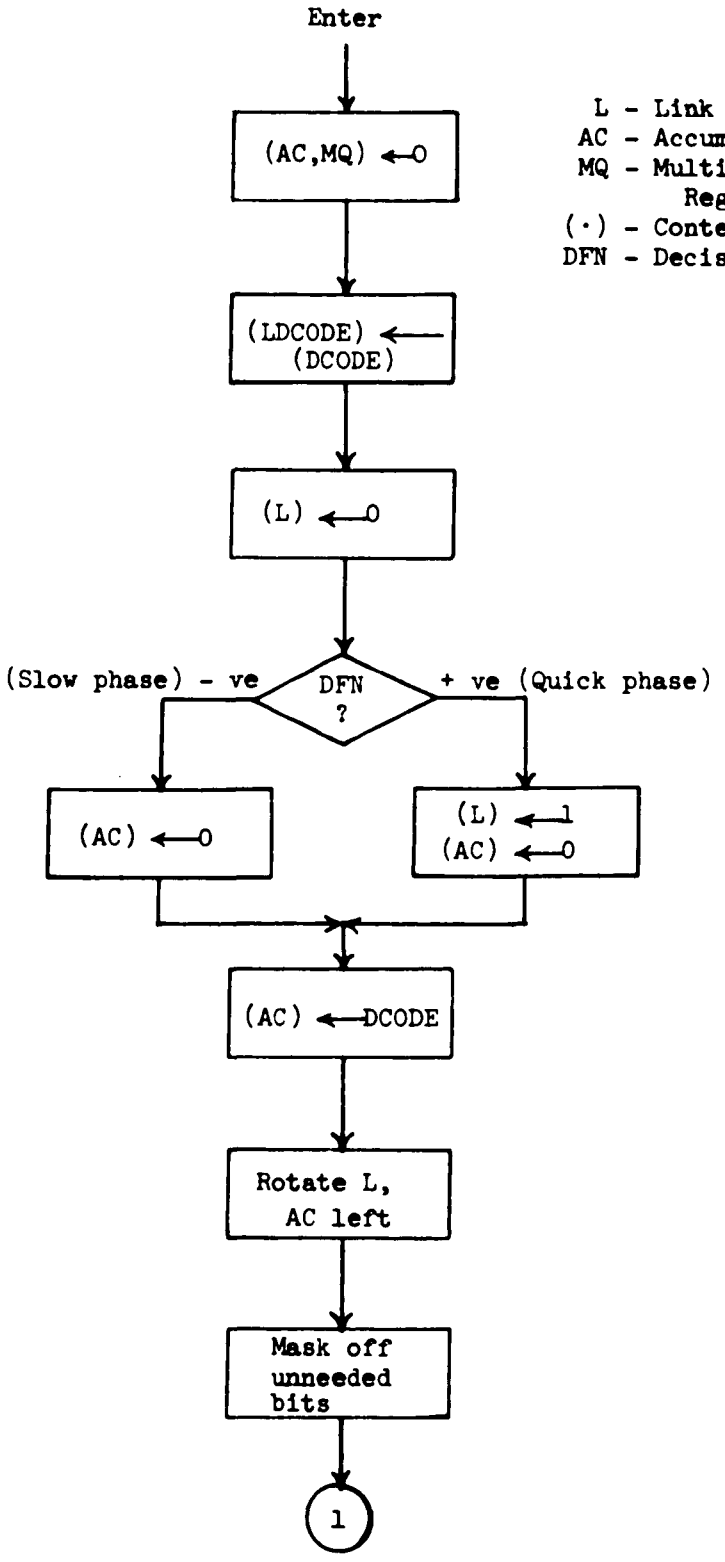

continued on next page

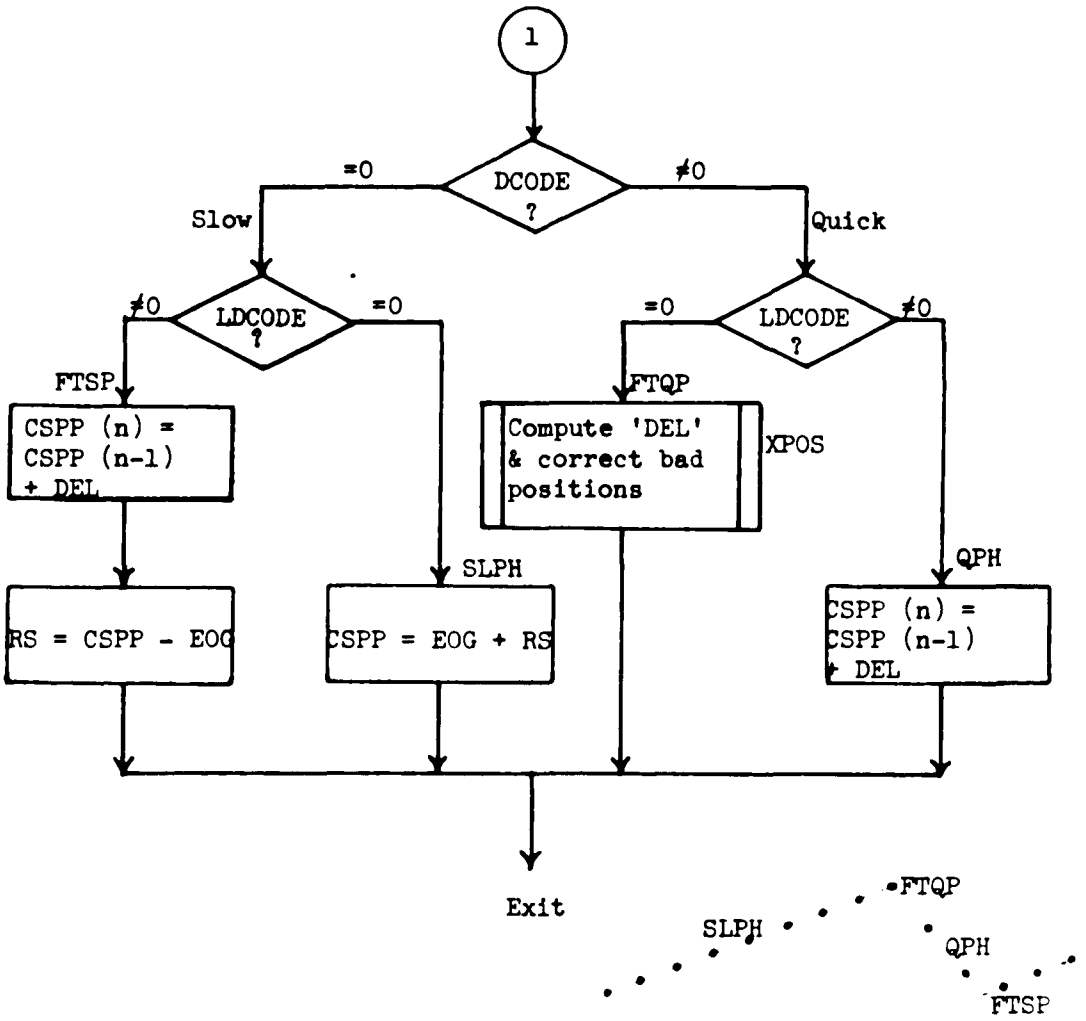

CSPP - Cumulative Slow Phase Position
DCODE - Decision Code
LDCODE - Last Value of DCODE
FTSP - First Time Slow Phase
SLPH - Slow Phase (continuation)
FTQP - First Time Quick Phase
QPH - Quick Phase (continuation)
RS - Running Sum (Accumulated quick phases)
DEL - Delta Change in Slow Phase Position (or CSPP)

Fig. 4.12. Flow chart of Cumulative Slow Phase Position subroutine.

filter or by any other low pass filter which can be implemented without adding too much to the timing requirements. In most cases filtering may not be needed at all.

The last major step of processing is to generate the slow phase velocity. Obviously, the slow phase velocity accuracy will depend on how accurately the cumulative slow phase position represents the slow phases in EOG. The slow phase velocity is obtained by differentiating the cumulative slow phase position; the digital differentiator used for the purpose was described in the last section. Filtering of the resulting velocity waveform may be required. The filtering may be done using the filter of the last section or any such algorithm implementable without jeopardizing on-line processing requirements.

The next section describes the implementation results of the algorithm described above. The results are shown using simulated data and actual experimental data.

4.4 Experimental Results

The algorithm described in the last section was implemented on PDP-8/E computer in assembly language. The incoming EOG data was stored in a full field of 4000_8 words. The cumulative slow phase position values as generated are stored in another field of 4000_8 words and the slow phase velocity in a third field. Even though not all 4000_8 points will be used at any time in any computation, it generates self-wrap-around for the pointer used to store a sample or a computed value into the memory. The algorithm program is stored in field zero of the computer memory. The listing of this program appears in Appendix B.

Fig. 4.13 shows the performance of algorithm in generating the cumulative slow phase position and the slow phase velocity waveform for a simulated waveform containing all types of saccades. The frequency of the saccade varies over a range of 1 to 15Hz for saccades to the left and to the right. The cumulative slow phase position and the corresponding slow phase velocity waveforms are as expected. The last part of Fig. 4.13 shows occurrence of pure saccades with no nystagmus. Those saccades are seen to be removed perfectly and no trace of saccades appear in the CSPP and the SPV. The program is run without any kind of filtering at any stage and it produces very smooth waveforms. The run time for these waveforms is less than 2msec and therefore a sampling of 2msec can be used without running into any real-time problems.

Fig. 4.14 shows how well the algorithm performs on an experimental EOG waveform to generate the cumulative slow phase position waveform and a waveform showing accumulation of quick phase jumps. The accumulated quick phases waveform also shows indirectly if a particular saccade was detected or missed. The waveform C in Fig. 4.14 is the CSPP waveform which is seen to be in accordance with the expected results. The run-time to generate these two waveforms is even less than that required to generate the waveforms in Fig. 4.13 since, in this case, differentiation is not done.

Fig. 4.15 shows the results of algorithm processing of a real EOG waveform. B is a waveform generated by the analog system, the nystagmus velocity coupler which differentiates the waveform and clips positive half or negative half as may be required. D is the cumulative

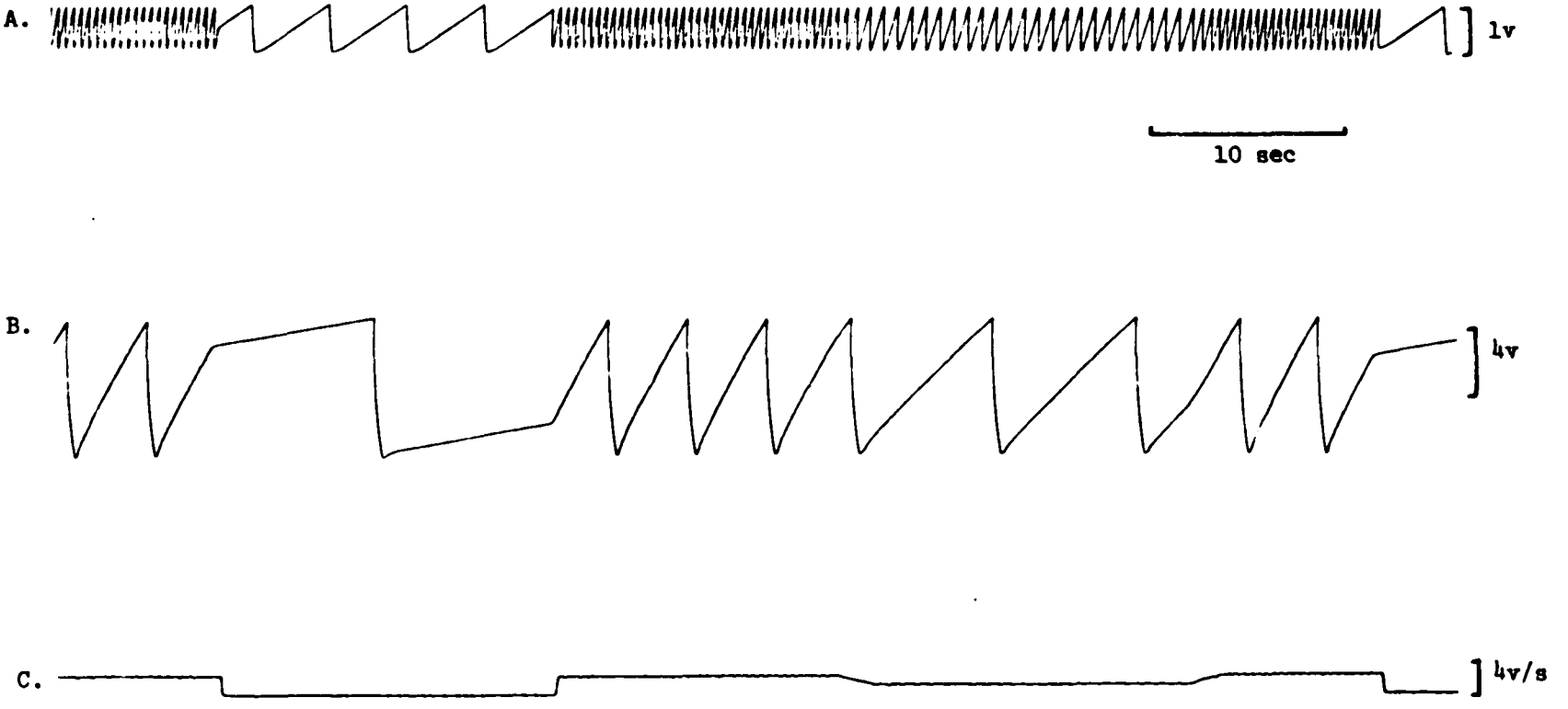

Fig. 4.13. Cumulative slow phase position and slow phase velocity for simulated waveform. A. Simulated waveform. B. Cumulative slow phase position. C. Slow phase velocity. (continued on next page.

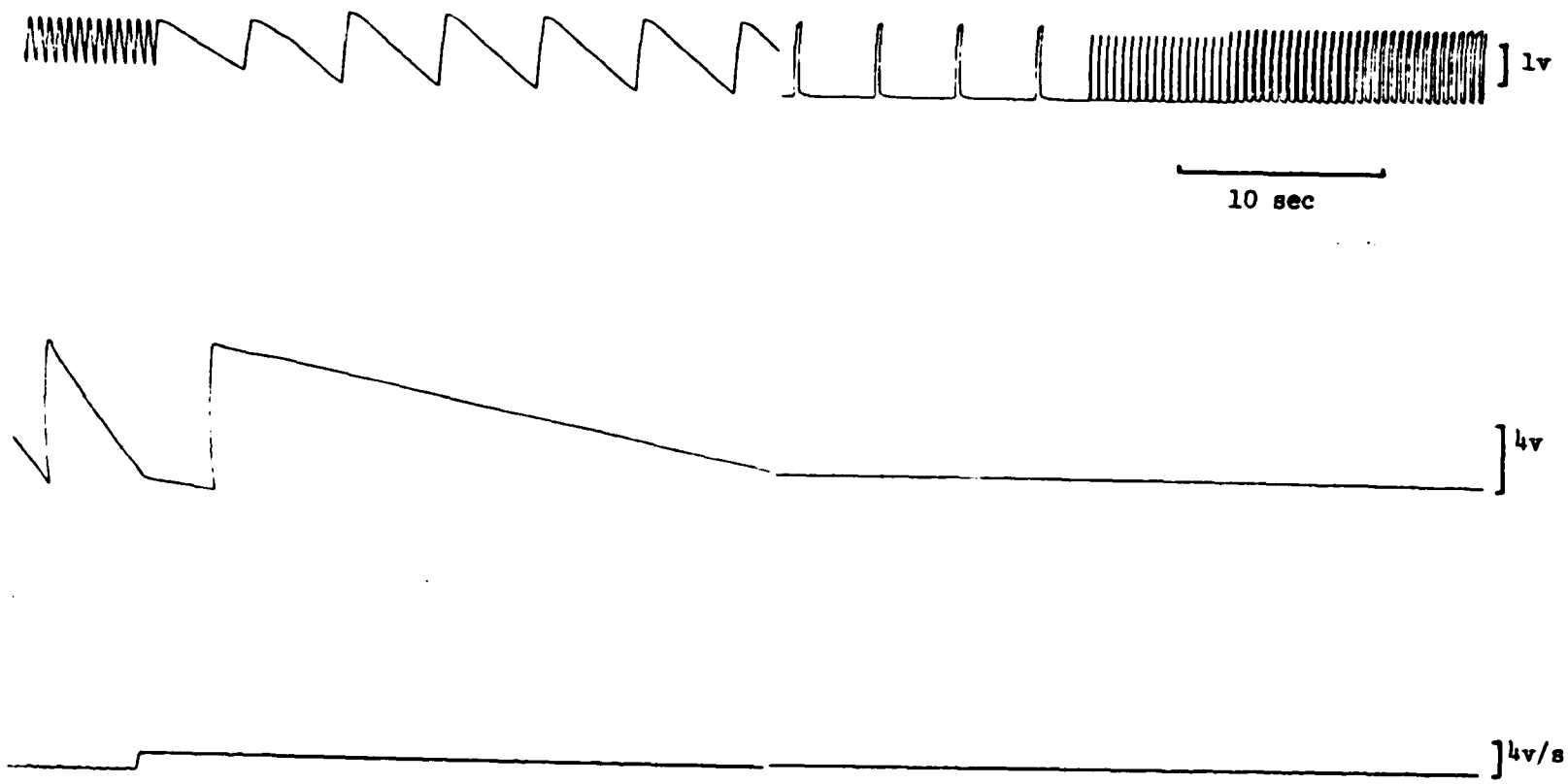

Fig. 4.13. Continued from last page.

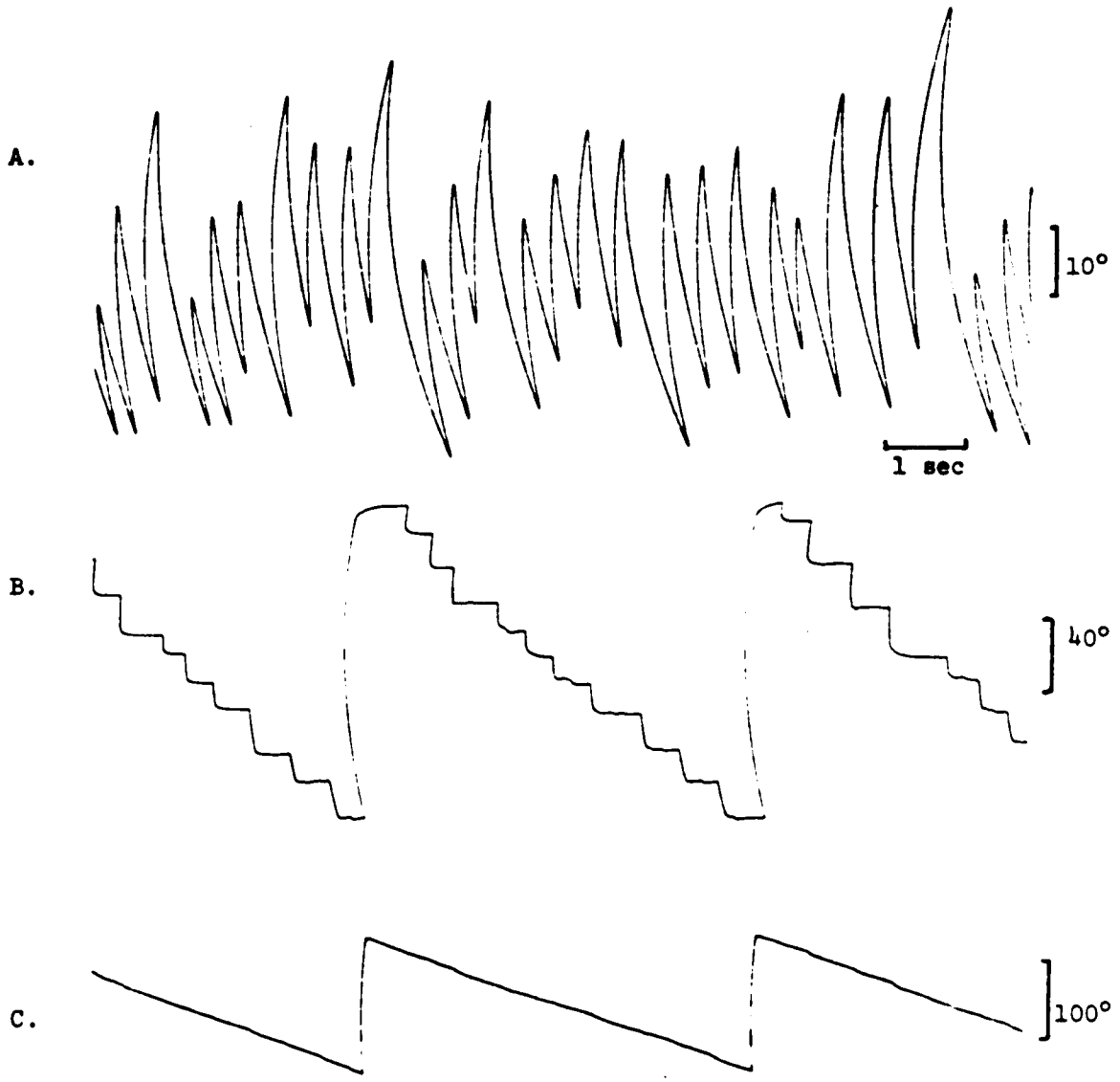

Fig. 4.14. A. EOG waveform. B. Accumulated quick phases waveform. C. Cumulative slow phase position (CSPP) waveform.

position waveform which follows the slow phases fairly well. The jumps are due to the wrap-around feature and therefore do not affect when differentiation is done. The waveform C is obtained after differentiation of the waveform D , and, therefore, represents the slow phase velocity waveform. The occasional kinks in the slow phase velocity waveform are the real manner in which the slow phases change. This is clear when one looks at the cumulative slow phase position, there is no jump which can be considered due to any quick phase eye movement. Secondly the velocity associated with these small kinks (Fig. 4.15 C) and comparing it with the velocity associated with the saccades (Fig. 4.15 B), one can come to the conclusion that these small variations in the slow phase velocity are primarily due to the real variations in the slow phase eye velocity. However, these kinks could have been tiny saccades which were undetected due to their time period being smaller than the width of the decision window (see Chapter 3 for details). This, however, leads us to redefine a saccadic movement based upon its time duration which will not be done here since it needs extremely small decision window and extremely fast computer to run the program on-line. All the waveforms generated in Fig. 4.15 are generated without any filtering at any stage of the processing. The low pass filtering on the SPV waveform may generate a smoother waveform, but will affect the transitions in the slow phase velocity and may not faithfully represent SPV during the time interval of a slow phase.

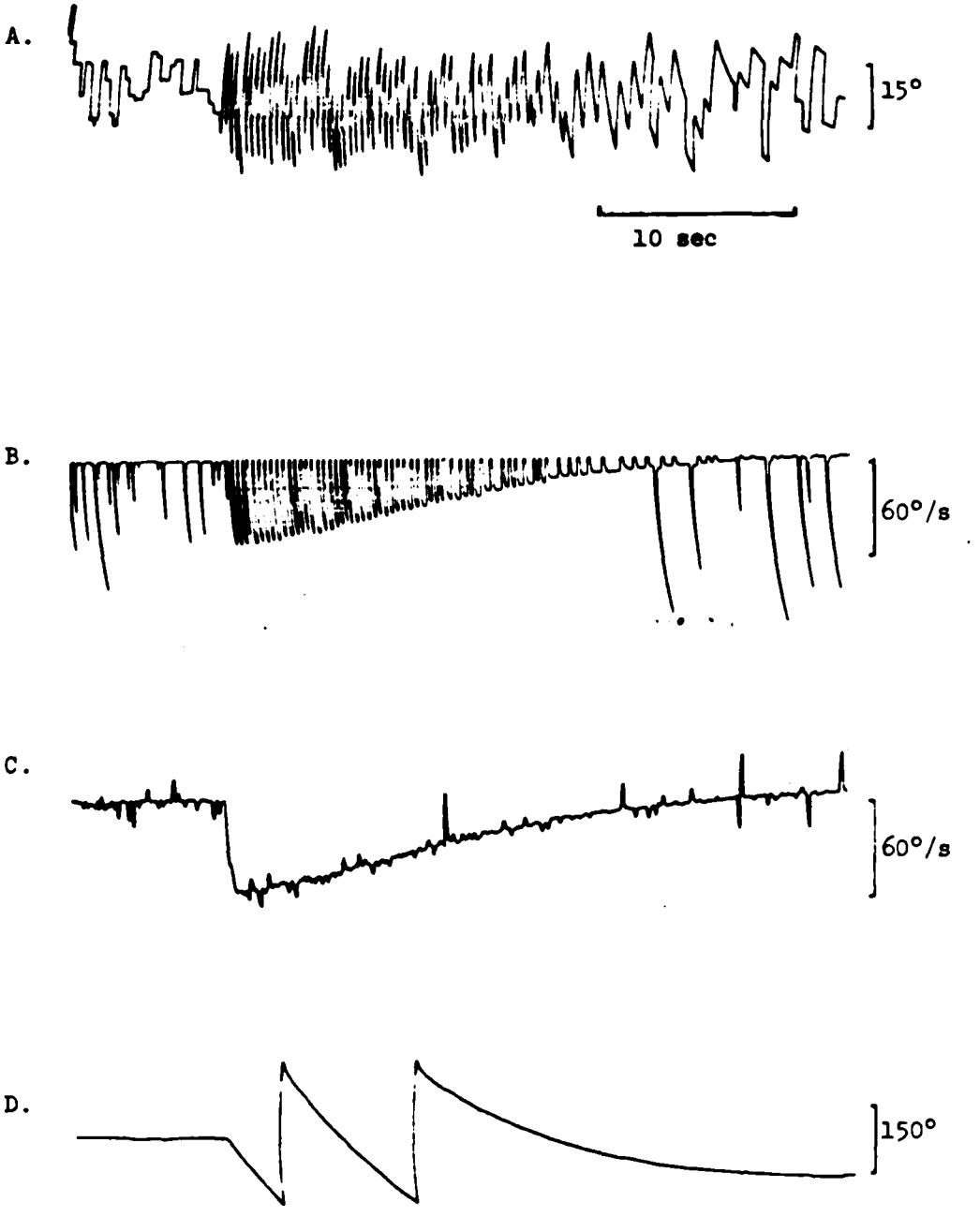

Fig. 4.15. Cumulative slow phase position and slow phase velocity as obtained by analog and computerized methods. A. EOG waveform. B. Differentiated EOG waveform - analog technique. C. Slow phase velocity waveform - computerized technique. D. Cumulative slow phase position waveform - computerized technique.

The precision with which the beginning and the end of a saccade are marked depends on how a slow phase turns into a quick phase and how a quick phase turns into a slow phase. Thus the extrapolated part of a waveform may not be an exact replacement for the saccadic interval. Secondly, since the extrapolation is based upon the slow phase portion just prior to the quick phase, the extrapolated waveform may not represent an accurate bridge between two slow phases. These processing errors affect the accuracy of a cumulative slow phase position waveform and the slow phase velocity waveform. If this poses a real problem, one may look into higher order function templates to define slow and quick phases for the detection scheme.

The next chapter will utilize the wavefroms generated in this chapter to identify the parameters of a slow-phase-generating system model.

CHAPTER 5

PARAMETER IDENTIFICATION FOR A MODEL OF SLOW PHASES OF OPTOKINETIC NYSTAGMUS

5.1 Introduction

This chapter considers the parameter identification of a model for slow phase eye velocity in response to full-field optokinetic stimuli. The specific model taken for identification is a subset of the one developed by Raphan and Cohen (Cohen et al, 1977; Raphan et al, 1979). The identification scheme uses the slow phase eye velocity of a monkey in response to a step. The model parameters are generated using a least squares error criterion.

The next section describes the slow phase model. The least squares parameter identification technique is described in section 5.3. The application of the technique to estimate the parameters of a slow phase model is the subject of section 5.4.

5.2 A Model for Slow Phase Generation

The model which will be utilized to demonstrate the behavior of the parameter identification algorithm is shown in Fig. 5.1 (Cohen et al, 1977). The response to a pulse input is shown in Fig. 5.2 and simulates the dominant characteristics of optokinetic nystagmus (OKN) and optokinetic after-nystagmus (OKAN) in response to a pulse (see Chapter 2).

Integration is assumed to be the basic element of OKN and OKAN system. The integrator stores activity during full-field optokinetic

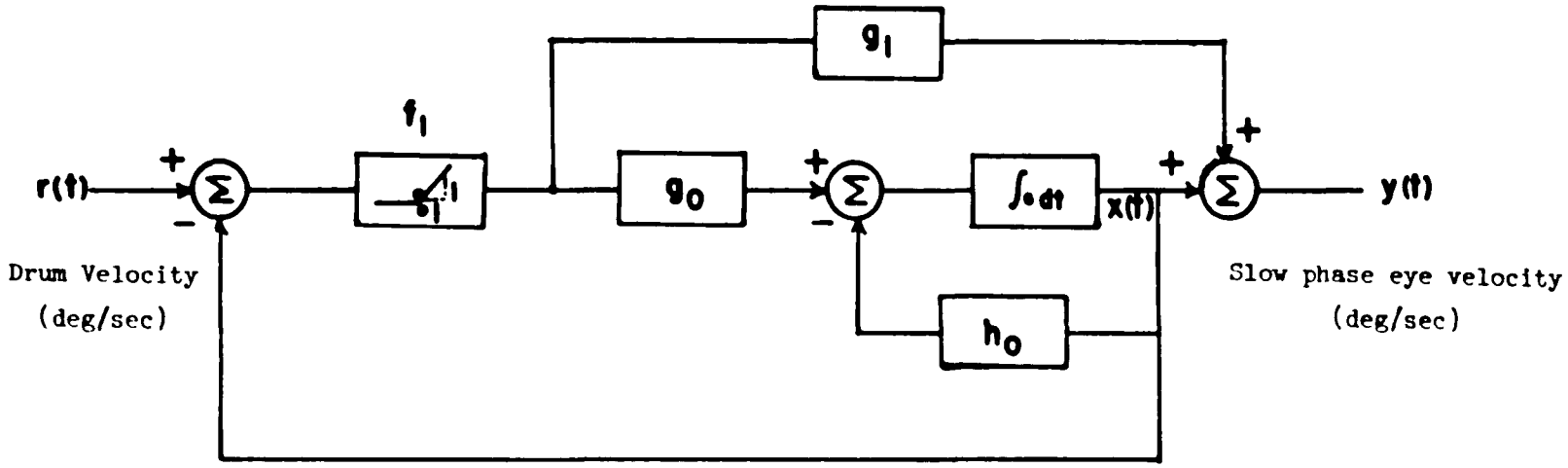

Fig. 5.1. Raphan-Cohen model of the neural mechanism responsible for producing OKN and OKAN.

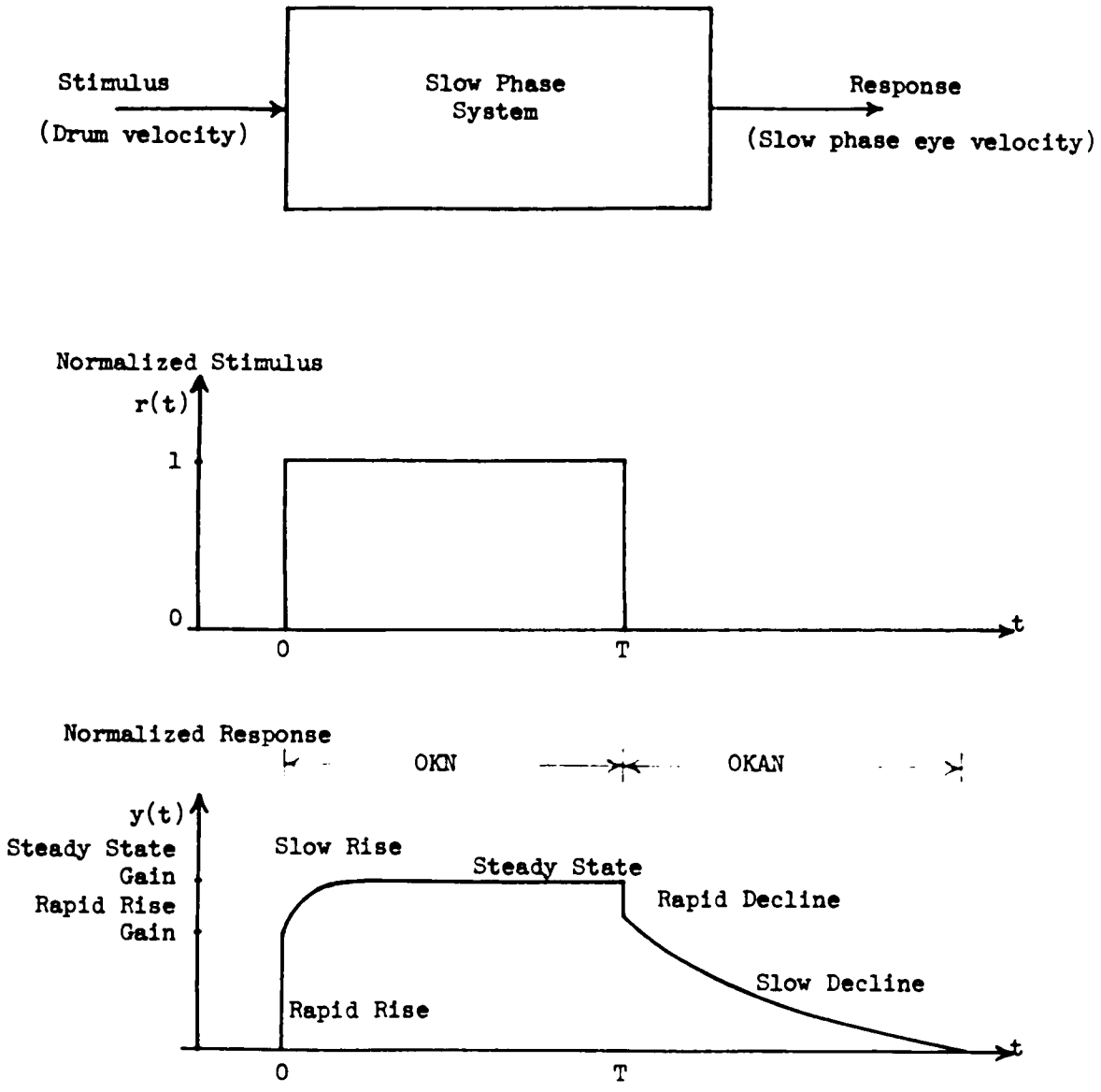

Fig. 5.2. An idealized pulse response of a slow phase system.

stimulation (OKN) which is later used to drive the eyes during OKAN. During OKN, r is assumed to be equal to the drum velocity and during OKAN r = 0. The nonlinear element f_1 allows transmission during OKN and shuts off during OKAN. The forward gain parameters g_0 and g_1 along with the feedback parameter h_0 determine the OKN characteristics like the rapid rise, slow rise and the steady state value. The feedback parameter h_0 determines the slow decline characteristics of OKAN. It is these parameters which will be identified.

The differential equation for the model in Fig. 5.2 is given by

$$\dot{x} = -h_0 x + g_0(r-x)\, u(r-x) \qquad (5.2.1)$$

$$y = x + g_1(r-x)\, u(r-x)$$

where $u(z) = 1$ for $z \geq 0$

$= 0$ for $z < 0$

The OKN response ($r > x$) of this model to an input similar to the one in Fig. 5.1B is given by

$$x(t) = \frac{g_0 V}{h_0+g_0} \left(1 - \exp -(h_0+g_0)t\right) \qquad (5.2.2)$$

$$y(t) = g_1 V + (1-g_1) \frac{g_0 V}{h_0+g_0} \left[1 - \exp\left(-(h_0+g_0)t\right)\right]$$

where V is the amplitude of the step input. From (5.2.2), one can obtain the following results relating the model parameters to the response parameters:

Rapid rise = $g_1 V$

Slow rise time constant = $1/(g_0+h_0)$

Steady state value y_s = $(g_1 h_0+g_0)V/ (h_0+g_0)$

Steady state value x_s = $g_0 V/(h_0+g_0)$

At t=T, when the stimulus is set to zero ($r \prec x$), the OKAN response as obtained from (5.2.1) is given by

$$x(t) = x_s \exp(-h_0(t - T)) \qquad (5.2.3)$$

$$y(t) = x(t)$$

From (5.2.3) one can obtain the following relations

Rapid decline = $g_1 h_0 V/(h_0+g_0)$

Slow decline time constant = $1/h_0$

The model is an approximation to a complex neural mechanism responsible for producing OKN and OKAN. The usefulness of this model lies in its simplicity coupled with reasonably good predictions [8]. This is explored in more detail when the model parameter identification is done in section 5.4 utilizing an actual experimental response of a monkey.

5.3 Identification of the Model Parameters

The parameter identification of the model is considered in this section. The nonlinear model structure imposes a constraint that separate identification must be done for the rising portion of the step response (when input is applied) and for

the decaying portion (when the input has been removed). This is because the system response in the two regions is not dependent upon the same parameters of the model. During OKN all the parameters g_1, g_0 and h_0 determine the response. During OKAN only h_0 determines the response.

The model state equation for $r(t)> x(t)$ is given by

$$\dot{x}(t) = -(h_0+g_0)\, x(t) + g_0 r(t) \tag{5.3.1}$$

$$z(t) = (1-g_1)\, x(t) + g_1 r(t) + n(t)$$

where $n(t)$ accounts for the measurement noise. The discrete equivalent of (5.3.1) is given by

$$x(k+1) = \exp(-(h_0+g_0)T)\, x(k) + \int_{kT}^{(k+1)T} \exp\left[-(h_0+g_0)\,[(k+1)T-\tau]\right] \cdot g_0 d\tau\, r(k) \tag{5.3.2}$$

$$z(k+1) = (1-g_1)\, x(k+1) + g_1 r(k+1) + n(k+1)$$

Eliminating the state variable $x(k+1)$ in (5.3.2) yields

$$z(k+1) = a\, z(k) + b\, r(k) + c\, r(k+1) + n(k+1) - a\, n(k) \tag{5.3.3}$$

where

$$a = \exp(-(h_0+g_0)T) \tag{5.3.4}$$

$$b = (1-g_1)g_0/(h_0+g_0) \cdot [1-\exp(-(h_0+g_0)T)] - g_1 \exp(-(h_0+g_0)T) \tag{5.3.5}$$

$$c = g_1 \tag{5.3.6}$$

Let the step input be defined by

$$r(k) = V\, u(k) \tag{5.3.7}$$

where V is the magnitude of the step input.

Substituting (5.3.7) in (5.3.3) yields

$$z(k+1) = a\, z(k) + b\, V\, u(k) + c\, V\, u(k+1) + n(k+1) - a\, n(k) \tag{5.3.8}$$

For $k \geq 0$ (5.3.8) becomes

$$z(k+1) = a\, z(k) + b\, V + cV + n(k+1) - a\, n(k) \qquad (5.3.9)$$

Equation (5.3.9) fails to satisfy output distinguishability conditions [13] and therefore can't be used to estimate all three parameters. One method to circumvent this problem is to use the initial response y(0) to estimate parameter c. This is accomplished by substituting k = -1 in (5.3.8) which yields

$$z(0) = cV\, u(0) + n(0) \qquad (5.3.10)$$

It is possible to derive least square estimate [19] of c if a number of step responses for different magnitudes of step inputs are available. In such a case (5.3.10) can be written as

$$z_i(0) = c\, V_i\, u(0) + n_i(0) \qquad (5.3.11)$$

where i denotes the particular experiment in each V_i u(0) is the input and $z_i(0)$ is the output at t=0 (or k=0). The least square estimate of c as obtained from (5.3.11) is given by

$$\hat{c} = (\phi^T \phi)^{-1} \phi^T z(0) \qquad (5.3.12)$$

where $\phi = [V_1 \;\; V_2 \cdots V_N]^T \qquad (5.3.13)$

and $z(0) = [z_1(0) \;\; z_2(0) \cdots z_N(0)]^T$

where N denotes the number of experiments used to estimate c.

To estimate parameters a and b, (5.3.8) is written as

$$z(k+1) = a\, z(k) + b\, V + z(0) - n(0) + n(k+1) - a\, n(k)$$

$$= a\, z(k) + \beta + w(k+1) \qquad k \geq 0 \qquad (5.3.14)$$

where $\beta = bV + (z(0) - n(0)) = (b + c)\, V \qquad (5.3.15)$

and $w(k+1) = n(k+1) - a\, n(k) \qquad (5.3.16)$

Least squares estimation [19] as applied to (5.3.14) yields a and β.

These estimates are given by

$$\begin{bmatrix} \hat{a}(m) \\ \hat{\beta}(m) \end{bmatrix} = [\Phi^T \Phi]^{-1} \Phi^T z \tag{5.3.17}$$

where m denotes the number of measurements (in addition to initial z(0)) used to estimate a and β.

$$z = [z(1) \quad z(2) \cdots \quad z(m)]^T \tag{5.3.18}$$

$$\Phi = \begin{bmatrix} z(0) & 1 \\ z(1) & 1 \\ z(2) & 1 \\ \vdots & \vdots \\ z(m-1) & 1 \end{bmatrix} \tag{5.3.19}$$

Equation (5.3.17) when expanded yields

$$\hat{a}(m) = \frac{m\sum z(i)\cdot z(i+1) - \sum z(i) \sum (z(i+1)}{m\sum z^2(i) - (\sum z(i))^2} \tag{5.3.20}$$

$$\hat{\beta}(m) = \frac{-\sum z(i) \sum z(i)\cdot z(i+1) + \sum z^2(i) \sum z(i+1)}{m\sum z^2(i) - (\sum z(i))^2} \tag{5.3.21}$$

where all summations $\sum$ s are taken from i = 0 to (m-1). The recursive realization of (5.3.20) and (5.3.21) can be carried out by defining intermediate variables as follows:

$$SZ(m) = \sum_0^{m-1} z(i) = \sum_0^{m-2} z(i) + z(m-1)$$

$$= SZ(m-1) + z(m-1) \tag{5.3.22}$$

$$SSZ(m) = \sum_0^{m-1} z^2(i) = \sum_0^{m-2} z^2(i) + z^2(m-1)$$

$$= SSZ(m-1) + z^2(m-1) \tag{5.3.23}$$

$$SZ1(m) = \sum_0^{m-1} z(i+1) = \sum_0^{m-2} z(i+1) + z(m)$$

$$+ SZ1(m-1) + z(m) \tag{5.3.24}$$

$$SZZ1(m) = \sum_{0}^{m-1} z(i).z(i+1)$$

$$= \sum_{0}^{m-2} z(i).z(i+1) + z(m-1).z(m)$$

$$= SZZ1(m-1) + z(m-1).z(m) \qquad (5.3.25)$$

Parameter estimation must begin with at least two measurements for two parameters. Alternatively the initial values (for m=1) for the variables defined in (5.3.22) to (5.3.25) are given by

$$\begin{aligned} SZ(1) &= z(0) \\ SSZ(1) &= z^2(0) \\ SZ1(1) &= z(1) \\ SZZ1(1) &= z(1).z(0) \end{aligned} \qquad (5.3.26)$$

In view of (5.3.22) to (5.3.25), (5.3.20) and (5.3.21) can be written as

$$\hat{a}(m) = \frac{m.\ SZZ1(m) - SZ(m).SZ1(m)}{m.\ SSZ(m) - (SZ(m))^2} \qquad (5.3.27)$$

$$\hat{\beta}(m) = \frac{SZ(m).SZZ1(m) + SSZ(m).SZ1(m)}{m.\ SSZ(m) - (SZ(m))^2} \qquad (5.3.28)$$

Thus equations (5.3.22) - (5.3.25) along with (5.3.27) and (5.3.28) can be implemented for recursive estimation of parameters a and β. The identification process may be stopped when the parameters settle with required acuracy.

The estimates of h_0, g_0 and g_1 can be obtained from the estimates of a, β, c and equations (5.3.4) - (5.3.6), (5.3.15). These estimates are given by

$$\hat{g}_0 = \ln[\hat{a}](\hat{b} + \hat{a}\,\hat{c}) \;/\; [(-T)(1-\hat{a})(1-\hat{c})]$$

$$\hat{h}_0 = \ln[\hat{a}](\hat{a} + \hat{b} + \hat{c}-1) \;/\; [T(1-\hat{a})(1-\hat{c})] \qquad (5.3.29)$$

$$\hat{g}_1 = \hat{c}$$

where $\hat{b} = \hat{\beta}/V - \hat{c}$

When r(t) = 0, the differential equation generating output (OKAN velocity) is given by

$$\dot{x}(t) = -h_0 x(t) \qquad (5.3.30)$$

$$z(t) = x(t) + n(t)$$

Discrete equivalent of (5.3.30) is given by

$$x(k+1) = \exp(-h_0 T)\, x(k) \qquad (5.3.31)$$

$$z(k+1) = x(k+1) + n(k+1)$$

Eliminating x(k+1) in (5.3.31) yields

$$z(k+1) = \alpha z(k) + w(k+1) \qquad (5.3.32)$$

where

$$\alpha = \exp(-h_0 T) \qquad (5.3.33)$$

and $w(k+1) = n(k+1) - n(k)$ (5.3.34)

Least square estimation of α from (5.3.32) gives

$$\hat{\alpha} = (\phi^T \phi)^{-1} \phi^T z \qquad (5.3.35)$$

where $z = [z(1) \quad z(2) \cdots z(m)]^T$

and $\phi = [z(0) \quad z(1) \ldots z(m-1)]^T$ (5.3.36)

The estimation of α leads to the estimation of h_0 from eqn. (5.3.33), i.e.

$$\hat{h}_0 = -\ln(\hat{\alpha})/T \qquad (5.3.37)$$

The least square parameter estimates are known to be biased [19]. The amount of bias can be estimated as follows. In general the estimate for the parameter vector Θ is given by

$$\hat{\Theta} = (\Phi^T \Phi)^{-1} \cdot \Phi^T z \tag{5.3.38}$$

where Φ is a matrix of past outputs and z is a vector of outputs given by

$$z = \Phi \Theta + w \tag{5.3.39}$$

where w is a noise vector.

Substituting (5.3.39) in (5.3.38) yields

$$\hat{\Theta} = \Theta + (\Phi^T \Phi)^{-1} \cdot \Phi^T w \tag{5.3.40}$$

From (5.3.40) bias on Θ is given by

$$\hat{\Theta}_{bias} = E\,[(\Phi^T \Phi)^{-1} \cdot \Phi^T w] \tag{5.3.41}$$

The bias is due to the reason that the system outputs are correlated with the past noises. If we assume that each output has significant correlation only with the finite past and then take data far enough apart in time such that each new equation is essentially independent of the past noises, we can minimize $\hat{\Theta}_{bias}$.

5.4 Experimental Results

The least square error parameter identification of the slow phase model described in section 5.3 was applied to the experimentally obtained OKN and OKAN responses of a monkey. The results of the identification are described in section 5.4.2. However, first the scheme used in collecting needed data for the identification is considered in section 5.4.1.

5.4.1 Data Acquisition for the Parameter Identification Program

The schematic which describes the steps used to generate the slow phase eye velocity and the identification of parameters is shown in Fig. 5.3. The EOG representing eye position and stimulus velocity were obtained from an analog tape (Honeywell). The eye velocity of the slow phases was estimated from the EOG waveform using the saccade detection program.

The saccades were detected (see chapter 3) and removed (see chapter 4) to generate cumulative slow phase position whose differentiation using one PDP-8/E computer yielded the slow phase velocity. A second computer (PDP-8/E) was used to smooth and store this velocity along with the stimulus velocity on a DEC tape. The various amplifiers used in the schematic were needed to scale the signals to proper amplitudes for the A/D converters. The data tape so prepared was then used to obtain the model parameters by running the parameter identification program off-line on a PDP-8/E computer. The identification program is shown in Appendix C.

5.4.2 Parameter Identification Results

The slow phase system response to a stimulus velocity pulse of 90°/sec to the right is considered for the parameter identification. The response along with the stimulus is shown in Fig. 5.4. The approximate response parameters as obtained graphically from Fig. 5.4B are also given in the figure. These parameters can be compared with the ones obtained by the least squares identification technique.

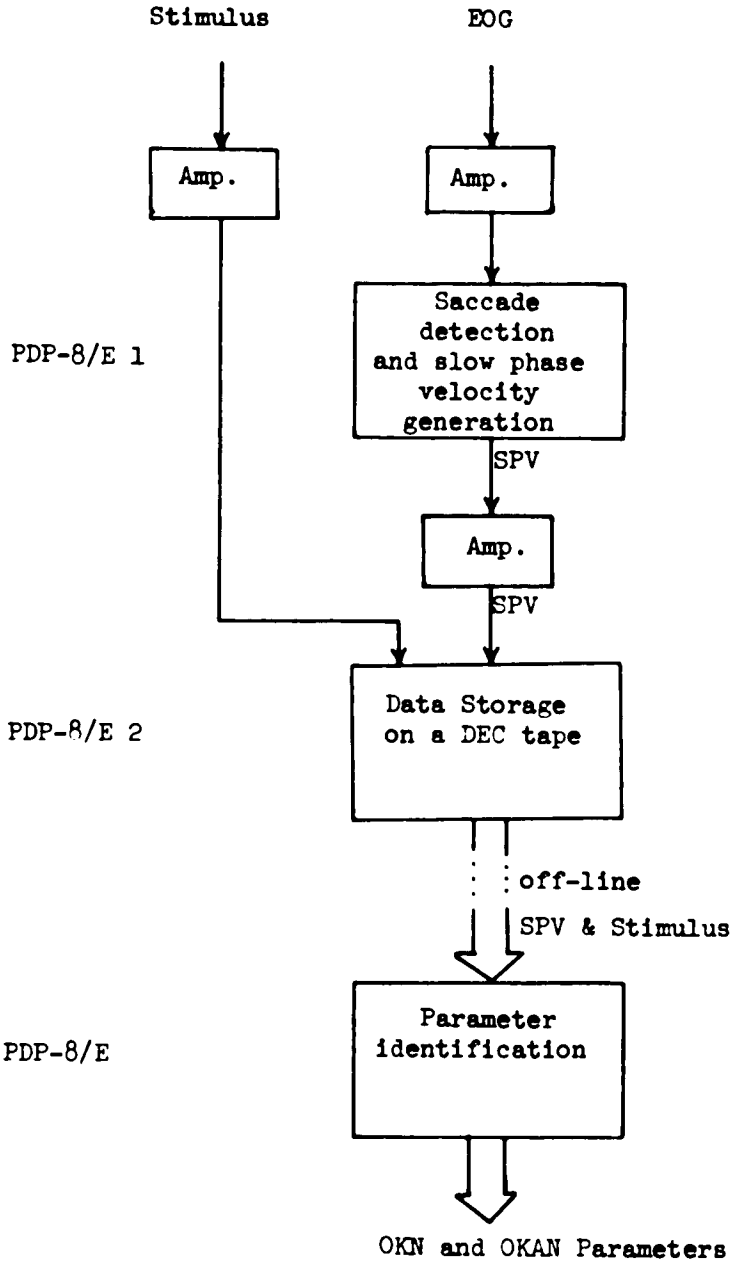

Fig. 5.3. The data-acquisition system for the parameter identification of OKN and OKAN model.

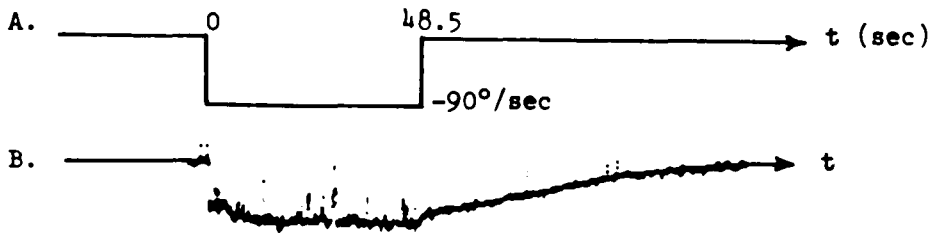

Fig. 5.4. OKN and OKAN response to a pulse input.

A. Stimulus velocity is -90°/sec

B. Eye velocity as obtained by the method discussed in Chapter 4. Graphical estimates of response parameters are as follows:

Rapid rise gain ≈ .65
Slow rise time constant ≈ 3 sec
Steady state gain ≈ 1
Rapid decline gain ≈ .15
Slow decline time constant ≈ 27 sec.

The least squares estimates for the OKN parameters c, a and β, for a -90°/sec nystagmus velocity, and a sampling interval of .2048 sec. are plotted in Fig. 5.5. Under these conditions

$\hat{c}$ = .575, $\hat{a}$ = .94 and $\hat{\beta}/V$ = .05 which correspond to $\hat{g}_1$ = .575, $\hat{h}_0$ = .13 and $\hat{g}_0$ = .16. The identification was repeated for various sampling intervals and the results are shown in Appendix D and summarized in Table 5.1. The mean of the estimates of g_1, h_0 and g_0 are .575, .18, .25 respectively. These results can be used to compute the response parameters for comparison with the graphical measurements.

The least squares estimate for the OKAN parameter α, for a sampling interval of 1.536 sec. is plotted in Fig. 5.6. It can be observed that $\hat{\alpha}$ = .94 which corresponds to the OKAN model parameter $\hat{h}_0$ = .0388. The identification was repeated for various sampling intervals and the results are shown in Appendix D and summarized in Table 5.2. The mean of the h_0 estimate is .03942, corresponding to an OKAN time constant of 25.38 seconds. These results are consistent with the graphical measurements from Fig. 5.4B. It seems that h_0 as obtained from OKAN is closer to the real value of h_0 when compared to the one obtained from OKN. The reason seems to be that response waveform during OKN is not an exponential rise. The OKAN response, however is closer to an exponential as implicitly assumed by the model. This fact has already been noted by Raphan et al, (1979).

The response parameters as computed from the model parameters are presented in Table 5.3 and they compare reasonably well to the ones determined graphically. This supports the contention that h_0 as obtained from OKAN is a better estimate of h_0.

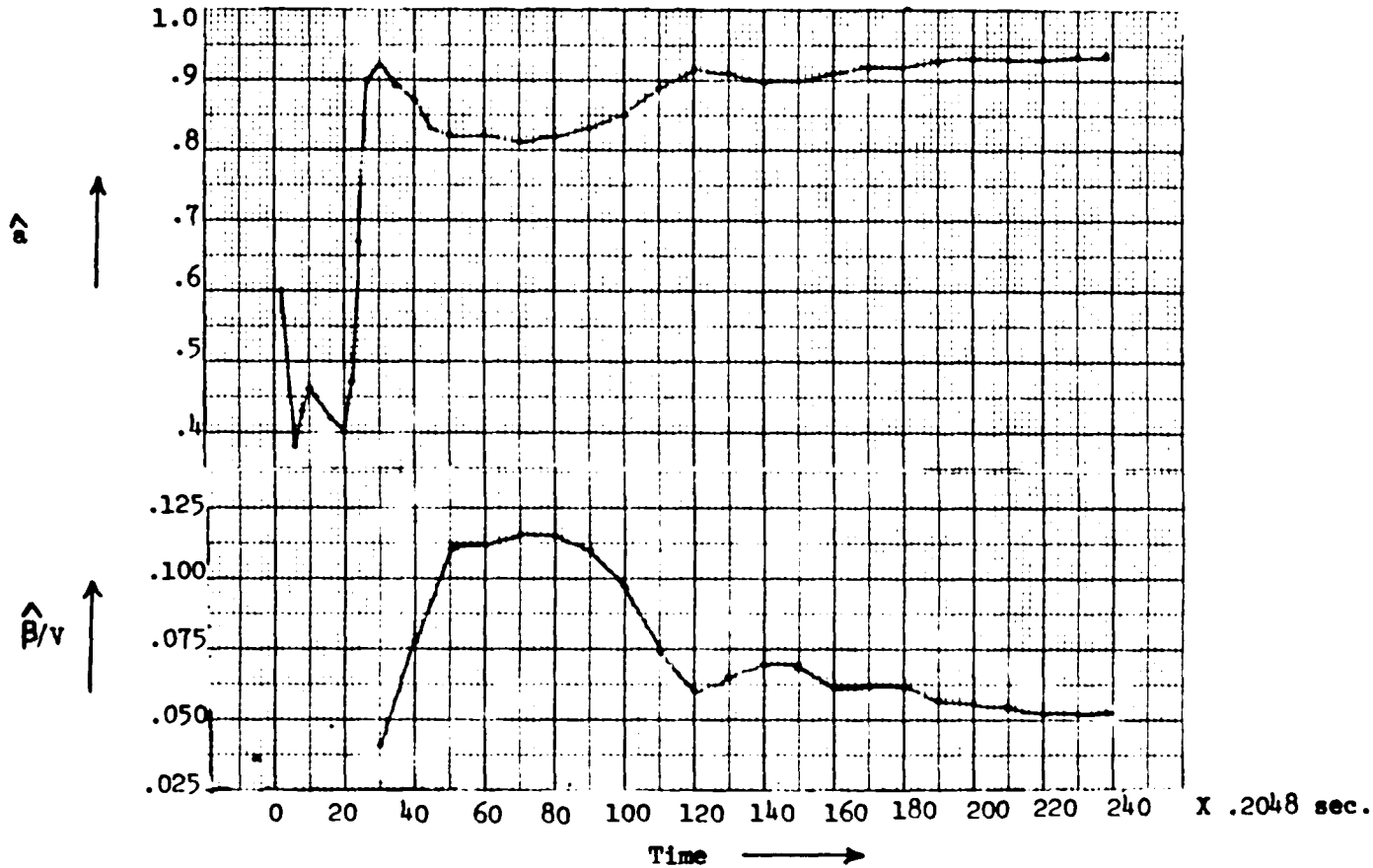

Fig. 5.5. OKN parameter identification. Sampling interval = .2048 sec.

Table 5.1. OKN parameter identification for various sampling intervals.

T (sec.)	$\hat{c}$	$\hat{a}$	$\hat{\beta}/V$	$\hat{g}_1$	$\hat{h}_o$	$\hat{g}_o$
.2048	.575	.94	.05	.575	.13	.16
.512	.575	.85	.12	.575	.15	.17
1.024	.575	.52	.40	.575	.24	.38
2.048	.575	.38	.52	.575	.18	.29

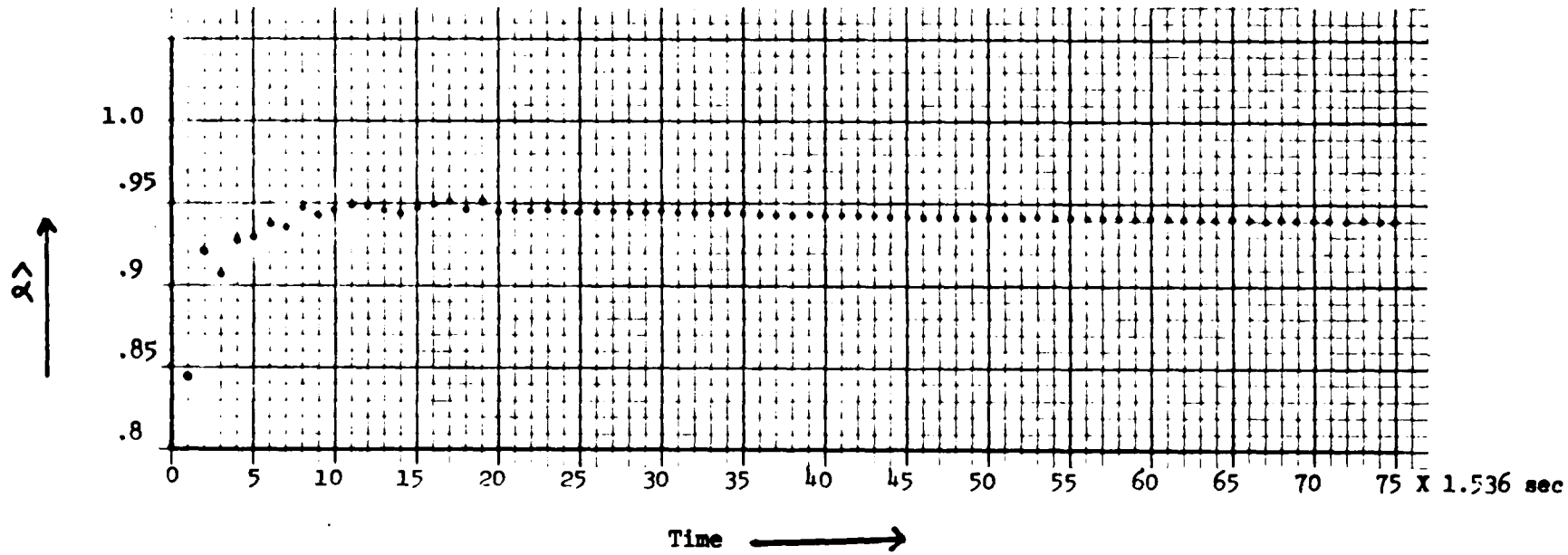

Fig. 5.6. OKAN parameter α identification. T = 1.536 sec.

Table 5.2. OKAN parameter identification for various sampling intervals.

T (sec.)	$\hat{\alpha}$	$\hat{h}_o$
.0512	.9975	.0391
.256	.9885	.0452
.512	.980	.0395
1.024	.961	.0388
1.536	.940	.0403
2.56	.902	.0394

Table 5.3. Response parameters as obtained from the OKN and OKAN model parameters.

Response parameter	Graphically from Fig. 5.4B	From identified model parameters
Rapid rise gain	.65	.575
Slow rise time constant	3 sec	3.45 sec ** (2.33 sec) *
Steady state gain	1	.94 ** (.82) *
Rapid decline gain	.15	.08 ** (.24) *
Slow decline time constant	27 sec	25.37 ** sec (5.6 sec) *

* h_o = .18 used in calculations (OKN identification)

** h_o = .04 used in calculations (OKAN identification)

To compare the parameter estimation of h_0 from OKN data with the parameter estimation from the OKAN data, the model outputs were generated using h_0 as estimated from these data. The simulated outputs were compared with the system outputs by defining a model error e(k) and the integral square error ISE(k) as follows:

$$e(k) = z(k) - \hat{z}(k)$$

$$ISE(k) = \sum_{i=k-1}^{k} e^2(i)$$

where z(k) is the system output and $\hat{z}(k)$ is the simulated model output. The '1' defines the length of the moving window for computing ISE(k).

The simulation program for this purpose is shown in Appendix E. The signal processing results are shown in Fig. 5.7. The traces in Fig. 5.7 show the model output, the model error and the integral square error for three cases: one, when the OKN parameter estimation was used to simulate the OKN model output and the OKAN parameter the OKAN model putput; two, when $\hat{h}_0$ from OKAN was used to simulate the model output; and three, when $\hat{h}_0$ from OKN was used to simulate the model output. These traces for various z(t), e(t) and ISE(t) show that the estimate of h_0 parameter of the OKN is not reliable and the OKAN must be used to estimate it. The parts which show OKN simulation in these traces demonstrate the fact that the value of h_0 is not a crucial factor in the OKN generation.

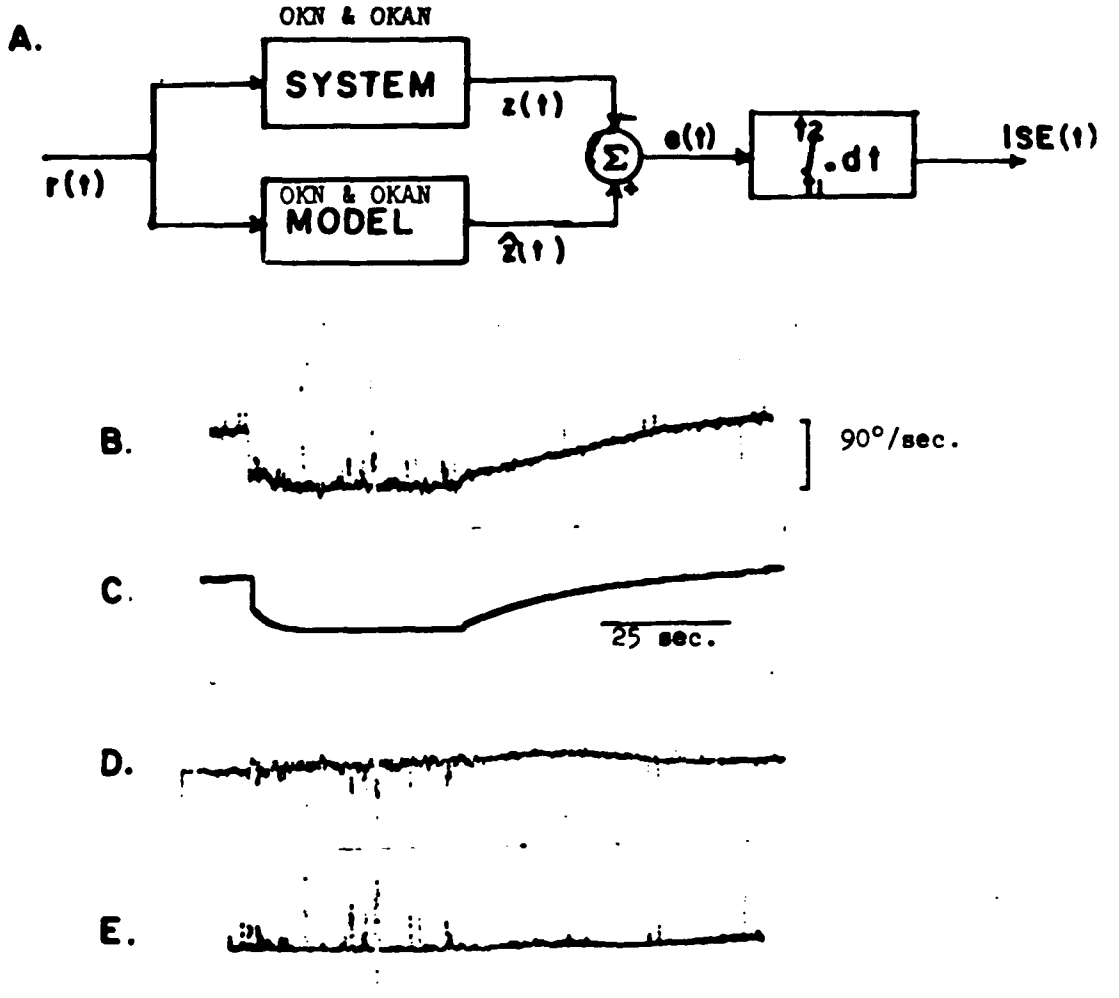

Fig. 5.7. The OKN & OKAN system response vs the OKN & OKAN model response.

A. Block diagram of the OKN & OKAN system vs model for comparison. Stimulus used was -90°/sec (Fig. 4B)

B. The OKN & OKAN system output z (t).

C. The OKN & OKAN model output $\hat{z}(t)$. The OKN was simulated using OKN parameter estimation and the OKAN using the OKAN parameter estimation.

D. The model error e(t) for the system output of B. and the model output of C.

E. The integral square error ISE (t) for the system output of B. and the model output of C.

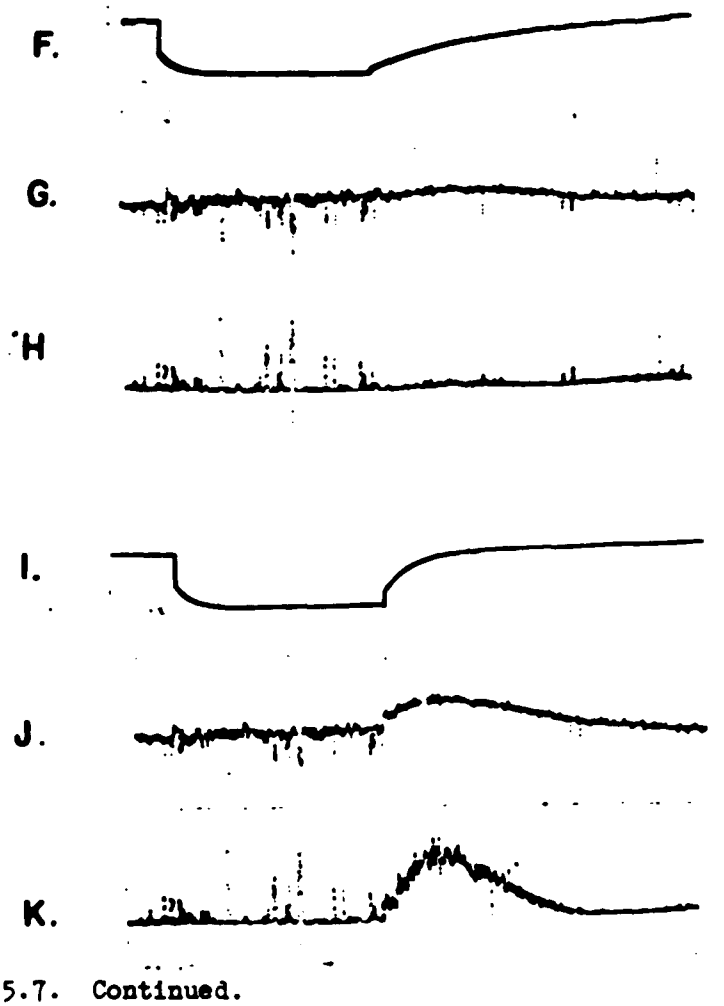

Fig. 5.7. Continued.

F. The OKN & OKAN model output $\hat{2}(t)$. Both OKN and OKAN were simulated using h_o as estimated from OKAN parameter estimation.

G. The model error e(t) for the system output of B. and the model output of F.

H. The integral square error ISE(t) for the system output of B. and the model output of F.

I. The OKN & OKAN model output $\hat{2}(t)$. Both OKN and OKAN were simulated using h_o as estimated from OKN parameter estimation.

J. The model error e(t) for the system output of B. and the model output of I.

K. The integral square error ISE(t) for the system output of B. and the model output of I.

CHAPTER 6

SUMMARY AND CONCLUSIONS

6.1 Summary

In this dissertation, an on-line digital signal processing technique has been developed to analyze the response of an oculomotor system subjected to an optokinetic stimulus or to a vestibular stimulus. The analyzed response is then utilized in the parameter identification of a slow phase subsystem model of the oculomotor system. Thus a technique has been developed which leads to the parameterization of the oculomotor system response. The response waveforms and the model parameters generated in this manner has the potential of being used in the diagnosis of oculomotor system problems and in the understanding of its functional behavior.

An important assumption on which the signal processing technique is based is that the two parts of the response (the slow phase and the quick phase or a saccade) are generated internally by two separate subsystems. This assumption allow treatment of a slow phase subsystem and its response independent of the quick phase or saccadic subsystem. Another assumption is that the quick phase saccadic duration is relatively much smaller than the slow phase duration. This leads to the assumption that during a quick/saccadic phase, the slow phase system state remains essentially unchanged. Still another assumption is that the slow phase response can be approximated by a straight line; this simplifies the implementation and reduces the timing requirements

of the on-line signal processing system.

An important feature of the signal processing developed in this work is that it lends itself to a microprocessor implementation for real-time analysis of waveforms. Special consideration was given in Chapter 4 to the implementation in terms of its timing requirements and the complexity of algorithms. Thus the results of this work serve as the foundation for the development of a microprocessor-based instrument for on-line oculomotor system analysis. The parameter identification of the slow phase system model replaces a cumbersome manual operation by an automatic identification procedure.

A crucial part of the signal processing technique is the detection of saccades and quick phases in an EOG waveform. This was achieved using 'Baye's Likelihood Ratio Criterion'. which minimizes the probability of a detection error. It leads to a detection technique with predictable performance and the control elements for adaptation to various experimental situations. The detection technique was described in section 3.3.1 and its probability of error was computed in section 3.3.3. The technique was tested on simulated waveforms in section 3.3.4 and on experimental waveforms in section 3.4. The results of these tests lead to the conclusion that it is an appropriate way to detect quick phases/saccade and the process of detection can be controlled by varying detection technique parameters, such as the number of samples used for detection, sampling interval and the functional description of the waveform sections.

Once saccades/quick phases are detected, the next step is to remove them to obtain a purely slow phase system response. The technique was based upon describing a slow phase by a straight line

and assuming that saccades/quick phases are much faster than the slow phases. The description of the technique which generates cumulative slow phase position (CSPP) is contained in section 4.2.1. The slow phase velocity (SPV) is obtained by differenting CSPP. A least squares error digital differentiator for this purpose was described in section 4.2.2. The applicability of this type of digital differentiator to EOG waveforms was tested mathematically by evaluating its frequency response and experimentally by applying it to real EOG waveforms. The digital differentiator has advantages over an analog differentiator most commonly used for obtaining SPV waveforms. The combined detection, CSPP and SPV generation program is presented in section 4.4 where a vestibular nystagmus was processed to detect/suppress quick phases and generate cumulative slow phase position and the slow phase velocity. The slow phase velocity generated in this manner is compared to an analog differentiator output. The conclusion is that the type of signal processing technique developed in this dissertation is capable of producing predictable performance and has a number of advantages over the ones which have been developed so far. These advantages include the detection of forward as well as reverse saccades, reproduction of slow phase velocity transitions, and control over detection parameters for optimal processing.

A state space model due to Raphan and Cohen [8] was considered to represent the slow phase subsystem responsible for producing OKN and OKAN response. The model is an approximation to a more complex and nonlinear system but is adequate to predict salient features of a step (or a long pulse) response. For this model, the parameter identification had to be carried using a step response and the response itself was very

noisy. A least square error technique which has a smoothing effect on the noise was considered for the parameter identification. The technique was described in section 5.3 and was applied to a 90°/sec nystagmus in section 5.4.2. The estimated parameters compare favorably to the ones measured manually. The bias in the least square estimation technique was minimized by using data samples sufficiently apart so as to reduce the noise correlation between them.

Control over the signal processing parameters allows one to adapt the technique described in this work to various experimental situations. The predictability of the technique leads to the pre-evaluation of its applicability to an experimental response. This initial step in the understanding of oculomotor system through signal processing has a potential in analyzing various kinds of oculomotor system responses and in evolving an optimal and adaptive technique for this purpose.

6.2 Recommendations for Future Research

Theoretical and practical future extensions of this research are listed below. A sound understanding of the measurement noise statistics should be obtained so that possibly a new detection scheme could be achieved. Specifically the following recommendations are made for further investigation in line with this thesis.

1. Consider the other forms of EOG noise statistics and derive other forms of saccade/quick phase detectors and the associated probabilities of detection error.

2. Change the functional descriptions of the quick and the slow phases of nystagmus to higher order functions. Specifically, higher order functions are needed to describe the beginning and the end of these movements. This may lead to a multiple-hypotheses detection problem. The detection based upon the solution to the multiple-hypothesis problem may lead to lower probability of detection error.
3. Optimize the functional descriptions for the slow and the quick phases for various nystagmus velocities and fit them into a functional so that the process of detection may be made self-adaptive.
4. Obtain noise vs time trade-off for the digital differentiator used to obtain slow phase velocities. Also consider other forms of digital differentiators to find an optimal one for the slow phase velocity generation.
5. Consider other forms of experiments for the on-line parameter identification of the slow phase system. This is to circumvent the difficulties associated with an on-line parameter identification from a step response.
6. Integrate the saccadic detector and the parameter identification so that these two schemes run simultaneously in an on-line manner. This will generate a system of results valuable for the real-time analysis of oculomotor system.
7. Implement the detection and the identification of a slow phase system on a microprocessor system. Such an implementation will lead to a portable instrument for the oculomotor system diagnosis.

APPENDIX A

COMPUTER PROGRAM FOR ERROR ANALYSIS OF EXAMPLE IN SECTION 3.3.4

TYPE ERROR1 FORTRAN

```
C       ERROR ANALYSIS OF DETECTION SYSTEM                              ERR00010
        REAL K                                                          ERR00020
        INTEGER X                                                       ERR00030
        DIMENSION F(10),G(10),Z(2),Y(2,10)                              ERR00040
        WRITE(6,1)                                                      ERR00050
1       FORMAT(///,5X,'N',10X,'S',10X,'Z11N',7X,'Z22N',7X,'X',4X,'Z21X',ERR00060
       A7X,'Z12X',//)                                                   ERR00070
        DO 500 N=2,6,2                                                  ERR00080
        S=0.5                                                           ERR00090
        DO 400 M=1,7                                                    ERR00100
        K=0.                                                            ERR00110
        Z(1)=0.                                                         ERR00120
        Z(2)=0.                                                         ERR00130
        S1=0.                                                           ERR00140
        DO 100 I=1,N                                                    ERR00150
        F(I)=.2*I                                                       ERR00160
        G(I)=-1.6*I                                                     ERR00170
        Z(1)=Z(1)+F(I)*(F(I)-G(I))                                      ERR00180
        Z(2)=Z(2)+G(I)*(F(I)-G(I))                                      ERR00190
        K=K+F(I)**2-G(I)**2                                             ERR00200
100     S1=S1+(F(I)-G(I))**2                                            ERR00210
        K=K/2+S**2*ALOG(.1)                                             ERR00220
        S1=S1**.5*S                                                     ERR00230
        Z(1)=.5*ERFC((K-Z(1))/(1.414*S1))+.5                            ERR00240
        Z(2)=.5*ERFC((K-Z(2))/(1.414*S1))                               ERR00250
        N1=N-1                                                          ERR00260
        YX=0.                                                           ERR00270
        DO 300 X=1,N1                                                   ERR00280
        Y(2,X)=0.                                                       ERR00290
        Y(1,X)=0.                                                       ERR00300
        N2=N-X                                                          ERR00310
```

```
      DO 200 I=1,N2                                                    ERR00320
      Y(2,X)=Y(2,X)+G(I)*(F(I)-G(I))                                   ERR00330
200   Y(1,X)=Y(1,X)+F(I)*(F(I)-G(I))                                   ERR00340
      N3=N-X+1                                                         ERR00350
      DO 250 I=N3,N                                                    ERR00360
      Y(2,X)=Y(2,X)+(G(N2)+F(I-N2))*(F(I)-G(I))                        ERR00370
250   Y(1,X)=Y(1,X)+(F(N2)+G(I-N2))*(F(I)-G(I))                        ERR00380
      Y(2,X)=.5*ERF((K-Y(2,X))/(S1*1.414))+.5                          ERR00390
      Y(1,X)=.5*ERFC((K-Y(1,X))/(S1*1.414))                            ERR00400
      WRITE(6,2) N,S,Z(1),Z(2),X,Y(2,X),Y(1,X)                         ERR00410
2     FORMAT(5X,I3,8X,F6.3,5X,F6.4,5X,F6.4,5X,I2,3X,F6.4,5X,F6.4)      ERR00420
300   YX=YX+Y(2,X)+Y(1,X)                                              ERR00430
      TOTEA=.9*Z(1)+.1*Z(2)                                            ERR00440
      TOTE=TOTEA+.002*YX                                               ERR00450
      WRITE(6,3)TOTEA,TOTE                                             ERR00460
3     FORMAT(/,20X,'TOTEA=',F6.4,/,20X'TOTE=',F6.4,//)                 ERR00470
400   G=G+.5                                                           ERR00480
500   CONTINUE                                                         ERR00490
      STOP                                                             ERR00500
      END                                                              ERR00510
```

APPENDIX B

A PROGRAM FOR PROCESSING EOG WAVEFORMS

The following pages contain listing of an assembly language program developed on PDP-8/E minicomputer to process raw EOG data and generate any combination of following waveforms.

i) Smoothed EOG waveform where smoothing is done by means of a 4-point averaging filter.

ii) A waveform indicating occurrences of saccades or quick phases in EOG waveform. The saccade detection algorithm is based upon the 'likelihood ratio detector' of Chapter 3.

iii) Cumulative slow phase position (CSPP) waveform. The algorithm is discussed in Chapter 4.

iv) Cumulative quick phases/saccades waveform. The algorithm is discussed in Chapter 4.

v) EOG velocity waveform. The digital differentiator used is designed using least square error straight line fit to EOG data. The slope of the line indicates velocity.

vi) EOG slow phase velocity waveform. Cumulative slow phase position and digital differentiator are used to generate slow phase velocity.

```
                /ON-LINE SACCADIC DETECTION AND SLOW PHASE VELOCITY GENERATION PROGRAM.

                /REM: THIS PROGRAM SAMPLES EOG WAVEFORM ON CHANNEL 0 AND GENERATES
                /SLOW-PHASE VELOCITY WAVEFORM ON CHANNEL X
                /AND CUMULATIVE POSITION WAVEFORM ON CHANNEL Y
                /SWITCH REGISTER SETTING: BITS 0-5 ABS(F1-F2),BITS 6-11 (F1+F2)
                /F1 DENOTES SLOW PHASE (1ST QUAD), F2 DENOTES QUICK PHASE (4TH QUAD)

                /LABORATORY PERIPHERALS DEFINITIONS

                /DK-8/EP CLOCK DEFINITIONS

6130                    CLZE=   6130            /ZEROS TO CLOCK ENABLE
6132                    CLOE=   6132            /ONES TO CLOCK ENABLE
6133                    CLAB=   6133            /LOAD BUFFER PRESET REGISTER

                /AD-8/eA A-D CONVERTOR DEFINITIONS

6531                    ADLM=   6531            /LOAD A-D MUX REGISTER
6532                    ADST=   6532            /START A-D CONVERTER
6533                    ADRB=   6533            /READ A-D BUFFER
6534                    ADSK=   6534            /SKIP ON A-D FLAG
6536                    ADLE=   6536            /LOAD A-D ENABLE REGISTER

                /D-A CONVERTOR DEFINITIONS

6551                    DALX=   6551            /LOAD X
6552                    DALY=   6552            /LOAD Y
6553                    DASK=   6553            /SKIP ON D-A FLAG
6554                    DINT=   6554            /INTENSIFY DISPLAY

                /GENERAL EQUIVALENCES

0177                    PROTMK=0177             /ROTATING MASK FOR PROTECTING TRAILING EDGE
0004                    SAMINT=4                /SAMPLING INTERVAL IN MSEC.
```

```
                /NUMERICAL CONSTANTS

        7300            NL0000= CLA CLL          /GET 0
        7301            NL0001= CLA CLL IAC      /GET 1
        7305            NL0002= CLA CLL IAC RAL  /GET 2
        7325            NL0003= CLA CLL CML IAC RAL /GET 3
        7307            NL0004= CLA CLL IAC RTL  /GET 4
        7327            NL0006= CLA CLL CML IAC RTL /GET 6
        7340            NL7777= CLA CLL CMA      /GET -1
        7344            NL7776= CLA CLL CMA RAL  /GET -2


                /PAGE ZERO LOCATIONS

       *0010            *10

00010   0367  XR,       BUFF-1                   /AUTO-INDEX FOR RAW EOG SAMPLES
00011   7777  XRE,      EBUFF-1                  /AUTO-INDEX FOR SMOOTHED EOG SAMPLES
00012   0020  XR1,      F1MF2                    /AUTO-INDEX FOR F1-F2
00013   0021  XR2,      F1PF2                    /AUTO-INDEX FOR F1+F2

       *0020            *20

00020   0512  F1MF2,    F1MF2T                   /F1-F2 TABLE ADDRESS POINTER
00021   0505  F1PF2,    F1PF2T                   /F1+F2 TABLE ADDRESS POINTER
00022   0400  PDETECT,  DETECT                   /POINTER TO DETECT SUBROUTINE
00023   0600  PCSPP,    CSPP                     /POINTER TO CUMULATIVE SLOW PHASE POSITION ROUTINE
00024   1200  PDIFF,    DIFF                     /POINTER TO DIFF. FILTER ROUTINE
00025   0000  PB1,      0                        /POINTER1
00026   0000  PB2,      0                        /POINTER2
00027   0000  CNT1,     0                        /INITIALIZING COUNTER
00030   0004  DWNWTH,   4                        /DECISION WINDOW WIDTH-1
00031   0000  DREF,     0                        /MOVING REFERENCE TO SCALE INPUT SAMPLES
```

```
00032  0000  DFN,     0                    /DECISION FUNCTION
00033  0000           0                    /DOUBLE PRECISION
00034  0000  DCODE,   0                    /DECISION CODE TO PROTECT TRAILING EDGE
00035  0000  LDCODE,  0                    /LAST VALUE OF DCODE
00036  0000  RS,      0                    /RUNNING SUM
00037  0000  SIGN,    0                    /SIGN SWITCH
00040  0000  DEL,     0                    /DELTA CHANGE IN CUM. POS.
00041  0000  VEL,     0                    /SLOW PHASE VELOCITY
00042  0000           0                    /DOUBLE PRECISION
00043  0000  VELDIS,  0                    /VELOCITY TO BE DISPLAYED
00044  0000  TEMP1,   0                    /TEMPORARY LOCATION
00045  0000  TEMP2,   0                    /DOUBLE-PRECISION
00046  0000           0                    /TEMPORARY LOCATION
00047  0000  TEMP3,   0                    /TEMPORARY LOCATION
00050  0000  TEMP4,   0                    /TEMPORARY LOCATION
00051  0000  TEMP5,   0                    /TEMPORARY LOCATION
00052  0000  TEMP6,   0                    /TEMPORARY LOCATION
00053  0000           0                    /DOUBLE PRECISION
       0000  EBUFF=   0                    /EOG BUFFER INITIALIZATION
00054  0000  EBUFDP,  EBUFF                /EOG DISPLAY POINT POINTER
00055  0104  YM1,     CBUFF+104            /Y(-1) POINTER
00056  0105  Y0,      CBUFF+105            /Y(0) POINTER
00057  0125  Y2N,     CBUFF+125            /Y(2N) POINTER
       0003  XDIVN=   3                    /DIVISION BY 'N' IN EXTRAPOLATION
       0010  DELWN=   10
       0001  DELN=    1                    /DIVISION CONSTANT FOR DEL AVERAGING
00060  0061  EBUFDS,  EBUFF+61            /START OF DECISION WINDOW POINTER
00061  0063  EBUFDM,  EBUFF+63            /DECISION WINDOW MID POINT POINTER
00062  0065  EBUFLP,  EBUFF+65            /LATEST EOG POINT POINTER
       0000  CBUFF=   0                    /CUM. POS. BUFFER INITIALIZATION
```

```
00063   0057  CBUFDP, CBUFF+57          /CUMULATIVE POS. DISPLAY POINT POINTER
00064   0060  DIFMM1, CBUFF+60          /DIFF. MID POINT-1
00065   0061  CDIFMP, CBUFF+61          /DIFF. MID POINT POINTER
00066   0062  DIFMP1, CBUFF+62          /DIFF. MID POINT+1
        0030  NM1B2=  30                /(TOTAL DIFF.PTS.-1)/2
00067   0131  CBUFN,  CBUFF+131         /FIRST POINT REPLACED-4 POINT POINTER
00070   0135  CBFNP1, CBUFF+135         /FIRST POINT REPLACED POINTER
        0006  CBUFRP= 6                 /CBUFF POINTS TO BE REPLACED
00071   0136  CBLPM1, CBUFF+136         /LATEST POINT-4 POINTER
00072   0142  CBUFLP, CBUFF+142         /LATEST CUMULATIVE POINT POINTER
00073   1464  DFILTS, DBUFF+64          /DIFF. FILTER START POINTER
00074   1500  DBLP,   DBUFF+100         /DIFF. BUFFER LATEST POINT POINTER
        0004  VGAIN=  4                 /VELOCITY GAIN CONTROL

       *0200          PAGE
```

```
                /MAIN PROGRAM

00200  6007  START,  CAF                    /CLEAN UP
00201  6201          CDF      00           /MAKE SURE DATA FIELD 0
00202  7431          SWAB                  /FORCE MODE B EAE
00203  7300          NL0000                /GET A/D 0
00204  6531          ADLM                  /LOAD MUX REG
00205  1377          TAD      (200         /ENABLE A-D BY CLOCK
00206  6536          ADLE                  /FOR INPUT ROUTINE
00207  6551          DALX                  /CENTER X, RAISING DONE FLAG
00210  6552          DALY                  /CENTER Y, RAISING DONE FLAG
00211  1177          TAD      (-SAMINT)    /SET SAMPLING INTERVAL
00212  6133          CLAB                  /PRESET CLOCK BUFFER
00213  7240          STA                   /-1
00214  6130          CLZE                  /CLEAR CLOCK
00215  0376          AND      (1340        /MODE 01, 1KHZ,A-D START
00216  6132          CLOE                  /LOAD CLOCK ENABLE
00217  4336  FEED,   JMS      SMOOTH       /OBTAIN A SMOOTHED EOG SAMPLE
00220  6211          CDF      10           /SAVE IN DATA FIELD 1
00221  3462          DCA I    EBUFLP       /THE LATEST SAMPLE
00222  6201          CDF      00           /RESTORE DATA FIELD
00223  1021          TAD      F1PF2        /INITILIZE POINTERS FOR TABLES
00224  3012          DCA      XR1
00225  1020          TAD      F1MF2
00226  3013          DCA      XR2
00227  7307          NL0004                /INITILIZE COUNTER
00230  7041          CIA
00231  3045          DCA      TEMP2
00232  3044          DCA      TEMP1        /CLEAN UP TEMP1
00233  7604  TABUP1, LAS                   /READ IN SWITCH REGISTER
00234  0375          AND      (77          /MASK  LEFT BITS
00235  1044          TAD      TEMP1        /ADD ON OLD SUM
00236  3044          DCA      TEMP1        /AND SAVE
00237  1044          TAD      TEMP1        /GET BACK SUM
00240  3412          DCA I    XR1          /UPDATE TABLE
```

```
00241  2045           ISZ     TEMP2          /DONE?
00242  5233           JMP     TABUP1         /NO
00243  3044           DCA     TEMP1          /CLEAN UP TEMP1
00244  7307           NL0004                 /INITIALIZE COUNTER
00245  7041           CIA
00246  3045           DCA     TEMP2
00247  7604  TABUP2,  LAS                    /READ IN SWITCH REGISTER
00250  7002           BSW                    /SWAP
00251  0375           AND     I77            /CLEAN UP LEFT BITS
00252  7041           CIA                    /NEGATE IT
00253  1044           TAD     TEMP1          /ADD ON OLD SUM
00254  3044           DCA     TEMP1          /AND SAVE
00255  1044           TAD     TEMP1          /GET IT BACK
00256  3413           DCA I   XR2            /UPDATE TABLE
00257  2045           ISZ     TEMP2          /DONE?
00260  5247           JMP     TABUP2         /NO
00261  4422           JMS I   PDETECT        /DETECT ROUTINE
00262  4423           JMS I   PCSPP          /COMPUTE COMULATIVE SLOW PHASE POSITION
00263  4424           JMS I   PDIFF          /COMPUTE VELOCITY
00264  7621           CAM                    /CLEAN UP
00265  6221           CDF     20             /OBTAIN FROM DATA FIELD 2
00266  1463           TAD I   CBUFDP         /THE CUMULATIVE POSITION DISPLAY POINT
00267  6201           CDF     00             /RESTORE DATA FIELD 0
00270  6552           DALY                   /DISPLAY
00271  7621           CAM                    /CLEAR AC AND MQ
00272  1043           TAD     VELDIS         /OBTAIN VELOCITY FOR DISPLAY
00273  6551           DALX                   /DISPLAY
00274  6553           DASK                   /D-A DONE?
00275  5274           JMP     .-1            /NO, WAIT
00276  6554           DINT                   /YES OUTPUT INTENSITY
```

```
                /UPDATE VARIOUS POINTERS:
00277  2054     ISZ     EBUFDP          /EOG DISPLAY POINT POINTER
00300  7000     NOP
00301  2055     ISZ     YM1             /Y(-1)  POINTER
00302  7000     NOP
00303  2056     ISZ     Y0              /Y(0) POINTER
00304  7000     NOP
00305  2057     ISZ     Y2N             /Y(2N) POINTER
00306  7000     NOP
00307  2060     ISZ     EBUFDS          /DECISION WINDOW START POINTER
00310  7000     NOP
00311  2061     ISZ     EBUFDM          /DECISION WINDOW MID POINT POINTER
00312  7000     NOP
00313  2062     ISZ     EBUFLP          /LATEST EOG POINT POINTER
00314  7000     NOP
00315  2063     ISZ     CBUFDP          /CUM. POS. DISPLAY POINT POINTER
00316  7000     NOP
00317  2064     ISZ     DIFMM1          /DIFF. MID PT.-1
00320  7000     NOP
00321  2065     ISZ     CDIFMP          /DIFF. MID POINT POINTER
00322  7000     NOP
00323  2066     ISZ     DIFMP1          /DIFF. MID PT.+1
00324  7000     NOP
00325  2067     ISZ     CBUFN           /FIRST REPLACED-1 POINT POINTER
00326  7000     NOP
00327  2070     ISZ     CBFNP1          /FIRST REPLACED POINT POINTER
00330  7000     NOP
00331  2071     ISZ     CBLPM1          /LATEST POINT-1 POINTER
00332  7000     NOP
00333  2072     ISZ     CBUFLP          /LATEST CUM. POS. POINT POINTER
00334  7000     NOP
00335  5217     JMP     FEED            /GO DO IT AGAIN
```

```
00336  0000  SMOOTH, 0                    /AVERAGING INPUT ROUTINE
00337  7344         NL7776                /-2
00340  3037         DCA     SIGN          /TO SIGN SWITCH
00341  1371         TAD     BUFF+1        /\
00342  3370         DCA     BUFF          / \
00343  1372         TAD     BUFF+2        /  \MOVE BACK
00344  3371         DCA     BUFF+1        /  /ONE PLACE
00345  1373         TAD     BUFF+3        / /
00346  3372         DCA     BUFF+2        //
00347  6534         ADSK                  /A-D READY?
00350  5347         JMP     .-1           /NO, WAIT FOR IT
00351  6533         ADRB                  /READ IT IN
00352  3373         DCA     BUFF+3        /STASH IT
00353  1370         TAD     BUFF          /\
00354  1371         TAD     BUFF+1        / \ADD UP
00355  1372         TAD     BUFF+2        / /FOUR POINTS
00356  1373         TAD     BUFF+3        //
00357  7500         SMA                   /NEGATIVE?
00360  2037         ISZ     SIGN          /NO,BUMP SIGN SWITCH
00361  7510         SPA                   /POSITIVE?
00362  7041         CIA                   /NO,TAKE ABSOLUTE VALUE
00363  7110         CLL RAR               /DIVIDE BY 2
00364  7110         CLL RAR               /DIVIDE BY 2
00365  2037         ISZ     SIGN          /INVERT BACK?
00366  7041         CIA                   /YES
00367  5736         JMP I   SMOOTH        /RETURN TO CALLER

00370  0000  BUFF,  ZBLOCK  4             /RAW EOG BUFFER

       *0375
00375  0077
00376  1340
00377  0200
       *0400         PAGE
```

```
                /LIKELIHOOD RATIO DETECTOR SUBROUTINE

00400  0000  DETECT, 0
00401  7621         CAM                    /CLEAN UP
00402  1377         TAD     (SBUFF         /RESTORE XRE TO
00403  3011         DCA     XRE            /START OF DATA WINDOW
00404  1020         TAD     F1MF2          /RESTORE XR1 TO
00405  3012         DCA     XR1            /START OF F1-F2
00406  1021         TAD     F1PF2          /RESTORE XR2 TO
00407  3013         DCA     XR2            /START OF F1+F2
00410  7421         MQL                    /ZERO LSPART OF DFN
00411  7445         DST;    DFN            /ZERO DFN
00412  0032
00413  1060         TAD     EBUFDS         /RESET PB1 TO
00414  3025         DCA     PB1            /FIRST SMOOTHED SAMPLE
00415  1377         TAD     (SBUFF         /RESET PB2 TO
00416  3026         DCA     PB2            /FIRST SCALED SAMPLE
00417  1030         TAD     DWNWTH         /RESTORE WINDOW COUNTER
00420  7041         CIA
00421  3027         DCA     CNT1           /TO -(DECISION WINDOW WIDTH-1)
00422  6211         CDF     10             /FROM DATA FIELD 1,
00423  1425         TAD I   PB1            /GET FIRST POINT
00424  6201         CDF     00             /RESTORE DATA FIELD 0
00425  7041         CIA                    /NEGATE IT
00426  3031         DCA     DREF           /SAVE IN DREF
00427  3426         DCA I   PB2            /ZERO IPO FIRST POINT
00430  2025  BACK1, ISZ     PB1            /INCREMENT PB1
00431  7000         NOP
00432  2026         ISZ     PB2            /INCREMENT PB2
00433  6211         CDF     10             /FROM DATA FIELD 1
00434  1425         TAD I   PB1            /GET NEXT POINT
00435  6201         CDF     00             /RESTORE DATA FIELD 0
00436  1031         TAD     DREF           /ADD -FIRST POINT
00437  7510         SPA                    /POSITIVE?
00440  7041         CIA                    /NO,NEGATE
00441  3426         DCA I   PB2            /SAVE IT
00442  2027         ISZ     CNT1           /DONE?
00443  5230         JMP     BACK1          /NO, DO IT AGAIN
```

```
                /DECISION FUNCTION "DFN" CALCULATIONS

00444  1030           TAD      DWNWTH          /SET COUNTER
00445  7041           CIA                      /TO
00446  3027           DCA      CNT1            /-(DECISION WINDOW WIDTH-1)
00447  7340  DECSN,   NL7777                   /-1
00450  3037           DCA      SIGN            /TO SIGN SWITCH
00451  1412           TAD I    XR1             /GET F1-F2
00452  7041           CIA                      /NEGATE
00453  7421           MQL                      /SAVE IN MQ
00454  1411           TAD I    XRE             /GET DATA SAMPLE R
00455  7104           CLL RAL                  /R*2
00456  7041           CIA                      /-R*2
00457  1413           TAD I    XR2             /FORM F1+F2-2R
00460  3044           DCA      TEMP1           /SAVE IN TEMP1
00461  1044           TAD      TEMP1           /GET F1+F2-2R
00462  7510           SPA                      /POSITIVE?
00463  7410           SKP                      /NO,SKIP TO INVERT
00464  5270           JMP      POSMUL          /YES,SKIP TO MULTIPLY
00465  7041           CIA                      /INVERT
00466  3044           DCA      TEMP1           /SAVE IN TEMP1
00467  2037           ISZ      SIGN            /SIGN=0 IF F1+F2-2R IS NEGATIVE
00470  7200  POSMUL,  CLA                      /CLEAR AC
00471  7405           MUY;     TEMP1           /(F1-F2)(F1+F2-2R)
00472  0044
00473  2037           ISZ      SIGN            /WAS NEGATIVE?
00474  7410           SKP                      /NO,SKIP TO SAVE
00475  7575           DCM                      /YES, ATTACH SIGN
00476  7443           DAD;     DFN             /ADD TO LAST DFN VALUE
00477  0032
00500  7445           DST;     DFN             /AND SAVE
00501  0032
00502  2027           ISZ      CNT1            /DONE?
00503  5247           JMP      DECSN           /NO,DO NEXT PT.
00504  5600           JMP I    DETECT          /RETURN
```

```
                /FUNCTION TABLES

00505  0000  F1PF2T, 0                        /F1+F2 TABLE
00506  0010          10
00507  0020          20
00510  0030          30
00511  0040          40

00512  0000  F1MF2T, 0                        /F1-F2 TABLE
00513  7772          7772
00514  7764          7764
00515  7756          7756
00516  7750          7750

00517  0000  SBUFF,  ZBLOCK  5                /SCALED EOG BUFFER

      *0577
00577  0517
      *0600          PAGE
```

```
                /CUMULATIVE SLOW PHASE POSITION "CSPP" LOGIC AND CALCULATIONS SUBROUTINE

00600  0000  CSPP,   0
00601  7621          CAM                     /CLEAN UP
00602  1034          TAD     DCODE           /REPLACE LDCODE
00603  3035          DCA     LDCODE          /BY DCODE
00604  7100          CLL                     /CLEAR LINK
00605  7443          DAD;    DFN             /GET DFN
00606  0032
00607  7700          SMA CLA                 /NEGATIVE?
00610  7120          STL                     /NO,SET LINK=1
00611  1034          TAD     DCODE           /GET LAST DECISION CODE
00612  7004          RAL                     /ROTATE LEFT
00613  0176          AND     [PROTMK]        /CLEAN LEFT OF DECISION-CODE
00614  3034          DCA     DCODE           /SAVE NEW DECISION-CODE
00615  1034          TAD     DCODE           /GET DECISION -CODE
00616  7450          SNA                     /NON-ZERO?
00617  5237          JMP     SLOW            /NO, SLOW-PHASE!
00620  7300  QUICK,  CLA CLL                 /CLEAN UP
00621  1035          TAD     LDCODE          /WAS LAST POINT QUICK PHASE
00622  7440          SZA                     /NO
00623  5226          JMP     QPH             /YES
00624  4673  FTQP,   JMS I   PXPOS           /EXTRAPOLATE CORRECTION FACTOR "DEL" AND
00625  5272          JMP     NEXT            /CORRECT BAD CUM.POSITIONS
00626  7621  QPH,    CAM
00627  6221          CDF     20              /FROM DATA FIELD 2
00630  1471          TAD I   CBLPM1          /GET LAST CUM. POS.
00631  6201          CDF     00              /RESTORE DATA FIELD 0
00632  1040          TAD     DEL             /ADD ON DEL. CHANGE
00633  6221          CDF     20              /SAVE IN DATA FIELD 2 THE
00634  3472          DCA I   CBUFLP          /EXTRAPOLATED CUMULATIVE POSITION
00635  6201          CDF     00              /RESTORE DATA FIELD 0
00636  5272          JMP     NEXT            /DO NEXT POINT
```

```
00637  1035  SLOW,   TAD      LDCODE          /GET LAST DCODE
00640  7450           SNA                     /BEGINNING OR CONTINUATION
00641  5262           JMP      SLPH
00642  7621  FTSP,    CAM
00643  6221           CDF      20             /FROM DATA FIELD 2
00644  1471           TAD I    CBLPM1         /GET LAST CUM. POS.
00645  6201           CDF      00             /RESTORE DATA FIELD 0
00646  1040           TAD      DEL            /ADD ON DEL CHANGE
00647  3045           DCA      TEMP2          /SAVE TEMPORARILY
00650  1045           TAD      TEMP2          /GET CUM. POS. BACK
00651  6221           CDF      20             /SAVE IN DATA FIELD 2 THE
00652  3472           DCA I    CBUFLP         /EXTRAPOLATED CUMULATIVE POSITION
00653  6211           CDF      10             /FROM DATA FIELD 1
00654  1462           TAD I    EBUFLP         /GET DECISION WINDOW MID POINT
00655  6201           CDF      00             /RESTORE DATA FIELD 0
00656  7041           CIA                     /NEGATE IT
00657  1045           TAD      TEMP2          /ADD ON CUM. POS.
00660  3036           DCA      RS             /AND SAVE RUNNING SUM
00661  5272           JMP      NEXT
00662  7621  SLPH,    CAM
00663  6211           CDF      10             /FROM DATA FIELD 1
00664  1462           TAD I    EBUFLP         /GET DECISION WINDOW MID POINT
00665  6201           CDF      00             /RESTORE DATA FIELD 0
00666  1036           TAD      RS             /ADD ON RUNNING SUM
00667  6221           CDF      20             /IN DATA FIELD 2
00670  3472           DCA I    CBUFLP         /SAVE CUM. POS.
00671  6201           CDF      00             /RESTORE DATA FIELD 0
00672  5600  NEXT,    JMP I    CSPP           /RETURN

00673  1000  PXPOS,   XPOS                     /POINTER TO EXTRAPOLATE CUMULATIVE POSITION

       *1000          PAGE
```

```
                /SUBROUTINE TO EXTRAPOLATE CUMULATIVE POSITION ACROSS SACCADES

01000  0000  XPOS,   0
01001  7621          CAM                    /CLEAN UP
01002  1377          TAD     (-DELWN        /SET COUNTER TO - OF
01003  3027          DCA     CNT1           /DELTAS FOR AVERAGING
01004  7445          DST;    TEMP6          /ZERO TEMP. LOCATION
01005  0052
01006  7621  LOOP,   CAM                    /CLEAR AC AND MQ
01007  6221          CDF     20             /FROM DATA FIELD 2
01010  1456          TAD I   Y0             /GET Y(0)
01011  7041          CIA                    /-Y(0)
01012  1457          TAD I   Y2N            /GET Y(2N)
01013  6201          CDF     00             /RESTORE DATA FIELD 0
01014  7415          ASR;    XDIVN          /DIVIDE BY N
01015  0003
01016  7443          DAD;    TEMP6          /ADD ON PREVIOUS SUM
01017  0052
01020  7445          DST;    TEMP6          /AND SAVE
01021  0052
01022  2056          ISZ     Y0             /UPDATE POINTERS Y0 & Y2N
01023  7000          NOP
01024  2057          ISZ     Y2N
01025  7000          NOP
01026  2027          ISZ     CNT1           /DONE?
01027  5206          JMP     LOOP           /NO, DO NEXT POINT
01030  7621          CAM                    /ZERO AC AND MQ
01031  7340          NL7777                 /DECREMENT POINTER Y0
01032  1056          TAD     Y0
01033  3056          DCA     Y0
01034  6221          CDF     20             /FROM DATA FIELD 2
01035  1456          TAD I   Y0             /GET Y(0)
01036  7041          CIA                    /-Y(0)
01037  1455          TAD I   YM1            /ADD ON Y(-1)
01040  6201          CDF     00             /RESTORE DATA FIELD 0
```

```
01041  7443          DAD;    TEMP6          /ADD ON SAVED SUM
01042  0052
01043  7415          ASR;    DELN           /AVERAGE OVER DELTAS
01044  0001
01045  3040          DCA     DEL            /SAVE DEL CHANGE IN CUMULATIVE POSITION
01046  7621          CAM
01047  1377          TAD     (-DELWN        /RESTORE POINTERS YO & Y2N
01050  1056          TAD     YO
01051  7001          IAC
01052  3056          DCA     YO
01053  1377          TAD     (-DELWN
01054  1057          TAD     Y2N
01055  3057          DCA     Y2N
01056  1376          TAD     (-CBUFRP       /- OF NO. OF POINTS TO BE REPLACED
01057  3027          DCA     CNT1
01060  1070          TAD     CBFNP1         /FIRST POINT TO BE REPLACED
01061  3050          DCA     TEMP4
01062  1067          TAD     CBUFN          /LAST SLOW PHASE POINT
01063  3051          DCA     TEMP5
01064  6221  HERE,   CDF     20             /FROM DATA FIELD 2
01065  1451          TAD I   TEMP5          /GET LAST CUM. POS.
01066  6201          CDF     00             /RESTORE DATA FIELD 0
01067  1040          TAD     DEL            /ADD ON DEL CHANGE
01070  6221          CDF     20             /IN DATA FIELD 2
01071  3450          DCA I   TEMP4          /SAVE EXTRAPOLATED CUM. POS.
01072  6201          CDF     00             /RESTORE DATA FIELD 0
01073  2050          ISZ     TEMP4          /UPDATE POINTERS
01074  7000          NOP
01075  2051          ISZ     TEMP5
01076  7000          NOP
01077  2027          ISZ     CNT1           /DONE?
01100  5264          JMP     HERE           /NO, DO  NEXT POINT
01101  5600          JMP I   XPOS           /RETURN

       *1176
01176  7772
01177  7770
       *1200          PAGE
```

```
                /DIFFERENTIATING FILTER SUBROUTINE

01200  0000  DIFF,   0
01201  7301          NL0001                  /SET TEMP1=1
01202  3044          DCA     TEMP1
01203  1064          TAD     DIFMM1          /SET PB2 TO DIFF. MID PT.-1
01204  3026          DCA     PB2
01205  1377          TAD     (-NM1B2         /(TOTAL DIFF. PTS.-1)/2
01206  3027          DCA     CNT1
01207  1066          TAD     DIFMP1          /SET PB1 TO DIFF. MID PT.+1
01210  3025          DCA     PB1
01211  7421          MQL                     /CLEAR MQ
01212  7445          DST;    VEL             /CLEAR VEL
01213  0041
01214  7344  BACK2,  NL7776                  /-2
01215  3037          DCA     SIGN            /TO SIGN
01216  6221          CDF     20
01217  1426          TAD I   PB2             /FORM F(K+J)-F(K-J)
01220  7041          CIA
01221  1425          TAD I   PB1
01222  6201          CDF     00
01223  7500          SMA                     /NEGATIVE?
01224  5227          JMP     .+3             /NO, SKIP TO SAVE
01225  7041          CIA                     /YES,MAKE IT POSITIVE
01226  2037          ISZ     SIGN            /SIGN=1 ON NEGATIVE
01227  7421          MQL                     /SAVE
01230  2025          ISZ     PB1             /INCREMENT PB1
01231  7000          NOP
01232  7340          NL7777                  /DECREMENT PB2
01233  1026          TAD     PB2
01234  3026          DCA     PB2
01235  7405          MUY;    TEMP1           /MULTIPLY WITH J
01236  0044
01237  2037          ISZ     SIGN            /INVERT BACK?
01240  7410          SKP                     /NO
```

```
01241  7575          DCM                    /YES
01242  7443          DAD;    VEL            /ADD ON PREVIOUS SUM
01243  0041
01244  7445          DST;    VEL            /AND SAVE
01245  0041
01246  2044          ISZ     TEMP1          /INCREMENT J
01247  2027          ISZ     CNT1           /DONE?
01250  5214          JMP     BACK2          /NO, DO NEXT POINT
01251  7413          SHL;    VGAIN          /ADJUST GAIN
01252  0004
01253  3043          DCA     VELDIS         /VELOCITY TO BE DISPLAYED
01254  3474          DCA I   DBLP           /PUT ON TOP
01255  1074          TAD     DBLP           /UPDATE POINTER
01256  7001          IAC
01257  0376          AND     (0177          /LIMIT TO 1 PAGE
01260  1375          TAD     (DBUFF
01261  3074          DCA     DBLP           /PUT AWAY
01262  5600          JMP I   DIFF           /RETURN

       *1375
01375  1400
01376  0177
01377  7750
       *1400          PAGE

01400  0000  DBUFF,  ZBLOCK  177            /DIFF. BUFFER

       *1600          PAGE

       *0176
00176  0177
00177  7774
```

ASSEMBLY STATISTICS

NO ERRORS DETECTED

NO LINKS GENERATED

5K MEMORY UTILIZED

1 FILE CREATED

103 SYMBOLS

APPENDIX C

OKN AND OKAN MODEL PARAMETER ESTIMATION PROGRAM

The following pages present the main part of an assembly program for the PDP-8/E computer. This program estimates the parameters of OKN and OKAN model from a given step response. The model, the parameter estimation technique and the relations between the estimated parameters and the model parameters are described in chapter 5.

```
                /PARAMETER IDENTIFICATION PROGRAM

                /THIS PROGRAM ESTIMATES THE PARAMETERS OF OKN AND OKAN MODEL.
                /STIMULUS VELOCITY IS STORED IN FIELD 2 STARTING AT 400
                /RESPONSE VELOCITY IS STORED IN FIELD 1 STARTING AT 400
                /SET SWITCH REGISTER POSITIVE FOR OKAN MODEL IDENTIFICATION AND
                /NEGATIVE STIMULUS VALUE FOR OKN MODEL IDENTIFICATION

        *0770
000770   1170
000771   0171
000772   0467
000773   0466
000774   0001
000775   0465
000776   7000
000777   0430
        *0014           *14
000014   0417   PTRDAT, 417                    /DATA POINTER(AUTO-INDEX)
000015   0417   PARPTR, 417                    /PARAMETER POINTER(AUTO-INDEX)

        *0070           *70
000070   0000   Y0,      ZBLOCK  3             /Y(0)
000073   0000   M,       ZBLOCK  3             /NO. OF MEASUREMENTS
000076   0000   YM1,     ZBLOCK  3             /Y(M-1)
000101   0000   YM,      ZBLOCK  3             /Y(M)
000104   0000   SY,      ZBLOCK  3             /Y(0)+Y(1)+....+Y(M-1)
000107   0000   SSY,     ZBLOCK  3             /Y(0)**2+....+Y(M-1)**2
000112   0000   SY1,     ZBLOCK  3             /(Y(1)+Y(2)+.........+Y(M)
000115   0000   SYY1,    ZBLOCK  3             /Y(0)(Y(1)+..........Y(M-1)Y(M)
000120   0000   TEMP1,   ZBLOCK  3             /TEMPORARY STORAGE
000123   0000   TEMP2,   ZBLOCK  3             /TEMPORARY STORAGE
000126   0001   ONE,     1                     /NUMERICAL 1
000127   2000            2000
000130   0000            0
000131   0000   MDIST,   0                     /MEASUREMENTS DISTANCE-1
                                               /CHANGE IT TO DEAL WITH CORRELATED NOISE
000132   1000   PLOOP,   LOOP                  /POINTER TO LOOP
```

```
000133  1105  PSPACE, PRSPACE                 /POINTER TO PRINT SPACE ROUTINE
000134  1125  PCRSUPP,CRSUPP                  /POINTER TO CR SUPPRESS ROUTINE
000135  1117  PCRREST,CRREST                  /POINTER TO CR RESTORE ROUTINE
000136  1200  POKANID,OKANID                  /POINTER TO OKAN PARAMETER IDENTIFICATION
000137  0000  R,      ZBLOCK  3               /INPUT STIMULUS
000142  0000  A,      ZBLOCK  3               /PARAMETER A
000145  0000  B,      ZBLOCK  3               /PARAMETER B
000150  0000  C,      ZBLOCK  3               /PARAMETER C
000153  6000  PARCTR, 6000                     /-2000 OCTAL

      *0651  *CONTIN
000651  0000  FROAN,  .-.                     /ANALIZE

000652  6221         CDF     20              /SET DATA FIELD =2
000653  7300  BEGIN,  CLA CLL                 /CLEAN UP AC & LINK
000654  1367         TAD     (7720           /-60 OCTAL
000655  1414         TAD I   PTRDAT          /ADD ON STIMULUS
000656  7510         SPA                     /STIMULUS ON?
000657  5253         JMP     BEGIN           /NO, SEARCH FOR IT
000660  6032         KCC                     /INITIALIZE KEYBOARD
000661  6046         TLS                     /AND TELEPRINTER
000662  7300         CLA CLL                 /CLEAN UP
000663  7604         LAS                     /READ IN SWITCH REGISTER
000664  7500         SMA                     /OKN?
000665  5347         JMP     OKAN            /NO, OKAN
000666  6201  OKN,    CDF     00              /SET TO FIELD 0
000667  7604         LAS                     /READ IN SWITCH REG FOR STIMULUS R
000670  3044         DCA     FLAC            /R IN FLOATING AC
000671  4407         FENT                    /ENTER FPP
000672  0014         FLOT                    /CONVERT TO FLOATING POINT NUMBER
000673  6137         FPUT    R               /SAVE IN R
000674  0000         FEXT                    /LEAVE FPP
000675  2014         ISZ     PTRDAT          /GET PAST DELAY IN OKN RESPONSE
000676  2014         ISZ     PTRDAT
000677  2014         ISZ     PTRDAT
000700  2014         ISZ     PTRDAT
```

```
000701  6211          CDF     10              /SET DATA FIELD =1
000702  1414          TAD I   PTRDAT          /GET Y(0)
000703  6201          CDF     00              /SET DATA FIELD=0
000704  3044          DCA     FLAC            /SAVE IN FLOATING AC
000705  4407          FENT                    /ENTER INTERPRETER
000706  0014          FLOT                    /CONVERT TO FLOATING POINT NUMBER
000707  6070          FPUT    Y0              /SAVE Y(0)
000710  0012          FOUT
000711  5126          FGET    ONE             /M=1
000712  6073          FPUT    M
000713  0000          FEXT                    /EXIT FPP
000714  7300          CLA CLL                 /CLEAN UP AC
000715  1014          TAD     PTRDAT          /COMPUTE MEASUREMENT SPACING
000716  1131          TAD     MDIST
000717  3014          DCA     PTRDAT
000720  6211          CDF     10              /SET DATA FIELD=1
000721  1414          TAD I   PTRDAT          /GET Y(1)
000722  6201          CDF     00              /SET DATA FIELD =0
000723  3044          DCA     FLAC            /IN FLOATING AC
000724  4407          FENT                    /ENTER INTERPRETER
000725  0014          FLOT                    /CONVERT TO FLOATING POINT NUMBER
000726  6101          FPUT    YM              /AND SAVE
000727  0012          FOUT
000730  5070          FGET    Y0              /SY(1)=Y0
000731  6104          FPUT    SY
000732  5070          FGET    Y0              /SSY(1)=Y(0)**2
000733  3070          FMPY    Y0
000734  6107          FPUT    SSY
000735  5101          FGET    YM              /SY1(1)=Y(1)
000736  6112          FPUT    SY1
000737  5101          FGET    YM              /SYY1(1)=Y(0)Y(1)
000740  3070          FMPY    Y0
000741  6115          FPUT    SYY1
```

```
000742  5070          FGET    YO              /C=Y(0)/R
000743  4137          FDIV    R
000744  6150          FPUT    C
000745  0012          FOUT                    /PRINT C
000746  0532          FJMP I  PLOOP           /NEXT FILE
000747  7300  OKAN,    CLA CLL
000750  1414          TAD I   PTRDAT          /GET STIMULUS
000751  7500          SMA                     /OKAN?
000752  5347          JMP     OKAN            /NO, SEARCH FOR IT
000753  6211          CDF     10              /SET DATA FIELD =1
000754  7300          CLA CLL                 /CLEAN UP
000755  1414          TAD I   PTRDAT          /GET Y(0)
000756  6201          CDF     00              /SET DATA FIELD =0
000757  3044          DCA     FLAC            /IN FPP AC
000760  4407          FENT                    /ENTER FPP
000761  0014          FLOT                    /FLOATING POINT NUMBER
000762  6101          FPUT    YM              /SAVE Y(0)
000763  0012          FOUT                    /PRINT Y(0)
000764  0536          FJMP I  POKANID         /IDENTIFY OKAN PARAMETERS

        *0767
000767  7720
        *1000         PAGE
```

```
       *1000          PAGE
              /IDENTIFICATION OF PARAMETERS A AND B

001000  5073  LOOP,   FGET    M               /M=M+1
001001  1126          FADD    ONE
001002  6073          FPUT    M
001003  0012          FOUT                    /PRINT M
001004  7325          FJMS    CRSUPP
001005  5101          FGET    YM              /SHIFT BACK ONE PLACE
001006  6076          FPUT    YMM1
001007  0000          FEXT                    /EXIT FPP
001010  7300          CLA CLL                 /CLEAN UP
001011  1014          TAD     PTRDAT          /COMPUTE MEASUREMENT SPACING
001012  1131          TAD     MDIST
001013  3014          DCA     PTRDAT
001014  6211          CDF     10              /SET DATA FIELD=1
001015  1414          TAD I   PTRDAT          /GET Y(M)
001016  6201          CDF     00              /SET DATA FIELD=0
001017  3044          DCA     FLAC            /IN FLOATING AC
001020  4407          FENT                    /ENTER INTERPRETER
001021  0014          FLOT                    /CONVERT TO FLOATING POINT NUMBER
001022  6101          FPUT    YM              /AND SAVE
001023  0012          FOUT
001024  5076          FGET    YMM1            /SY=SY+Y(M-1)
001025  1104          FADD    SY
001026  6104          FPUT    SY
001027  5076          FGET    YMM1            /SSY=SSY+Y(M-1)**2
001030  3076          FMPY    YMM1
001031  1107          FADD    SSY
001032  6107          FPUT    SSY
001033  5101          FGET    YM              /SY1=SY1+Y(M)
001034  1112          FADD    SY1
001035  6112          FPUT    SY1
```

```
001036  5101          FGET    YM              /SYY1=SYY1+Y(M-1)Y(M)
001037  3076          FMPY    YMM1
001040  1115          FADD    SYY1
001041  6115          FPUT    SYY1
001042  5073          FGET    M               /M*SYY1-SY*SY1
001043  3115          FMPY    SYY1
001044  6120          FPUT    TEMP1
001045  5104          FGET    SY
001046  3112          FMPY    SY1
001047  0010          FNEG
001050  1120          FADD    TEMP1
001051  6120          FPUT    TEMP1
001052  5104          FGET    SY              /M*SSY-SY**2
001053  3104          FMPY    SY
001054  0010          FNEG
001055  6123          FPUT    TEMP2
001056  5073          FGET    M
001057  3107          FMPY    SSY
001060  1123          FADD    TEMP2
001061  6123          FPUT    TEMP2
001062  5120          FGET    TEMP1           /PARAMETER A
001063  4123          FDIV    TEMP2
001064  7305          FJMS    PRSPACE         /PRINT SPACE
001065  6142          FPUT    A
001066  0012          FOUT                    /TYPE OUT A
001067  5115          FGET    SYY1            /-SY*SYY1+SSY*SY1
001070  3104          FMPY    SY
001071  0010          FNEG
001072  6120          FPUT    TEMP1
001073  5107          FGET    SSY
001074  3112          FMPY    SY1
001075  1120          FADD    TEMP1
001076  4123          FDIV    TEMP2
001077  4137          FDIV    R               /PARAMETER B
001100  7305          FJMS    PRSPACE         /PRINT SPACE
001101  6145          FPUT    B
001102  7317          FJMS    CRLEST          /RESTORE CR AND LF
001103  0012          FOUT                    /TYPE OUT B
001104  0200          FJMP    LOOP            /DO IT AGAIN
```

```
001105  0000  PRSPACE,0                    /PRINT SPACE SUBROUTINE
001106  0000        FEXT                   /EXIT FPP
001107  7200        CLA                    /CLEAR AC
001110  1377        TAD     I240           /ASCII FOR SPACE
001111  6041        TSF                    /READY?
001112  5311        JMP     .-1            /NO
001113  6046        TLS                    /PRINT
001114  7300        CLA CLL                /CLEAN UP
001115  4407        FENT                   /ENTER FPP
001116  0705        FJMP I  PRSPACE        /RETURN

001117  0000  CRREST, 0                    /CR,LF RESTORE ROUTINE
001120  0000        FEXT                   /LEAVE FPP
001121  7203        CLA IAC BSW            /NON-ZERO IN AC
001122  3055        DCA     R55            /R55 IS NON-ZERO
001123  4407        FENT                   /ENTER  FPP
001124  0717        FJMP I  CRREST         /RETURN

001125  0000  CRSUPP, 0                    /CR,LF SUPPRESS ROUTINE
001126  0000        FEXT                   /LEAVE FPP
001127  7200        CLA                    /ZERO IN AC
001130  3055        DCA     R55            /R55 IS ZERO
001131  4407        FENT                   /ENTER FPP
001132  0725        FJMP I  CRSUPP         /RETURN

      *1177
001177  0240
      *1200        PAGE
```

```
                / OKAN PARAMETER IDENTIFICATION

001200  0000  OKANID, FEXT                    /LEAVE FPP
001201  1377        TAD     (400             /INITIALIZE PARAMETER POINTER
001202  3015        DCA     PARPTR
001203  4407        FENT                     /ENTER FPP
001204  5073  REPET, FGET    M                /M=M+1
001205  1126        FADD    ONE
001206  6073        FPUT    M
                /     FOUT                   /PRINT M
                /     FJMS I  PCRSUPP
001207  5101        FGET    YM               /SHIFT BACK ONE PLACE
001210  6076        FPUT    YMM1
001211  0000        FEXT                     /EXIT FPP
001212  7300        CLA CLL                  /CLEAN UP
001213  1014        TAD     PTRDAT           /COMPUTE MEASUREMENT SPACING
001214  1131        TAD     MDIST
001215  3014        DCA     PTRDAT
001216  6211        CDF     10               /SET DATA FIELD =1
001217  1414        TAD I   PTRDAT           /GET Y(M)
001220  6201        CDF     00               /SET DATA FIELD =0
001221  3044        DCA     FLAC             /IN FLOATING AC
001222  4407        FENT                     /ENTER FPP
001223  0014        FLOT                     /CONVERT TO FLOATING POINT NUMBER
001224  6101        FPUT    YM               /AND SAVE
                /     FOUT                   /PRINT IT OUT
001225  5076        FGET    YMM1             /SSY=SSY+Y(M-1)**2
001226  3076        FMPY    YMM1
001227  1107        FADD    SSY
001230  6107        FPUT    SSY
001231  5101        FGET    YM               /SYY1=SYY1+Y(M-1)Y(M)
001232  3076        FMPY    YMM1
001233  1115        FADD    SYY1
001234  6115        FPUT    SYY1
001235  4107        FDIV    SSY              /ALPHA=SYY1/SSY
                /     FJMS I  PSPACE
                /     FJMS I  PCRREST
001236  0000        FEXT                     /EXIT FPP
001237  4250        JMS     DNORM            /TO 12-BIT NUMBER
001240  6221        CDF     20
```

```
001241  3415          DCA I   PARPTR          /SAVE IN FIELD 2
001242  6201          CDF     00
001243  4407          FENT                    /ENTER FPP
001244  0153          FISZ    PARCTR          /PARAMETER FIELD FULL?
001245  0204          FJMP    REPET           /DO IT AGAIN
001246  0000          FEXT                    /LEAVE FPP
001247  4267          JMS     PLOT            /GO DISPLAY

001250  0000  DNORM,  .-.                     /CONVERT FP NUMBER TO 12 BIT NUMBER ROUTINE
001251  7200          CLA
001252  1044          TAD     44              /GET EXPONENT
001253  7500          SMA                     /NEGATIVE?
001254  5257          JMP     .+3             /NO
001255  7200          CLA                     /YES, INTEGER VALUE =0
001256  5266          JMP     GG
001257  7041          CIA
001260  1376          TAD     I4              /COMPUTE SHIFTS NEEDED TO MAKE IT INTEGER
001261  3265          DCA     SHFTCNT
001262  7431          SWAB                    /MODE B EAE
001263  1045          TAD     45              /GET MANTISSA
001264  7415          ASR                     /SHIFT TO MAKE IT INTEGER
001265  0000  SHFTCNT,000
001266  5650  GG,     JMP I   DNORM           /RETURN

001267  0000  PLOT,   .-.                     /DATA PLOT ROUTINE
001270  6201  FF,     CDF     00              /DATA FIELD=0
001271  7300          CLA CLL                 /CLEAN UP
001272  1375          TAD     I3220           /POINTS TO BE DISPLAYED
001273  3325          DCA     COUNT1
001274  1374          TAD     I477            /FIRST DATA POINT
001275  3014          DCA     PTRDAT
001276  1014          TAD     PTRDAT          /FIRST PARAMETER POINT
001277  3015          DCA     PARPTR
001300  3120          DCA     TEMP1           /DELAY FOR DISPLAY
001301  7621  EE,     CAM                     /CLEAN UP
001302  6221          CDF     20              /DATA FIELD =2
001303  1414          TAD I   PTRDAT          /GET POINT TO BE PLOTTED
001304  6201          CDF     00
001305  7413          SML;    4               /GAIN CONTROL
001306  0004
```

```
001307  7000            NOP
001310  6551            6551                    /DISPLAY IT
001311  7621            CAM
001312  6211            CDF     10              /FIELD 1
001313  1415            TAD I   PARPTR          /GET DISPLAY POINT
001314  6201            CDF     00              /FIELD 0
001315  7413            SNL;    4               /GAIN CONTROL
001316  0004
001317  6552            6552                    /DISPLAY ON Y CHANNEL
001320  2120  DELY,     ISZ     TEMP1           /DELAY LOOP
001321  5320            JMP     DELY
001322  2325            ISZ     COUNT1          /COUNT UP
001323  5301            JMP     EE
001324  5270            JMP     FF              /REPLOT

001325  0000  COUNT1,    0                       /DELAY COUNTER
        *1374
001374  0477
001375  3220
001376  0004
001377  0400
        *0156
000156  1000
000157  0613
000160  0634
000161  0334
000162  0200
000163  0324
000164  7600
000165  0537
000166  7774
000167  0177
000170  4000
000171  3777
000172  0077
000173  7700
000174  0600
000175  0377
000176  7777
000177  7000
```

ASSEMBLY STATISTICS

NO ERRORS DETECTED

NO LINKS GENERATED

6K MEMORY UTILIZED

1 FILE CREATED

209 SYMBOLS

APPENDIX D

OKN AND OKAN PARAMETER IDENTIFICATION

The following pages contain the results of the least square parameter identification as applied to a nystagmus of -90°/sec. The results are printed in the following formats for the various sampling intervals.

OKN identification:

z(0)		
z(1)		
2		
z(2)	$\hat{a}(2)$	$\hat{\beta}(2)/V$
3		
.	.	.
.	.	.
.	.	.
.	.	.
m		
z(m)	$\hat{a}(m)$	$\hat{\beta}(m)/V$
.	.	.
.	.	.
.	.	.

OKAN identification:

z(0)	
1	
z(1)	$\hat{\alpha}(1)$
2	
.	
.	
.	
.	
m	
z(m)	$\hat{\alpha}(m)$
.	.
.	.
.	.
.	.

OKN Model Identification, sampling interval = .2048 sec.

```
BLOCK NO:600
 -23.000
 -28.000
  +0.575
  +2.000
 -31.000    +0.600    +0.355
  +3.000
 -29.000    +0.173    +0.615
  +4.000
 -26.000    +0.043    +0.683
  +5.000
 -24.000    +0.210    +0.546
  +6.000
 -24.000    +0.384    +0.417
  +7.000
 -25.000    +0.426    +0.387
  +8.000
 -26.000    +0.428    +0.385
  +9.000
 -28.000    +0.422    +0.393
 +10.000
 -29.000    +0.462    +0.370
 +11.000
 -27.000    +0.418    +0.396
 +12.000
 -26.000    +0.412    +0.398
 +13.000
 -26.000    +0.418    +0.393
 +14.000
 -27.000    +0.415    +0.396
 +15.000
 -27.000    +0.415    +0.396
 +16.000
 -28.000    +0.420    +0.394
 +17.000
 -26.000    +0.391    +0.411
 +18.000
 -26.000    +0.397    +0.406
 +19.000
 -27.000    +0.393    +0.409
 +20.000
 -29.000    +0.403    +0.405
 +21.000
 -29.000    +0.437    +0.384
 +22.000
 -29.000    +0.463    +0.367
 +23.000
 -24.000    +0.362    +0.431
 +24.000
 -16.000    +0.670    +0.214
 +25.000
 -12.000    +1.041    -0.038
 +26.000
 -15.000    +0.903    +0.055
 +27.000
 -16.000    +0.898    +0.059
 +28.000
 -15.000    +0.923    +0.041
 +29.000
 -15.000    +0.930    +0.036
 +30.000
 -16.000    +0.923    +0.041
 +31.000
 -18.000    +0.908    +0.051
 +32.000
 -19.000    +0.904    +0.054
 +33.000
 -22.000    +0.890    +0.065
 +34.000
 -25.000    +0.885    +0.070
 +35.000
 -28.000    +0.889    +0.070
 +36.000
 -28.000    +0.890    +0.069
 +37.000
 -29.000    +0.896    +0.067
 +38.000
 -30.000    +0.902    +0.064
 +39.000
 -27.000    +0.888    +0.071
 +40.000
 -19.000    +0.868    +0.078
 +41.000
 -17.000    +0.881    +0.069
 +42.000
 -23.000    +0.847    +0.092
 +43.000
 -32.000    +0.839    +0.102
 +44.000
 -32.000    +0.846    +0.098
 +45.000
 -29.000    +0.833    +0.105
 +46.000
 -25.000    +0.821    +0.111
 +47.000
 -23.000    +0.820    +0.110
 +48.000
 -24.000    +0.820    +0.111
 +49.000
 -25.000    +0.819    +0.112
 +50.000
 -24.000    +0.819    +0.111
```

OKN Model Identification, sampling interval = .2048 sec.

+51.000		
-24.000	+0.819	+0.111
+52.000		
-24.000	+0.819	+0.111
+53.000		
-26.000	+0.818	+0.113
+54.000		
-27.000	+0.820	+0.112
+55.000		
-29.000	+0.824	+0.110
+56.000		
-29.000	+0.827	+0.109
+57.000		
-27.000	+0.822	+0.111
+58.000		
-26.000	+0.821	+0.112
+59.000		
-24.000	+0.819	+0.112
+60.000		
-24.000	+0.819	+0.112
+61.000		
-25.000	+0.819	+0.113
+62.000		
-28.000	+0.820	+0.114
+63.000		
-27.000	+0.818	+0.114
+64.000		
-25.000	+0.816	+0.115
+65.000		
-23.000	+0.815	+0.115
+66.000		
-23.000	+0.816	+0.114
+67.000		
-25.000	+0.814	+0.116
+68.000		
-26.000	+0.814	+0.116
+69.000		
-26.000	+0.814	+0.116
+70.000		
-26.000	+0.814	+0.116
+71.000		
-25.000	+0.813	+0.116
+72.000		
-23.000	+0.813	+0.116
+73.000		
-23.000	+0.814	+0.116
+74.000		
-25.000	+0.811	+0.117
+75.000		
-26.000	+0.812	+0.118
+76.000		
-26.000	+0.812	+0.118
+77.000		
-27.000	+0.813	+0.117
+78.000		
-27.000	+0.813	+0.117
+79.000		
-29.000	+0.817	+0.116
+80.000		
-29.000	+0.819	+0.115
+81.000		
-29.000	+0.821	+0.114
+82.000		
-31.000	+0.829	+0.110
+83.000		
-30.000	+0.828	+0.110
+84.000		
-28.000	+0.824	+0.112
+85.000		
-28.000	+0.825	+0.112
+86.000		
-29.000	+0.828	+0.110
+87.000		
-31.000	+0.834	+0.107
+88.000		
-29.000	+0.830	+0.109
+89.000		
-27.000	+0.827	+0.111
+90.000		
-27.000	+0.827	+0.111
+91.000		
-29.000	+0.829	+0.110
+92.000		
-30.000	+0.833	+0.108
+93.000		
-29.000	+0.832	+0.109
+94.000		
-28.000	+0.831	+0.109
+95.000		
-30.000	+0.834	+0.108
+96.000		
-32.000	+0.842	+0.104
+97.000		
-33.000	+0.849	+0.099
+98.000		
-33.000	+0.853	+0.097
+99.000		
-32.000	+0.853	+0.097
+100.000		
-31.000	+0.853	+0.097

OKN Model Identification, sampling interval = .2048 sec.

+101.000		
-32.000	+0.857	+0.095
+102.000		
-34.000	+0.866	+0.090
+103.000		
-36.000	+0.878	+0.082
+104.000		
-36.000	+0.884	+0.079
+105.000		
-35.000	+0.884	+0.079
+106.000		
-33.000	+0.880	+0.082
+107.000		
-32.000	+0.879	+0.082
+108.000		
-33.000	+0.883	+0.080
+109.000		
-34.000	+0.887	+0.077
+110.000		
-35.000	+0.893	+0.074
+111.000		
-35.000	+0.895	+0.072
+112.000		
-36.000	+0.901	+0.069
+113.000		
-36.000	+0.904	+0.067
+114.000		
-35.000	+0.903	+0.068
+115.000		
-36.000	+0.908	+0.065
+116.000		
-38.000	+0.917	+0.059
+117.000		
-37.000	+0.916	+0.060
+118.000		
-36.000	+0.915	+0.060
+119.000		
-35.000	+0.914	+0.061
+120.000		
-35.000	+0.915	+0.060
+121.000		
-34.000	+0.914	+0.061
+122.000		
-32.000	+0.911	+0.063
+123.000		
-31.000	+0.910	+0.063
+124.000		
-30.000	+0.910	+0.064
+125.000		
-28.000	+0.908	+0.064
+126.000		
-26.000	+0.908	+0.064
+127.000		
-25.000	+0.909	+0.063
+128.000		
-26.000	+0.908	+0.064
+129.000		
-26.000	+0.908	+0.064
+130.000		
-29.000	+0.907	+0.065
+131.000		
-31.000	+0.908	+0.065
+132.000		
-29.000	+0.906	+0.066
+133.000		
-24.000	+0.904	+0.066
+134.000		
-24.000	+0.904	+0.066
+135.000		
-32.000	+0.896	+0.073
+136.000		
-35.000	+0.901	+0.071
+137.000		
-35.000	+0.902	+0.070
+138.000		
-33.000	+0.899	+0.071
+139.000		
-32.000	+0.898	+0.072
+140.000		
-33.000	+0.900	+0.071
+141.000		
-34.000	+0.902	+0.070
+142.000		
-35.000	+0.905	+0.068
+143.000		
-34.000	+0.904	+0.069
+144.000		
-33.000	+0.903	+0.069
+145.000		
-33.000	+0.904	+0.069
+146.000		
-32.000	+0.903	+0.069
+147.000		
-33.000	+0.905	+0.068
+148.000		
-32.000	+0.904	+0.069
+149.000		
-29.000	+0.901	+0.070
+150.000		
-26.000	+0.900	+0.070

OKN Model Identification, sampling interval = .2048 sec.

+151.000		
-27.000	+0.900	+0.071
+152.000		
-27.000	+0.900	+0.071
+153.000		
-26.000	+0.900	+0.070
+154.000		
-30.000	+0.898	+0.072
+155.000		
-34.000	+0.900	+0.072
+156.000		
-35.000	+0.903	+0.070
+157.000		
-37.000	+0.907	+0.067
+158.000		
-38.000	+0.911	+0.065
+159.000		
-38.000	+0.913	+0.064
+160.000		
-37.000	+0.912	+0.064
+161.000		
-36.000	+0.912	+0.065
+162.000		
-35.000	+0.911	+0.065
+163.000		
-35.000	+0.912	+0.064
+164.000		
-36.000	+0.914	+0.063
+165.000		
-36.000	+0.915	+0.063
+166.000		
-36.000	+0.916	+0.062
+167.000		
-37.000	+0.918	+0.060
+168.000		
-35.000	+0.916	+0.062
+169.000		
-34.000	+0.915	+0.062
+170.000		
-34.000	+0.916	+0.062
+171.000		
-33.000	+0.915	+0.063
+172.000		
-32.000	+0.914	+0.063
+173.000		
-31.000	+0.914	+0.063
+174.000		
-30.000	+0.913	+0.063
+175.000		
-30.000	+0.913	+0.063
+176.000		
-30.000	+0.913	+0.063
+177.000		
-32.000	+0.914	+0.063
+178.000		
-35.000	+0.916	+0.062
+179.000		
-36.000	+0.918	+0.061
+180.000		
-35.000	+0.917	+0.062
+181.000		
-33.000	+0.915	+0.063
+182.000		
-33.000	+0.916	+0.063
+183.000		
-35.000	+0.917	+0.062
+184.000		
-36.000	+0.919	+0.060
+185.000		
-36.000	+0.920	+0.060
+186.000		
-36.000	+0.920	+0.060
+187.000		
-38.000	+0.924	+0.058
+188.000		
-37.000	+0.923	+0.058
+189.000		
-37.000	+0.924	+0.057
+190.000		
-37.000	+0.925	+0.057
+191.000		
-36.000	+0.924	+0.057
+192.000		
-36.000	+0.924	+0.057
+193.000		
-35.000	+0.924	+0.058
+194.000		
-35.000	+0.924	+0.057
+195.000		
-36.000	+0.925	+0.056
+196.000		
-36.000	+0.926	+0.056
+197.000		
-36.000	+0.926	+0.056
+198.000		
-36.000	+0.927	+0.056
+199.000		
-35.000	+0.926	+0.056
+200.000		
-35.000	+0.927	+0.056

OKN Model Identification, sampling interval = .2048 sec.

+201.000		
-34.000	+0.926	+0.056
+202.000		
-36.000	+0.928	+0.055
+203.000		
-38.000	+0.930	+0.054
+204.000		
-38.000	+0.931	+0.053
+205.000		
-36.000	+0.929	+0.054
+206.000		
-34.000	+0.927	+0.056
+207.000		
-33.000	+0.927	+0.056
+208.000		
-33.000	+0.927	+0.056
+209.000		
-34.000	+0.927	+0.055
+210.000		
-36.000	+0.929	+0.055
+211.000		
-36.000	+0.929	+0.054
+212.000		
-38.000	+0.932	+0.053
+213.000		
-38.000	+0.932	+0.052
+214.000		
-38.000	+0.933	+0.052
+215.000		
-38.000	+0.934	+0.052
+216.000		
-37.000	+0.933	+0.052
+217.000		
-36.000	+0.932	+0.052
+218.000		
-35.000	+0.932	+0.053
+219.000		
-35.000	+0.932	+0.053
+220.000		
-34.000	+0.931	+0.053
+221.000		
-33.000	+0.931	+0.053
+222.000		
-34.000	+0.931	+0.053
+223.000		
-35.000	+0.932	+0.053
+224.000		
-37.000	+0.934	+0.052
+225.000		
-39.000	+0.936	+0.050
+226.000		
-40.000	+0.938	+0.049
+227.000		
-37.000	+0.935	+0.051
+228.000		
-34.000	+0.932	+0.053
+229.000		
-34.000	+0.932	+0.053
+230.000		
-37.000	+0.934	+0.052
+231.000		
-39.000	+0.936	+0.050
+232.000		
-38.000	+0.935	+0.051
+233.000		
-38.000	+0.936	+0.051
+234.000		
-37.000	+0.935	+0.051
+235.000		
-36.000	+0.935	+0.051
+236.000		
-37.000	+0.936	+0.051
+237.000		
-36.000	+0.935	+0.051
+238.000		
-35.000	+0.935	+0.051

OKN Model Identification, sampling interval = .512 sec.

BLOCK NO:600

-23.000		
-24.000		
+0.575		
+2.000		
-29.000	+1.130	-0.001
+3.000		
-27.000	+1.037	+0.004
+4.000		
-29.000	+1.046	+0.004
+5.000		
-12.000	+0.878	+0.014
+6.000		
-16.000	+0.871	+0.029
+7.000		
-28.000	+0.882	+0.054
+8.000		
-19.000	+0.827	+0.059
+9.000		
-29.000	+0.846	+0.073
+10.000		
-24.000	+0.824	+0.076
+11.000		
-29.000	+0.845	+0.077
+12.000		
-24.000	+0.827	+0.080
+13.000		
-23.000	+0.826	+0.080
+14.000		
-26.000	+0.834	+0.082
+15.000		
-26.000	+0.837	+0.081
+16.000		
-29.000	+0.849	+0.081
+17.000		
-28.000	+0.850	+0.081
+18.000		
-27.000	+0.850	+0.081
+19.000		
-30.000	+0.860	+0.080
+20.000		
-31.000	+0.867	+0.078
+21.000		
-35.000	+0.886	+0.073
+22.000		
-35.000	+0.891	+0.071
+23.000		
-36.000	+0.899	+0.068
+24.000		
-35.000	+0.899	+0.069
+25.000		
-28.000	+0.877	+0.076
+26.000		
-29.000	+0.878	+0.076
+27.000		
-32.000	+0.884	+0.076
+28.000		
-33.000	+0.888	+0.074
+29.000		
-33.000	+0.890	+0.074
+30.000		
-26.000	+0.875	+0.079
+31.000		
-34.000	+0.878	+0.082
+32.000		
-37.000	+0.888	+0.079
+33.000		
-36.000	+0.888	+0.079
+34.000		
-34.000	+0.885	+0.080
+35.000		
-30.000	+0.878	+0.082
+36.000		
-35.000	+0.884	+0.082
+37.000		
-36.000	+0.888	+0.081
+38.000		
-37.000	+0.892	+0.079
+39.000		
-36.000	+0.892	+0.079
+40.000		
-35.000	+0.891	+0.079
+41.000		
-36.000	+0.894	+0.078
+42.000		
-36.000	+0.895	+0.078
+43.000		
-38.000	+0.901	+0.076
+44.000		
-34.000	+0.893	+0.079
+45.000		
-39.000	+0.901	+0.077
+46.000		
-37.000	+0.898	+0.078
+47.000		
-36.000	+0.897	+0.078

OKN Model Identification, sampling interval = .512 sec.

+48.000		
-21.000	+0.875	+0.087
+49.000		
-13.000	+0.887	+0.074
+50.000		
-36.000	+0.828	+0.125
+51.000		
-35.000	+0.828	+0.125
+52.000		
-36.000	+0.831	+0.124
+53.000		
-38.000	+0.835	+0.122
+54.000		
-36.000	+0.834	+0.123
+55.000		
-34.000	+0.833	+0.123
+56.000		
-36.000	+0.836	+0.123
+57.000		
-36.000	+0.837	+0.122
+58.000		
-37.000	+0.839	+0.121
+59.000		
-36.000	+0.839	+0.121
+60.000		
-37.000	+0.842	+0.120
+61.000		
-36.000	+0.842	+0.120
+62.000		
-36.000	+0.843	+0.120
+63.000		
-41.000	+0.849	+0.117
+64.000		
-40.000	+0.850	+0.117
+65.000		
-40.000	+0.852	+0.116
+66.000		
-34.000	+0.845	+0.119
+67.000		
-39.000	+0.848	+0.119
+68.000		
-37.000	+0.847	+0.119
+69.000		
-38.000	+0.849	+0.118
+70.000		
-39.000	+0.852	+0.117
+71.000		
-37.000	+0.850	+0.118
+72.000		
-36.000	+0.850	+0.118
+73.000		
-37.000	+0.852	+0.118
+74.000		
-38.000	+0.853	+0.117
+75.000		
-38.000	+0.854	+0.116
+76.000		
-34.000	+0.851	+0.118
+77.000		
-37.000	+0.853	+0.118
+78.000		
-37.000	+0.853	+0.117
+79.000		
-36.000	+0.853	+0.118
+80.000		
-30.000	+0.849	+0.119
+81.000		
-36.000	+0.848	+0.121
+82.000		
-35.000	+0.848	+0.121
+83.000		
-34.000	+0.848	+0.121
+84.000		
-34.000	+0.848	+0.121
+85.000		
-37.000	+0.849	+0.121
+86.000		
-37.000	+0.850	+0.121
+87.000		
-38.000	+0.851	+0.120
+88.000		
-37.000	+0.851	+0.121

OKAN Model Identification, sampling interval = .0512 sec.

BLOCK NO: 600

-38.000		+25.000		+50.000	
+1.000		-32.000	+0.993	-29.000	+0.995
-39.000	+1.026	+26.000		+51.000	
+2.000		-33.000	+0.994	-30.000	+0.995
-39.000	+1.013	+27.000		+52.000	
+3.000		-33.000	+0.995	-31.000	+0.996
-38.000	+1.000	+28.000		+53.000	
+4.000		-33.000	+0.995	-30.000	+0.995
-37.000	+0.993	+29.000		+54.000	
+5.000		-32.000	+0.994	-29.000	+0.995
-36.000	+0.990	+30.000		+55.000	
+6.000		-32.000	+0.994	-28.000	+0.994
-37.000	+0.995	+31.000		+56.000	
+7.000		-33.000	+0.995	-27.000	+0.994
-37.000	+0.996	+32.000		+57.000	
+8.000		-32.000	+0.995	-27.000	+0.994
-37.000	+0.996	+33.000		+58.000	
+9.000		-32.000	+0.995	-29.000	+0.995
-39.000	+1.003	+34.000		+59.000	
+10.000		-33.000	+0.996	-31.000	+0.996
-39.000	+1.002	+35.000		+60.000	
+11.000		-34.000	+0.996	-33.000	+0.997
-39.000	+1.002	+36.000		+61.000	
+12.000		-34.000	+0.996	-32.000	+0.997
-38.000	+1.000	+37.000		+62.000	
+13.000		-33.000	+0.996	-32.000	+0.997
-38.000	+1.000	+38.000		+63.000	
+14.000		-32.000	+0.995	-31.000	+0.996
-38.000	+1.000	+39.000		+64.000	
+15.000		-31.000	+0.995	-31.000	+0.996
-37.000	+0.998	+40.000		+65.000	
+16.000		-31.000	+0.995	-31.000	+0.996
-36.000	+0.997	+41.000		+66.000	
+17.000		-30.000	+0.994	-32.000	+0.997
-34.000	+0.994	+42.000		+67.000	
+18.000		-30.000	+0.994	-34.000	+0.998
-35.000	+0.995	+43.000		+68.000	
+19.000		-31.000	+0.995	-35.000	+0.998
-34.000	+0.994	+44.000		+69.000	
+20.000		-31.000	+0.995	-35.000	+0.998
-35.000	+0.996	+45.000		+70.000	
+21.000		-31.000	+0.995	-34.000	+0.998
-34.000	+0.995	+46.000		+71.000	
+22.000		-31.000	+0.995	-33.000	+0.997
-33.000	+0.994	+47.000		+72.000	
+23.000		-32.000	+0.996	-32.000	+0.997
-32.000	+0.993	+48.000		+73.000	
+24.000		-31.000	+0.995	-30.000	+0.996
-32.000	+0.993	+49.000		+74.000	
		-30.000	+0.995	-31.000	+0.997

OKAN Model Identification, sampling interval = .0512 sec.

+75.000		+100.000		+125.000	
-30.000	+0.996	-28.000	+0.996	-28.000	+0.997
+76.000		+101.000		+126.000	
-29.000	+0.996	-28.000	+0.996	-28.000	+0.997
+77.000		+102.000		+127.000	
-29.000	+0.996	-28.000	+0.997	-27.000	+0.997
+78.000		+103.000		+128.000	
-30.000	+0.996	-28.000	+0.997	-28.000	+0.997
+79.000		+104.000		+129.000	
-31.000	+0.997	-28.000	+0.997	-28.000	+0.997
+80.000		+105.000		+130.000	
-31.000	+0.997	-27.000	+0.996	-28.000	+0.997
+81.000		+106.000		+131.000	
-31.000	+0.997	-27.000	+0.996	-28.000	+0.997
+82.000		+107.000		+132.000	
-31.000	+0.997	-27.000	+0.996	-29.000	+0.997
+83.000		+108.000		+133.000	
-30.000	+0.997	-28.000	+0.997	-28.000	+0.997
+84.000		+109.000		+134.000	
-29.000	+0.996	-27.000	+0.996	-26.000	+0.997
+85.000		+110.000		+135.000	
-29.000	+0.996	-27.000	+0.996	-26.000	+0.997
+86.000		+111.000		+136.000	
-29.000	+0.996	-29.000	+0.997	-27.000	+0.997
+87.000		+112.000		+137.000	
-30.000	+0.997	-30.000	+0.997	-29.000	+0.997
+88.000		+113.000		+138.000	
-31.000	+0.997	-30.000	+0.997	-30.000	+0.998
+89.000		+114.000		+139.000	
-31.000	+0.997	-29.000	+0.997	-29.000	+0.997
+90.000		+115.000		+140.000	
-30.000	+0.997	-29.000	+0.997	-28.000	+0.997
+91.000		+116.000		+141.000	
-30.000	+0.997	-28.000	+0.997	-28.000	+0.997
+92.000		+117.000		+142.000	
-29.000	+0.997	-29.000	+0.997	-29.000	+0.997
+93.000		+118.000		+143.000	
-29.000	+0.997	-29.000	+0.997	-30.000	+0.998
+94.000		+119.000		+144.000	
-30.000	+0.997	-29.000	+0.997	-31.000	+0.998
+95.000		+120.000		+145.000	
-31.000	+0.997	-29.000	+0.997	-31.000	+0.998
+96.000		+121.000		+146.000	
-31.000	+0.997	-29.000	+0.997	-30.000	+0.998
+97.000		+122.000		+147.000	
-30.000	+0.997	-30.000	+0.997	-28.000	+0.997
+98.000		+123.000		+148.000	
-29.000	+0.997	-30.000	+0.997	-28.000	+0.997
+99.000		+124.000		+149.000	
-29.000	+0.997	-29.000	+0.997	-27.000	+0.997

OKAN Model Identification, sampling interval = 1.536 sec.

BLOCK NO:600

-38.000		+25.000		+50.000	
+1.000		-8.000	+0.944	-1.000	+0.940
-32.000	+0.842	+26.000		+51.000	
+2.000		-7.000	+0.943	-1.000	+0.940
-33.000	+0.921	+27.000		+52.000	
+3.000		-7.000	+0.944	-1.000	+0.940
-30.000	+0.917	+28.000		+53.000	
+4.000		-7.000	+0.944	-1.000	+0.940
-29.000	+0.927	+29.000		+54.000	
+5.000		-4.000	+0.942	-1.000	+0.940
-27.000	+0.928	+30.000		+55.000	
+6.000		-4.000	+0.943	-1.000	+0.940
-27.000	+0.936	+31.000		+56.000	
+7.000		-1.000	+0.942	-1.000	+0.940
-25.000	+0.935	+32.000		+57.000	
+8.000		-3.000	+0.942	-1.000	+0.940
-27.000	+0.948	+33.000		+58.000	
+9.000		-5.000	+0.942	-1.000	+0.940
-24.000	+0.942	+34.000		+59.000	
+10.000		+0.000	+0.941	-1.000	+0.940
-24.000	+0.946	+35.000		+60.000	
+11.000		-1.000	+0.941	-1.000	+0.940
-24.000	+0.949	+36.000		+61.000	
+12.000		+0.000	+0.941	-1.000	+0.940
-22.000	+0.948	+37.000		+62.000	
+13.000		+1.000	+0.941	-1.000	+0.940
-20.000	+0.946	+38.000		+63.000	
+14.000		+1.000	+0.941	-1.000	+0.940
-18.000	+0.944	+39.000		+64.000	
+15.000		+0.000	+0.941	-1.000	+0.940
-19.000	+0.947	+40.000		+65.000	
+16.000		+1.000	+0.941	-1.000	+0.940
-19.000	+0.949	+41.000		+66.000	
+17.000		+2.000	+0.941	-1.000	+0.940
-19.000	+0.951	+42.000		+67.000	
+18.000		+2.000	+0.941	-1.000	+0.940
-16.000	+0.947	+43.000		+68.000	
+19.000		+4.000	+0.941	-1.000	+0.940
-17.000	+0.950	+44.000		+69.000	
+20.000		+3.000	+0.941	-1.000	+0.940
-13.000	+0.945	+45.000		+70.000	
+21.000		+3.000	+0.941	-1.000	+0.940
-12.000	+0.945	+46.000		+71.000	
+22.000		-1.000	+0.940	-1.000	+0.940
-11.000	+0.945	+47.000		+72.000	
+23.000		-1.000	+0.940	-1.000	+0.940
-12.000	+0.946	+48.000		+73.000	
+24.000		-1.000	+0.940	-1.000	+0.940
-9.000	+0.944	+49.000		+74.000	
		-1.000	+0.940	-1.000	+0.940

APPENDIX E

OKN AND OKAN MODEL SIMULATION PROGRAM

The following pages contain an assembly program for the PDP-8/E computer. This program simulates OKN and OKAN response for a given set of model parameters and a step input. The program also computes the model error and the integral square error. These response curves can be plotted by using the PLOT subroutine in the program. Note that only the main program is included here, the system configuration definitions are the same as in the program in Appendix C.

```
                /OKN AND OKAN SIMULATION PROGRAM

       *0010            *10
000010  0000  PTRDAT,  0                    /POINTER TO DATA
000011  0000  PARPTR,  0                    /POINTER TO DATA
000012  0000  PTRERR,  0                    /ERROR POINTER
       *0070            *70
000070  0006  R,        0006                /40 AS FP NUMBER
000071  2400             2400
000072  0000             0000
000073  0000  A,        0000                /.9852o7 AS FP NUMBER
000074  3742             3742
000075  0000             0000
000076  7772  BETA,     7772                /.0136o73 AS FP NUMBER
000077  3434             3434
000100  0000             0000
000101  0000  ALPHA,    0000                /.9979541 AS FP NUMBER
000102  3774             3774
000103  0000             0000
000104  0000  C,        0000                /.575 AS FP NUMBER
000105  2232             2232
000106  0000             0000
000107  0002  QCKDRP,   0002                /QUICK DROP =3
000110  3000             3000
000111  0000             0000
000112  0000  TEMP1,    ZBLOCK 3
000115  7620  COUNT1,   7620                /-(657-477), BEFORE OKN STARTS
000116  6117  COUNT2,   6117                /-(2540-657), OKN DURATION
000117  5261  COUNT3,   5261                /-(5257-2540), OKAN DURATION
000120  0000  YMM1,     ZBLOCK 3            /Y(M-1)
000123  0000  ISE,      ZBLOCK  2           /INTEGRAL SQUARE ERROR
```

```
       *0200          *200

000200  6201          CDF     00              /SET DATA FIELD =0
000201  7300          CLA CLL                 /CLEAN UP
000202  1377          TAD     I477            /TO THE BEGINNING OF SIMULATED DATA
000203  3010          DCA     PTRDAT
000204  6221  AA,     CDF     20              /SET DATA FIELD =2
000205  3410          DCA I   PTRDAT          /ZERO BEFORE OKN BEGINNING
000206  6201          CDF     00              /DATA FIELD =0
000207  2115          ISZ     COUNT1          /DONE?
000210  5204          JMP     AA              /NO
000211  4407          FENT                    /ENTER FPP
000212  5104          FGET    C               /Y(0)=CR
000213  3070          FMPY    R
000214  6120          FPUT    YMM1
000215  0000          FEXT                    /EXIT FPP
000216  4264          JMS     DNORM           /FPP NUMBER TO 12 BIT NUMBER
000217  6221          CDF     20              /PREPARE FOR STORAGE
000220  3410          DCA I   PTRDAT          /STORE IT
000221  6201          CDF     00              /BACK TO FIELD 0
000222  2116          ISZ     COUNT2          /COUNT UP
000223  4407  BB,     FENT                    /ENTER FPP
000224  5120          FGET    YMM1            /A*Y(M-1)+BETA*R=Y(M)
000225  3073          FMPY    A
000226  6120          FPUT    YMM1
000227  5076          FGET    BETA
000230  3070          FMPY    R
000231  1120          FADD    YMM1
000232  6120          FPUT    YMM1
000233  0000          FEXT                    /LEAVE  FPP
000234  4264          JMS     DNORM           /CONVERT FP NUMBER TO 12 BIT NUMBER
000235  6221          CDF     20
000236  3410          DCA I   PTRDAT          /SAVE IN FIELD 2
000237  6201          CDF     00              /FIELD 0
000240  2116          ISZ     COUNT2          /OKN DONE?
000241  5223          JMP     BB              /NO
000242  4407          FENT                    /ENTER FPP
000243  5120          FGET    YMM1            /ADD QUICK DROP
000244  2107          FSUB    QCKDRP
000245  6120          FPUT    YMM1
```

```
000246  4407  CC,     FENT                    /ENTER FPP
000247  5120           FGET    YMM1            /Y(M)=ALPHA*Y(M-1)
000250  3101           FMPY    ALPHA
000251  6120           FPUT    YMM1
000252  0000           FEXT                    /LEAVE FPP
000253  4264           JMS DNORM               /CONVERT FP NUMBER TO 12 BIT NUMBER
000254  6221           CDF     20
000255  3410           DCA I   PTRDAT          /SAVE IN FIELD 2
000256  6201           CDF     00              /FIELD 0
000257  2117           ISZ     COUNT3          /DONE?
000260  5246           JMP     CC              /NO

                /SELECT CURVE TO BE PLOTTED

000261  4341           JMS     MISALN          /COMPUTE MODEL ERROR
000262  4765           JMS I   PEVAL           /COMPUTE ISE
000263  4303           JMS     PLOT            /PLOT SIMULATED DATA

000264  0000  DNORM,   .-.                     /CONVERT FP NUMBER TO 12 BIT NUMBER ROUTINE
000265  7200           CLA
000266  1044           TAD     44              /GET EXPONENT
000267  7500           SMA                     /NEGATIVE?
000270  5273           JMP     .+3             /NO
000271  7200           CLA                     /YES, INTEGER VALUE =0
000272  5302           JMP     GG
000273  7040           CMA
000274  1376           TAD     (14             /COMPUTE SHIFTS NEEDED TO MAKE IT INTEGER
000275  3301           DCA     SHFTCNT
000276  7431           SWAB                    /MODE B EAE
000277  1045           TAD     45              /GET MANTISSA
000300  7415           ASR                     /SHIFT TO MAKE IT INTEGER
000301  0000  SHFTCNT,000
000302  5664  GG,      JMP I   DNORM           /RETURN
```

```
000303  0000  PLOT,   .-.
000304  6201  FF,     CDF     00          /DATA PLOT ROUTINE
000305  7300           CLA CLL             /DATA FIELD=0
000306  1375           TAD     (3220       /CLEAN UP
000307  3115           DCA     COUNT1      /POINTS TO BE DISPLAYED
000310  1377           TAD     (477
000311  3010           DCA     PTRJAT      /FIRST DATA POINT
000312  1010           TAD     PTRDAT
000313  3011           DCA     PARPTR      /FIRST PARAMETER POINT
000314  3112           DCA     TEMP1
000315  7621  EE,     CAM                 /DELAY FOR DISPLAY
000316  6221           CDF     20          /CLEAN UP
000317  1410           TAD I   PTRDAT      /DATA FIELD =2
000320  6201           CDF     00          /GET POINT TO BE PLOTTED
000321  7413           SML;    4
000322  0004                               /GAIN CONTROL
000323  7000           NOP
000324  6551           6551
000325  7621           CAM                 /DISPLAY IT
000326  6211           CDF     10
000327  1411           TAD I   PARPTR      /FIELD 1
000330  6201           CDF     00          /GET DISPLAY POINT
000331  7413           SML;    4           /FIELD 0
000332  0004                               /GAIN CONTROL
000333  6552           6552                /DISPLAY ON Y CHANNEL
000334  2112  DELY,   ISZ     TEMP1       /DELAY LOOP
000335  5334           JMP     DELY
000336  2115           ISZ     COUNT1      /COUNT UP
000337  5315           JMP     EE
000340  5304           JMP     FF          /REPLOT
```

```
000341  0000  MISALN, .-.                    /ERROR SUBROUTINE
000342  7300          CLA CLL
000343  6201          CDF     00             /DATA FIELD 0
000344  1377          TAD     (477           /SET AUTO INDEX POINTERS
000345  3010          DCA     PTRDAT         /FIELD1
000346  1010          TAD     PTRDAT
000347  3011          DCA     PARPTR         /FIELD 2, SIMULATED OUTPUT
000350  1010          TAD     PTRDAT
000351  3012          DCA     PTRERR         /FIELD 2,ERROR
000352  1375          TAD     (3220          /POINTS TOTAL
000353  3115          DCA     COUNT1
000354  6211  DD,     CDF     10             /SET DATA FIELD 1
000355  1411          TAD I   PARPTR         /E(M)=Y(M)-Z(M)
000356  6221          CDF     20             /SET DATA FIELD 2
000357  1410          TAD I   PTRDAT
000360  3412          DCA I   PTRERR
000361  2115          ISZ     COUNT1         /DONE?
000362  5354          JMP     DD             /NO
000363  6201          CDF     00             /DATA FIELD 0
000364  5741          JMP I   MISALN         /RETURN

000365  0400  PEVAL, EVAL                     /POINTER TO EVAV ROUTINE

        *0375
000375  3220
000376  0014
000377  0477
        *0400          PAGE
```

```
                /PARAMETER ESTIMATION EVALUATION ROUTINE

000400  0000  EVAL,   .-.
000401  7300          CLA CLL                 /CLEAN UP
000402  6201          CDF     00              /FIELD 0
000403  1377          TAD     (477            /INITIALIZE POINTERS
000404  3012          DCA     PTRERR
000405  1012          TAD     PTRERR
000406  3010          DCA     PTRDAT
000407  1012          TAD     PTRERR
000410  3011          DCA     PARPTR
000411  1376          TAD     (3230           /INITIALIZE COUNTERS
000412  3115          DCA     COUNT1          /COUNT1=-3220+NO.OF POINTS IN INTEG. WINDOW
000413  1375          TAD     (7767           /COUNT2=-  NO. OF POINTS IN INTEG. WINDOW
000414  3116          DCA     COUNT2
000415  7431          SWAB                    /MODE B EAE
000416  7421          MQL                     /INITIAL ISE=0
000417  7445          DST;    ISE
000420  0123
000421  7300  INTEG1, CLA CLL                 /CLEAN UP
000422  6221          CDF     20              /DATA FIELD 2
000423  1412          TAD I   PTRERR          /GENERATE ISE
000424  6201          CDF     00
000425  7510          SPA
000426  7041          CIA
000427  3112          DCA     TEMP1
000430  1112          TAD     TEMP1
000431  7421          MQL
000432  7405          MUY;    TEMP1
000433  0112
000434  7443          DAD;    ISE             /ADD ON NEW SQUARED DATA
000435  0123
000436  7445          DST;    ISE             /AND SAVE
000437  0123
000440  2116          ISZ     COUNT2          /WINDOW DONE?
000441  5221          JMP     INTEG1          /NO
```

```
000442  6221  INTEG2, CDF     20              /DATA FIELD 2
000443  1410          TAD I   PTRDAT          /GET POINT BEFORE WINDOW
000444  6201          CDF     00              /DATA FIELD 0
000445  7510          SPA                     /GET ABSOLUTE VALUE
000446  7041          CIA
000447  3112          DCA     TEMP1
000450  7501          MQA                     /GET LAST ISE
000451  6221          CDF     20
000452  3411          DCA I   PARPTR          /SAVE IT
000453  6201          CDF     00
000454  1112          TAD     TEMP1           /GET LAST POINT
000455  7421          MQL                     /IN MQ REGISTER
000456  7405          MUY;    TEMP1           /SQUARE IT
000457  0112
000460  7575          DCM                     /SUBRACT FROM LAST ISE
000461  7443          DAD;    ISE
000462  0123
000463  7445          DST;    ISE             /SAVE IT
000464  0123
000465  6221          CDF     20              /GET NEXT POINT
000466  1412          TAD I   PTRERR
000467  6201          CDF     00
000470  7510          SPA
000471  7041          CIA
000472  3112          DCA     TEMP1           /SAVE IN TEMP1
000473  1112          TAD     TEMP1           /SQUARE IT
000474  7421          MUL
000475  7405          MUY;    TEMP1
000476  0112
000477  7443          DAD;    ISE             /ADD ON LAST VALUE OF ISE EXPRESSION
000500  0123
000501  7445          DST;    ISE             /SAVE IT
000502  0123
000503  2115          ISZ     COUNT1          /DONE?
000504  5242          JMP     INTEG2          /NO
000505  5600          JMP I   EVAL            /RETURN
        *0575
000575  7767
000576  3230
000577  0477
```

ASSEMBLY STATISTICS

NO ERRORS DETECTED

NO LINKS GENERATED

6K MEMORY UTILIZED

1 FILE CREATED

155 SYMBOLS

BIBLIOGRAPHY

1. Allum, J.H.J., "A Least Mean Squares Cubic Fit Algorithm for On-Line Differentiation of Sampled Analog Signals", IEEE Trans. on Comp., vol. C-24, pp. 585-590, June 1975.

2. Allum, J.H.J., Tole, J.R. and Weiss, A.D., "MITNYS-II A Digital Program for On-Line Analysis of Nystagmus", IEEE Trans. Biomed. Eng., vol. BME-22, pp. 196-202, May 1975.

3. Bahill, A.T., Clark, M.R. and Stark, L., "The Main Sequence, A Tool for Studying Human Eye Movements", Math. Biosciences, vol. 24, pp. 191-204, 1975.

4. Baloh, R.W., Kumley, W.E., Sills, A.W., Honrubia, V. and Konrad, H.R., "Quantitative Measurements of Smooth Pursuit Eye Movements", Am. Otol., vol. 85, pp. 111-119, 1976.

5. Baloh, R.W., Sills, A.W., Kumley, W.E. and Honrubia, V., "Quantitative Measurements of Saccade Amplitude, Duration and Velocity", Neurology, vol. 25, no. 11, pp. 1065-1070, Nov. 1975.

6. Bekey, G.A. and Yamashiro, S.M., "Parameter Estimation in Mathematical Models of Biological Systems", in Advances in Biomedical Engineering, ed. J.H.U. Brown and Dickson, J.F., vol. 6, pp. 1-43, 1976.

7. Bond, H.W. and Ho, P., "Solid Miniature Silver-Silver Chloride Electrodes for Chronic Implantation", Electroenceph. Clin. Neurophysiol., vol. 28, pp. 206-208, 1970.

8. Cohen, B., Matsuo, V. and Raphan, T., "Quantitative Analysis of the Velocity Characteristics of Optokinetic Nystagmus and Optokinetic After-Nystagmus", Journ. Physiol., vol. 270, pp. 321-344, 1977.

9. Cohen, B., Uemura, T. and Takemori, S., "Effects of Labyrinthectomy on Optokinetic Nystagmus (OKN) and Optokinetic-After Nystagmus (OKAN)", Equil. Res., vol. 3, pp. 88-93, 1973.

10. Digital Equipment Corp., Small Computer Handbook, 1973.

11. Fuchs, A.F., "Saccadic and Smooth Pursuit Eye Movements in the Monkey", J. Physiol., vol. 191, pp. 609-631, 1967.

12. Fuchs, A.F. and Robinson, D.A., "A Method for Measuring Horizontal and Vertical Eye Movements Chronically in the Monkey", J. Appl. Physiol., vol. 21, pp. 1068-1070, 1966.

13. Grewal, M.S. and Glover, K., "Identifiability of Linear and Nonlinear Dynamical Systems", IEEE Trans. Automat. Control, vol. AC-21, no. 6, pp. 833-837, Dec. 1976.

14. Hamming, R.W., Numerical Methods for Scientists and Engineers, McGraw-Hill Book Co., New York, 1973.

15. Hamming, R.W., Digital Filters, Prentice-Hall, Englewood Cliffs, N.J., 1977.

16. Henriksson, N.G., "An Electrical Method for Registration and Analysis of the Movements of the Eyes in Nystagmus", Acta Oto-Laryngologica, vol. 45, fase-I, pp. 25-41, 1955.

17. Isermann, R., Baur, U., Bamberger, W., Kneppo, P. and Siebert, H., "Comparison of Six On-Line Identification and Parameter Estimation Methods", Automatica, vol. 10, pp. 81-103, 1974.

18. Jackson, B., Kaiser, J.F. and McDonald, H.S., "An Approach to the Implementation of Digital Filters", IEEE Trans. Audio and Electroacoustics, vol. AU-16, no. 3, Sept. 1968.

19. Lee, R.C.K., Optimal Estimation, Identification and Control, MIT Press, Cambridge, Massachusetts, 1964.

20. Lesh, M.D., Mansour, J.M. and Simon, S.R., "A Gait Analysis Subsystem for Smoothing and Differentiation of Human Motion Data", Jr. Biomech. Eng., vol. 101, pp. 205-212, Aug. 1979.

21. Mekel, R. and Singh, A., "System Identification via a Microcomputer", 12th Annual Conf. on Man. Control, Univ. of Illinois, May 1976.

22. Michaels, D.L. and Tole, J.R., "A Microprocessor-Based Instrument for Nystagmus Analysis", Proc. IEEE, vol. 65, no. 5, pp. 730-735, May 1977.

23. Rabiner, L.R. and Steiglitz, K., "The Design of Wide-Band Recursive and Nonrecursive Digital Differentiators", IEEE Trans. Audio and Electroacoust., vol. AU-18, no. 2, pp. 204-209, June 1970.

24. Raphan, T., "A Parameter Adaptive Approach to Oculomotor System Modeling", Ph.D. Thesis, The City University of New York, 1976.

25. Raphan, T. and Cohen, B., "Brainstem Mechanisms for Rapid and Slow Eye Movements", Ann. Rev. Physiol., pp. 527-52, 1978.

26. Raphan, T., Cohen, B. and Matsuo, V., "A Velocity-Storage Mechanism Responsible for Optokinetic Nystagmus (OKN), Optokinetic After-Nystagmus (OKAN) and Vestibular Nystagmus", In Control of Gaze by Brainstem Neurons, ed. R. Baker and A. Berthoz, Elsevier/North Holland Biomedical Press, Amsterdam, 1977.

27. Raphan, T., Matsuo, V. and Cohen, B., "Velocity Storage in the Vestibulo-Ocular Reflex Arc (VOR)", Exp. Brain Research, vol. 35, pp. 229-248, 1979.

28. Rashbass, C., "The Relationship between Saccadic and Smooth Tracking Eye Movements", Journ. Physiol., vol. 159, pp. 326-338, 1961.

29. Robinson, D.A., "A Method of Measuring Movements using a Scleral Search Coil in a Magnetic Field:, IEEE Trans. on Biomed. Elect., vol. BME 1, pp. 137-145, 1963.

30. Robinson, D.A., "The Mechanics of Human Saccadic Eye Movement", Journ. Physiol., vol. 174, pp. 245-264, 1964.

31. Robinson, D.A., "The Mechanics of Human Smooth Pursuit Eye Movements", Journ. Physiol., vol. 180, pp. 569-591, 1965.

32. Robinson, D.A., "The Oculomotor Control System: A Review", Proc. of IEEE, vol. 56, no. 6, June 1968.

33. Singh, A., Thau, F.E., Raphan, T. and Cohen, B., "Detection of Saccades by a Maximum Likelihood Ratio Criterion", 34th ACEMB, Houston, Texas, p. 136, 21-23 Sept. 1981.

34. Steiglitz, K., "Computer-Aided Design of Recursive Digital Filters", IEEE Trans. Audio and Electroacoust., vol. AU-18, no. 2, pp. 123-129, June 1970.

35. Swanson, G.D., "Biological Signal Conditioning for System Identification", Proc. IEEE, vol. 65, no. 5, pp. 735-740, May 1977.

36. Thomas, A.T., "Architecture and Applications of a 12-Bit CMOS Microprocessor", Proc. IEEE, vol. 64, no. 6, pp. 873-881, June 1976.

37. Tole, J.R. and Young, L.R., "MITNYS. A Hybrid Program for On-Line Analysis of Nystagmus", Aerosp. Med., vol. 42, pp. 508-511, 1971.

38. VanTrees, H.L., Detection, Estimation and Modulation Theory, Part I, Wiley, New York, 1968.

39. Wheeless, L.L., Boynton, R.M. and Cohen, G.H., "Eye Movement Responses to Step and Pulse-Step Stimuli", J. Opt. Soc. Am., vol. 56, pp. 956-960, 1966.

40. Westheimer, G., "Eye Movement Responses to a Horizontally Moving Visual Stimulus", A.M.A. Arch Ophthalmol., vol. 52, pp. 932-941, 1954.

41. Young, L.R., "Measuring Eye Movements", The American Journal of Med. Electronics, pp. 300-307, Oct.-Dec. 1963.

42. Young, L.R. and Sheena, D., "Eye-Movement Measurement Techniques", American Psychologist, vol. 30, no. 3, March 1975.

43. Young, L.R. and Stark, L., "A Discrete Model for Eye Tracking Movements", IEEE Trans. on Military Electronics, vol. MIL-7, no. 2 &3, April-July 1963.